

AD-A107 590

FACTORY MUTUAL RESEARCH CORP NORWOOD MASS

F/G 21/2

MODELING OF CEILING FIRE SPREAD AND THERMAL RADIATION.(U)

OCT 81 R L ALPERT, M K MATHEWS, A T MODAK

DOT-FA79NA-6019

UNCLASSIFIED

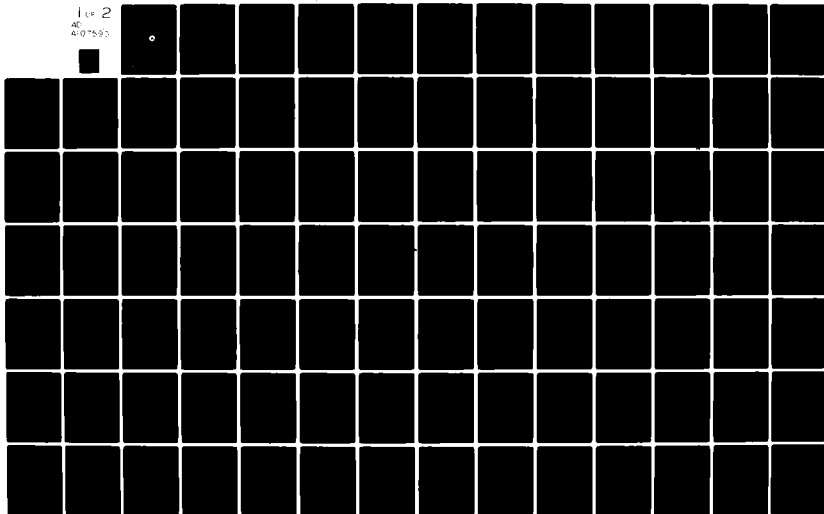
RC81-BR-3

DOT/FAA-CT-81-70

NL

1 of 2

407590



LEVEL

12

MODELING OF CEILING FIRE SPREAD AND THERMAL RADIATION

R. L. Alpert
M. K. Mathews
A. T. Modak

FEDERAL AVIATION ADMINISTRATION TECHNICAL CENTER
Atlantic City Airport, New Jersey 08405



NOT FOR
CIRCULATION
WHICH DO NOT

FINAL REPORT

OCTOBER 1981

Document is available to the U.S. public through
the National Technical Information Service,
Springfield, Virginia 22161.

Prepared for

U. S. DEPARTMENT OF TRANSPORTATION
FEDERAL AVIATION ADMINISTRATION
Systems Research & Development Service
Washington, D. C. 20590

DTIC FILE COPY

AD A107590

83

NOTICE

This document is disseminated under the sponsorship of the Department of Transportation in the interest of information exchange. The United States Government assumes no liability for the contents or use thereof.

The United States Government does not endorse products or manufacturers. Trade or manufacturer's names appear herein solely because they are considered essential to the object of this report.

DISCLAIMER NOTICE

**THIS DOCUMENT IS BEST QUALITY
PRACTICABLE. THE COPY FURNISHED
TO DTIC CONTAINED A SIGNIFICANT
NUMBER OF PAGES WHICH DO NOT
REPRODUCE LEGIBLY.**

Technical Report Documentation Page

1. Report No. DOT/FAA/CT-81-70		2. Government Accession No. AD-A107590		3. Recipient's Catalog No.	
4. Title and Subtitle Modeling of Ceiling Fire Spread and Thermal Radiation				5. Report Date October 1981	
				6. Performing Organization Code	
7. Author(s) R. L. Alpert, M. K. Mathews, A. T. Modak				8. Performing Organization Report No. OEON8.BU; RC81-BR-3	
9. Performing Organization Name and Address Factory Mutual Research Corporation 1151 Boston-Providence Turnpike Norwood, Massachusetts 02062				10. Work Unit No. (TRAIS)	
				11. Contract or Grant No. DOT-FA79NA-6019	
12. Sponsoring Agency Name and Address U.S. Department of Transportation Federal Aviation Administration Technical Center Atlantic City Airport, New Jersey 08405				13. Type of Report and Period Covered May 25, 1979-March 1981	
				14. Sponsoring Agency Code	
15. Supplementary Notes FAA Technical Center, formerly National Aviation Facilities Experimental Center (NAFEC)					
16. Abstract → The pressure modeling technique is used to study fire spread under five different ceiling materials and analytical and numerical techniques are used to compute thermal radiation to floor level from the resultant layer of hot gases near the ceiling. In the physical modeling part of the study, measurements are obtained at one atmosphere (full-scale) and at elevated air pressure characterizing fire growth in a ceiling channel exposed to a developing PMMA wall fire. Pressure modeling predictions of flame spread rates under a PMMA ceiling and flame lengths under an inert ceiling are found to be in reasonable agreement with full-scale behavior. Although fire spread under aircraft material ceilings occurs only at elevated pressure and not at one atmosphere (due to charring effects and the use of full-scale material thickness in the models), exponential growth factors characterizing fire spread rates, mass loss rates and radiant heat loss in the model tests are used to group the five ceiling materials according to fire growth hazard. In the second phase of the study, an exact, numerical solution technique is formulated for computing the radiant flux from hot gas layers with arbitrary, three-dimensional variations in gas temperature and absorption coefficient. A simplified, analytic approximation involving the use of a suitably averaged gas temperature and absorption coefficient is compared with the exact technique for the calculation of radiant flux to targets below the ceiling gas layer. It is found that the analytic approximation is adequate even when gradients in temperature are much larger than those expected from real aircraft cabin fires. ←					
17. Key Words Radiant Heat Loss Flame Spreading Ceiling Layer Radiation Aircraft Materials Fire Modeling Pressure Modeling				18. Distribution Statement Document is available to the U.S. public through the National Technical Information Service, Springfield, Virginia 22161	
19. Security Classif. (of this report)		20. Security Classif. (of this page)		21. No. of Pages	
				22. Price	

Approximate Conversions from Metric Measures			
Symbol	When You Know	Multiply by	To Find
	<u>LENGTH</u>		
in	inches	2.5	centimeters
ft	feet	30	centimeters
yd	yards	0.9	meters
m	miles	1.6	kilometers
	<u>AREA</u>		
in ²	square inches	6.5	square centimeters
ft ²	square feet	0.09	square meters
yd ²	square yards	0.8	square meters
m ²	square miles	2.6	square kilometers
	acres	0.4	hectares
	<u>MASS (weight)</u>		
oz	ounces	28	grams
lb	pounds	0.45	kilograms
	short tons (2000 lb)	0.9	tonnes
	<u>VOLUME</u>		
tsp	teaspoons	5	milliliters
Tbsp	tablespoons	15	milliliters
fl oz	fluid ounces	30	milliliters
c	cups	0.24	liters
pt	pints	0.47	liters
qt	quarts	0.95	liters
gal	gallons	3.8	liters
ft ³	cubic feet	0.03	cubic meters
yd ³	cubic yards	0.76	cubic meters
	<u>TEMPERATURE (exact)</u>		
Fahrenheit temperature	5/9 (after subtracting 32)		Celsius temperature
	<u>TEMPERATURE (exact)</u>		
Celsius temperature	9/5 (then add 32)		Fahrenheit temperature

Copyright © 1994 by The McGraw-Hill Companies, Inc. All rights reserved. Printed in the United States of America. This book is a trademark of The McGraw-Hill Companies, Inc.

1. The first two columns of the table are the names of the authors and the titles of the papers. The third column is the year of publication. The fourth column is the journal or book in which the paper was published. The fifth column is the volume number. The sixth column is the page number. The seventh column is the price of the paper. The eighth column is the name of the publisher. The ninth column is the name of the distributor. The tenth column is the name of the agent. The eleventh column is the name of the printer. The twelfth column is the name of the binder. The thirteenth column is the name of the cover. The fourteenth column is the name of the spine. The fifteenth column is the name of the title page. The sixteenth column is the name of the table of contents. The seventeenth column is the name of the introduction. The eighteenth column is the name of the first chapter. The nineteenth column is the name of the second chapter. The twentieth column is the name of the third chapter. The twenty-first column is the name of the fourth chapter. The twenty-second column is the name of the fifth chapter. The twenty-third column is the name of the sixth chapter. The twenty-fourth column is the name of the seventh chapter. The twenty-fifth column is the name of the eighth chapter. The twenty-sixth column is the name of the ninth chapter. The twenty-seventh column is the name of the tenth chapter. The twenty-eighth column is the name of the eleventh chapter. The twenty-ninth column is the name of the twelfth chapter. The thirtieth column is the name of the thirteenth chapter. The thirty-first column is the name of the fourteenth chapter. The thirty-second column is the name of the fifteenth chapter. The thirty-third column is the name of the sixteenth chapter. The thirty-fourth column is the name of the seventeenth chapter. The thirty-fifth column is the name of the eighteenth chapter. The thirty-sixth column is the name of the nineteenth chapter. The thirty-seventh column is the name of the twentieth chapter. The thirty-eighth column is the name of the twenty-first chapter. The thirty-ninth column is the name of the twenty-second chapter. The fortieth column is the name of the twenty-third chapter. The forty-first column is the name of the twenty-fourth chapter. The forty-second column is the name of the twenty-fifth chapter. The forty-third column is the name of the twenty-sixth chapter. The forty-fourth column is the name of the twenty-seventh chapter. The forty-fifth column is the name of the twenty-eighth chapter. The forty-sixth column is the name of the twenty-ninth chapter. The forty-seventh column is the name of the thirtieth chapter. The forty-eighth column is the name of the thirty-first chapter. The forty-ninth column is the name of the thirty-second chapter. The fiftieth column is the name of the thirty-third chapter. The fifty-first column is the name of the thirty-fourth chapter. The fifty-second column is the name of the thirty-fifth chapter. The fifty-third column is the name of the thirty-sixth chapter. The fifty-fourth column is the name of the thirty-seventh chapter. The fifty-fifth column is the name of the thirty-eighth chapter. The fifty-sixth column is the name of the thirty-ninth chapter. The fifty-seventh column is the name of the fortieth chapter. The fifty-eighth column is the name of the forty-first chapter. The fifty-ninth column is the name of the forty-second chapter. The sixtieth column is the name of the forty-third chapter. The sixty-first column is the name of the forty-fourth chapter. The sixty-second column is the name of the forty-fifth chapter. The sixty-third column is the name of the forty-sixth chapter. The sixty-fourth column is the name of the forty-seventh chapter. The sixty-fifth column is the name of the forty-eighth chapter. The sixty-sixth column is the name of the forty-ninth chapter. The sixty-seventh column is the name of the fiftieth chapter. The sixty-eighth column is the name of the fifty-first chapter. The sixty-ninth column is the name of the fifty-second chapter. The seventieth column is the name of the fifty-third chapter. The seventy-first column is the name of the fifty-fourth chapter. The seventy-second column is the name of the fifty-fifth chapter. The seventy-third column is the name of the fifty-sixth chapter. The seventy-fourth column is the name of the fifty-seventh chapter. The seventy-fifth column is the name of the fifty-eighth chapter. The seventy-sixth column is the name of the fifty-ninth chapter. The seventy-seventh column is the name of the sixtieth chapter. The seventy-eighth column is the name of the sixty-first chapter. The seventy-ninth column is the name of the sixty-second chapter. The eightieth column is the name of the sixty-third chapter. The eighty-first column is the name of the sixty-fourth chapter. The eighty-second column is the name of the sixty-fifth chapter. The eighty-third column is the name of the sixty-sixth chapter. The eighty-fourth column is the name of the sixty-seventh chapter. The eighty-fifth column is the name of the sixty-eighth chapter. The eighty-sixth column is the name of the sixty-ninth chapter. The eighty-seventh column is the name of the seventieth chapter. The eighty-eighth column is the name of the seventy-first chapter. The eighty-ninth column is the name of the seventy-second chapter. The ninetieth column is the name of the seventy-third chapter. The ninety-first column is the name of the seventy-fourth chapter. The ninety-second column is the name of the seventy-fifth chapter. The ninety-third column is the name of the seventy-sixth chapter. The ninety-fourth column is the name of the seventy-seventh chapter. The ninety-fifth column is the name of the seventy-eighth chapter. The ninety-sixth column is the name of the seventy-ninth chapter. The ninety-seventh column is the name of the eightieth chapter. The ninety-eighth column is the name of the eighty-first chapter. The ninety-ninth column is the name of the eighty-second chapter. The hundredth column is the name of the eighty-third chapter.

PREFACE

This work was sponsored by the Federal Aviation Administration, through a contract from the FAA Technical Center, Atlantic City, New Jersey. The Contracting Officer's Technical Representative was Dr. Thor I. Eklund, whose valuable advice and encouragement during the entire course of this work are gratefully acknowledged.

Mr. Francis B. Kiley, aided by Mr. Lawney Crudup, Jr., ably performed the experiments described herein at the Factory Mutual Research Corporation. The support and patience of Dr. John de Ris, Manager, FMRC Basic Research and Dr. Raymond Friedman, Manager, FMRC Research Division, are sincerely appreciated.

Accession for	✓
1975-1976	
1976-1977	
1977-1978	
1978-1979	
1979-1980	
1980-1981	
1981-1982	
1982-1983	
1983-1984	
1984-1985	
1985-1986	
1986-1987	
1987-1988	
1988-1989	
1989-1990	
1990-1991	
1991-1992	
1992-1993	
1993-1994	
1994-1995	
1995-1996	
1996-1997	
1997-1998	
1998-1999	
1999-2000	
2000-2001	
2001-2002	
2002-2003	
2003-2004	
2004-2005	
2005-2006	
2006-2007	
2007-2008	
2008-2009	
2009-2010	
2010-2011	
2011-2012	
2012-2013	
2013-2014	
2014-2015	
2015-2016	
2016-2017	
2017-2018	
2018-2019	
2019-2020	
2020-2021	
2021-2022	
2022-2023	
2023-2024	
2024-2025	
2025-2026	
2026-2027	
2027-2028	
2028-2029	
2029-2030	
2030-2031	
2031-2032	
2032-2033	
2033-2034	
2034-2035	
2035-2036	
2036-2037	
2037-2038	
2038-2039	
2039-2040	
2040-2041	
2041-2042	
2042-2043	
2043-2044	
2044-2045	
2045-2046	
2046-2047	
2047-2048	
2048-2049	
2049-2050	
2050-2051	
2051-2052	
2052-2053	
2053-2054	
2054-2055	
2055-2056	
2056-2057	
2057-2058	
2058-2059	
2059-2060	
2060-2061	
2061-2062	
2062-2063	
2063-2064	
2064-2065	
2065-2066	
2066-2067	
2067-2068	
2068-2069	
2069-2070	
2070-2071	
2071-2072	
2072-2073	
2073-2074	
2074-2075	
2075-2076	
2076-2077	
2077-2078	
2078-2079	
2079-2080	
2080-2081	
2081-2082	
2082-2083	
2083-2084	
2084-2085	
2085-2086	
2086-2087	
2087-2088	
2088-2089	
2089-2090	
2090-2091	
2091-2092	
2092-2093	
2093-2094	
2094-2095	
2095-2096	
2096-2097	
2097-2098	
2098-2099	
2099-2100	
2100-2101	
2101-2102	
2102-2103	
2103-2104	
2104-2105	
2105-2106	
2106-2107	
2107-2108	
2108-2109	
2109-2110	
2110-2111	
2111-2112	
2112-2113	
2113-2114	
2114-2115	
2115-2116	
2116-2117	
2117-2118	
2118-2119	
2119-2120	
2120-2121	
2121-2122	
2122-2123	
2123-2124	
2124-2125	
2125-2126	
2126-2127	
2127-2128	
2128-2129	
2129-2130	
2130-2131	
2131-2132	
2132-2133	
2133-2134	
2134-2135	
2135-2136	
2136-2137	
2137-2138	
2138-2139	
2139-2140	
2140-2141	
2141-2142	
2142-2143	
2143-2144	
2144-2145	
2145-2146	
2146-2147	
2147-2148	
2148-2149	
2149-2150	
2150-2151	
2151-2152	
2152-2153	
2153-2154	
2154-2155	
2155-2156	
2156-2157	
2157-2158	
2158-2159	
2159-2160	
2160-2161	
2161-2162	
2162-2163	
2163-2164	
2164-2165	
2165-2166	
2166-2167	
2167-2168	
2168-2169	
2169-2170	
2170-2171	
2171-2172	
2172-2173	
2173-2174	
2174-2175	
2175-2176	
2176-2177	
2177-2178	
2178-2179	
2179-2180	
2180-2181	
2181-2182	
2182-2183	
2183-2184	
2184-2185	
2185-2186	
2186-2187	
2187-2188	
2188-2189	
2189-2190	
2190-2191	
2191-2192	
2192-2193	
2193-2194	
2194-2195	
2195-2196	
2196-2197	
2197-2198	
2198-2199	
2199-2200	
2200-2201	
2201-2202	
2202-2203	
2203-2204	
2204-2205	
2205-2206	
2206-2207	
2207-2208	
2208-2209	
2209-2210	
2210-2211	
2211-2212	
2212-2213	
2213-2214	
2214-2215	
2215-2216	
2216-2217	
2217-2218	
2218-2219	
2219-2220	
2220-2221	
2221-2222	
2222-2223	
2223-2224	
2224-2225	
2225-2226	
2226-2227	
2227-2228	
2228-2229	
2229-2230	
2230-2231	
2231-2232	
2232-2233	
2233-2234	
2234-2235	
2235-2236	
2236-2237	
2237-2238	
2238-2239	
2239-2240	
2240-2241	
2241-2242	
2242-2243	
2243-2244	
2244-2245	
2245-2246	
2246-2247	
2247-2248	
2248-2249	
2249-2250	
2250-2251	
2251-2252	
2252-2253	
2253-2254	
2254-2255	
2255-2256	
2256-2257	
2257-2258	
2258-2259	
2259-2260	
2260-2261	
2261-2262	
2262-2263	
2263-2264	
2264-2265	
2265-2266	
2266-2267	
2267-2268	
2268-2269	
2269-2270	
2270-2271	
2271-2272	
2272-2273	
2273-2274	
2274-2275	
2275-2276	
2276-2277	
2277-2278	
2278-2279	
2279-2280	
2280-2281	
2281-2282	
2282-2283	
2283-2284	
2284-2285	
2285-2286	
2286-2287	
2287-2288	
2288-2289	
2289-2290	
2290-2291	
2291-2292	
2292-2293	
2293-2294	
2294-2295	
2295-2296	
2296-2297	
2297-2298	
2298-2299	
2299-2300	
2300-2301	
2301-2302	
2302-2303	
2303-2304	
2304-2305	
2305-2306	
2306-2307	
2307-2308	
2308-2309	
2309-2310	
2310-2311	
2311-2312	
2312-2313	
2313-2314	
2314-2315	
2315-2316	
2316-2317	
2317-2318	
2318-2319	
2319-2320	
2320-2321	
2321-2322	
2322-2323	
2323-2324	
2324-2325	
2325-2326	
2326-2327	
2327-2328	
2328-2329	
2329-2330	
2330-2331	
2331-2332	
2332-2333	
2333-2334	
2334-2335	
2335-2336	
2336-2337	
2337-2338	
2338-2339	
2339-2340	
2340-2341	
2341-2342	
2342-2343	
2343-2344	
2344-2345	
2345-2346	
2346-2347	
2347-2348	
2348-2349	
2349-2350	
2350-2351	
2351-2352	
2352-2353	
2353-2354	
2354-2355	
2355-2356	
2356-2357	
2357-2358	
2358-2359	
2359-2360	
2360-2361	
2361-2362	
2362-2363	
2363-2364	
2364-2365	
2365-2366	
2366-2367	
2367-2368	
2368-2369	
2369-2370	
2370-2371	
2371-2372	
2372-2373	
2373-2374	
2374-2375	
2375-2376	
2376-2377	
2377-2378	
2378-2379	
2379-2380	
2380-2381	
2381-2382	
2382-2383	
2383-2384	
2384-2385	
2385-2386	
2386-2387	
2387-2388	
2388-2389	
2389-2390	
2390-2391	
2391-2392	
2392-2393	
2393-2394	
2394-2395	
2395-2396	
2396-2397	
2397-2398	
2398-2399	
2399-2400	
2400-2401	
2401-2402	
2402-2403	
2403-2404	
2404-2405	
2405-2406	
2406-2407	
2407-2408	
2408-2409	
2409-2410	
2410-2411	
2411-2412	
2412-2413	
2413-2414	
2414-2415	
2415-2416	
2416-2417	
2417-2418	
2418-2419	
2419-2420	
2420-2421	
2421-2422	
2422-2423	
2423-2424	
2424-2425	
2425-2426	
2426-2427	
2427-2428	
2428-2429	
2429-2430	
2430-2431	
2431-2432	
2432-2433	
2433-2434	
2434-2435	
2435-2436	
2436-2437	
2437-2438	
2438-2439	
2439-2440	
2440-2441	
2441-2442	
2442-2443	
2443-2444	
2444-2445	
2445-2446	
2446-2447	
2447-2448	
2448-2449	
2449-2450	
2450-2451	
2451-2452	
2452-2453	
2453-2454	
2454-2455	
2455-2456	
2456-2457	
2457-2458	
2458-2459	
2459-2460	
2460-2461	
2461-2462	
2462-2463	
2463-2464	
2464-2465	
2465-2466	
2466-2467	
2467-2468	
2468-2469	
2469-2470	
2470-2471	
2471-2472	
2472-2473	
2473-2474	
2474-2475	
2475-2476	
2476-2477	
2477-2478	
2478-2479	
2479-2480	
2480-2481	
2481-2482	
2482-2483	
2483-2484	
2484-2485	
2485-2486	
2486-2487	
2487-2488	
2488-2489	
2489-2490	
2490-2491	
2491-2492	
2492-2493	
2493-2494	
2494-2495	
2495-2496	
2496-2497	
2497-2498	
2498-2499	
2499-2500	
2500-2501	
2501-2502	
2502-2503	
2503-2504	
2504-2505	
2505-2506	
2506-2507	
2507-2508	
2508-2509	
2509-2510	
2510-2511	
2511-2512	
2512-2513	
2513-2514	
2514-2515	
2515-2516	
2516-2517	
2517-2518	
2518-2519	
2519-2520	
2520-2521	
2521-2522	
2522-2523	
2523-2524	
2524-2525	

TABLE OF CONTENTS

<u>Section</u>	<u>Title</u>	<u>Page</u>
I	INTRODUCTION	1
	1.1 Purpose	1
	1.2 Background	1
II	PRESSURE MODELING OF CEILING FIRE GROWTH	3
	2.1 Experimental Arrangement	3
	2.2 Experimental Results: Full-Scale Tests	10
	2.3 Experimental Results: Model Tests	15
	2.4 Analysis of Modeling Results	27
	2.5 Comparison of Ceiling Fire Growth	36
III	ANALYTICAL MODELING OF THERMAL RADIATION FROM LONG CEILING CHANNELS	41
	3.1 Mathematical Formulation	41
	3.2 Approximate Solution	47
	3.3 Application to Full-Scale Test Results	48
	3.4 Use of the Approximate Radiation Model	57
IV	SUMMARY OF RESULTS	58
V	CONCLUSIONS	59
	REFERENCES	60
	APPENDIX A	62

LIST OF FIGURES

<u>Number</u>	<u>Title</u>	<u>Page</u>
1	Side View of Channel	4
2	End View of Channel	5
3	Flame Lengths under Full-Scale Ceilings	12
4	Correlation of Flame Length under Inert Ceilings	16
5	Correlation of Flame Length under No 234 Model Ceilings	17
6	Correlation of Flame Length under No B8811 Model Ceilings	18
7	Correlation of Flame Length under No. 223 Model Ceilings	19
8	Correlation of Flame Length under PMMA Ceilings	20
9	Correlation of Flame and Inert Ceiling Radiance	22
10	Correlation of Flame and No. 234 Model Ceiling Radiance	23
11	Correlation of Flame and No. B8811 Model Ceiling Radiance	24
12	Correlation of Flame and No. 223 Model Ceiling Radiance	25
13	Correlation of Flame and PMMA Ceiling Radiance	26
14	Correlation of Mass Loss Rate for Inert Model Ceilings	28
15	Correlation of Mass Loss Rate for No. 234 Model Ceilings	29
16	Correlation of Mass Loss Rate for No. B8811 Model Ceilings	30
17	Correlation of Mass Loss Rate for No. 223 Model Ceilings	31
18	Correlation of Mass Loss Rate for PMMA Model Ceilings	32
19	Predicted Behavior of Square of Net Heat Flux to Thermally Thick Fuel Surface	35
20	Predicted Behavior of Flame and Fuel Surface Radiance	37
21A	Elevation, End and Plan Views of Enclosure of Length-L, Breadth-B, Height-H ₂	44
21B	Detail of Elevation, End and Plan Views of Rectangular Parallelepiped No. 1 of Length-b, Breadth-a, Height-H ₂	45
22	Basic Temperature Distribution Used for Calculated Results in Tables 5 and 6	49

LIST OF TABLES

<u>Number</u>	<u>Title</u>	<u>Page</u>
1	Description of Ceiling Materials	7
2	Measurement Instruments for Full-Scale Tests	8
3	Ceiling Fire Exponential Growth Factors	38
4	Maximum Mass Loss Rate and Radiance of Ceiling Fires	40
5	Radiant Flux to Target Located Below Center of Layer	50
6	Radiant Flux to Target Located Below End of Layer	51
7	Computed and Observed Heat Losses, Full-Scale Test 6-19-80, Inert Ceiling	54
8	Computed and Observed Radiant Heat Losses, Full-Scale Test 8-5-80, PMMA Ceiling	55
9	Computed and Observed Radiant Heat Losses, Full-Scale Test 8-20-80, PMMA Ceiling Burning Steadily	56
A-1	Upward Flame Spread on PMMA Wall, Test 6-10-80, Inert Ceiling	62
A-2	Upward Flame Spread on PMMA Wall, Test 6-19-80, Inert Ceiling	63
A-3	Mass Loss Rate of PMMA Wall Test 6-10-80, Inert Ceiling Mass Loss Rate of PMMA Wall Test 6-19-80, Inert Ceiling	64
A-4	Flame Extent Under Inert Ceiling, Test 6-10-80	65
A-5	Flame Extent Under Inert Ceiling, Test 6-19-80	66
A-6	Flame Extent Under NAFEC #234 Ceiling, Test 7-9-80	67
A-7	Flame Extent Under NAFEC #B8811 Ceiling, Test 7-22-80	68
A-8	Flame Extent Under NAFEC #223 Ceiling, Test 7-30-80	69
A-9	Flame Spread Under PMMA Ceiling, Test 8-5-80	70
A-10	Temperature and Radiation Measurements, Full-Scale Test 6-10-80, Inert Ceiling	71
A-11	Temperature and Radiation Measurements, Full-Scale Test 6-19-80, Inert Ceiling	74
A-12	Temperature and Radiation Measurements, Full-Scale Test 7-9-80, NAFEC #234 Ceiling	78
A-13	Temperature and Radiation Measurements, Full-Scale Test 7-22-80, NAFEC #B8811 Ceiling	82
A-14	Temperature and Radiation Measurements, Full-Scale Test 7-30-80, NAFEC #223 Ceiling	86
A-15	Temperature and Radiation Measurements, Full-Scale Test 8-5-80, PMMA Ceiling	90
A-16	Temperature and Radiation Measurements, Full-Scale Test 8-20-80, Fully Developed PMMA Ceiling Fire	95

LIST OF SYMBOLS

a	width of parallelepiped section of ceiling layer
b	length of parallelepiped section of ceiling layer
C	specific heat of wall or ceiling material
d	flame thickness or gas layer depth
H_1	height of lower edge of ceiling layer above target
H_2	height of upper edge of ceiling layer above target
k	infrared absorption coefficient
L_m	radiation mean-beam-length
ℓ	optical path length in ceiling layer
m	mass of wall or ceiling material
\dot{m}	mass loss rate
N	radiance of ceiling layer for ray normal to ceiling
\vec{n}	unit normal vector to target surface
p	absolute gas pressure
\dot{q}''	heat flux or power per unit area
\vec{r}_0	radius vector from target along ray to far edge of ceiling layer
T	gas temperature
t	time
V_f	flame spread rate
W	width of gas layer or channel
x_f	flame length from end-wall
x	longitudinal Cartesian coordinate
y	lateral Cartesian coordinate
z	vertical Cartesian coordinate
z_0	vertical coordinate at far edge of ceiling layer
z_1	vertical distance below ceiling surface
α	reradiation constant, between zero and unity
γ	exponential growth factor
θ	polar angle
λ	thermal conductivity
ρ	density
σ	Stefan-Boltzmann constant
ϕ	azimuthal angle

Superscripts

' at absolute pressure, p

Subscripts

c convective

g gas

ℓ lower limit of integration

o reference or normal, one-atmosphere condition

s ceiling or wall surface

u upper limit of integration

I

INTRODUCTION

1.1 PURPOSE

The purpose of this project is 1) to model the fire growth which can occur along ceiling channels (simulating an aircraft fuselage) through the use of small-scale experiments at elevated air pressure and 2) to model the radiant heat transfer from ceiling fire gases in a long channel through analytical and numerical techniques.

1.2 BACKGROUND

Fire growth within an aircraft cabin environment can occur by several different modes. One such mode is by upward fire spread on vertical surfaces, a process which can be very rapid. In a previous study¹, the feasibility of modeling upward fire spread on vertical walls through the use of small-scale experiments at elevated air pressure (pressure modeling) was proven for a fuel with simple vaporization characteristics, polymethylmethacrylate (PMMA). Relative rates of upward spread among 15 different aircraft materials at elevated air pressures were also investigated in this study. As a result of the work in reference 1, it was found that samples of aircraft materials could be conveniently ranked by characteristic rate of upward fire spread, with such a ranking being reasonably independent of absolute air pressure in the range from 10 to 30 atmospheres.

Another mode for fire growth in a fuselage type of enclosure is by flame spread on the long ceiling channel formed by the cabin ceiling and walls. The hot gas layer near the ceiling resulting from such fire spread can lead to full enclosure involvement in fire due to radiative heat transfer to lower levels at large distances from the ignition location. Fire spread under ceilings as well as steady burning of ceilings has not been studied in detail compared to other modes of fire spread. Recent progress in this area has resulted from work which appears in references 2-8. Babrauskas² estimates flame lengths under open and channeled inert ceilings due to pool fire plume impingement. A simplified mass flow calculation procedure is used in reference 2 to obtain results for comparison with extensive measurements by You and Faeth⁷ on small-scale (less than 0.34 m height) axisymmetric impinging flames and by Hinkley et al¹¹ on flames along large-scale channels. Flame spread in the direction of forced convective flows is analyzed by Fernandez-Pello⁶ and by Annamalai and Sibulkin³ for the laminar case where thermal radiation is unimportant and by Carrier et al⁵ for the tunnel geometry used in the ASTM E84 flammability test. In the latter reference⁵, numerical solution of a very complex mathematical formulation is required. Movement of smoke or combustion products in large-scale ceiling channels has been analyzed recently by Delichatsios⁴ while Hwang et al⁹ have previously studied product flow along the ceilings of ventilated ducts. Work done by Alpert¹⁰ establishes simplified integral models for nonreacting ceiling-jets in two-dimensional channels. The flow studied in

reference 10 results from impingement of a line plume across the entire channel width rather than from axisymmetric plume impingement, as in reference 4. None of the preceding theoretical work directly addresses the problem of predicting self-sustained fire spread in ceiling channels, although many of the results can eventually be applied to making such predictions.

Because of the absence of proven theoretical predictive techniques, the first part of the present study investigates the possibility of physical modeling of the ceiling fire spread phenomenon through use of the pressure modeling technique. In this first section of the report, small-scale tests run at elevated ambient pressure yield measurements of transient flame lengths, mass loss rates and radiant heat loss for five different ceiling materials exposed to a PMMA wall fire at one end of a long channel. Full-scale tests with the same five materials and an analysis of the effect of pressure on radiant heat loss are used to evaluate modeling success. Results show the modeling to be surprisingly accurate for both inert and PMMA ceilings in spite of relatively thick hot-gas layers, radiation from which cannot be readily modeled at elevated air pressure. However, it is shown that the flame spread process is not modeled for three aircraft material ceilings, probably due to charring effects and the impracticality of changing the thickness of complex, composite materials. (A factor of 10 decrease in full-scale thickness is required for modeling at 31 atmospheres.)

In the second part of the report, radiant heat loss from realistic, corridor-like ceiling fires is examined in detail. As part of this study, the consistency of several different ceiling layer temperature and heat flux measurements made during the series of full-scale tests is analyzed. Exact numerical calculation of radiant heat flux from hot gases in a long ceiling channel (such as an aircraft cabin) are then shown to be in very good agreement with results from an approximate, analytical technique. This analytical procedure greatly simplifies the task of calculating radiant emission from inhomogeneous hot gas layers of known size, composition and temperature.

II
PRESSURE MODELING OF CEILING FIRE GROWTH

2.1 EXPERIMENTAL ARRANGEMENT

2.1.1 MODELING TECHNIQUE. The pressure modeling technique for prediction of transient, large-scale fire phenomena from small-scale experiments is fully described in references 12-14. As explained in these references, the modeling scheme requires the reduction of all characteristic length scales as the minus $2/3$ power of absolute air pressure. This type of scaling preserves the full-scale relationship among gas phase inertial, buoyant and viscous forces. Solid phase thermal response and vaporization characteristics will also model full-scale phenomena, but on a time scale which is reduced as the minus $4/3$ power of absolute air pressure. The previous study of upward fire spread has shown that the modeling scheme may not generally be successful if thermal radiation from solid surfaces or from thick gas layers is the dominant heat transfer mode in fire growth.

2.1.2 WALL-CHANNEL CONFIGURATION. The prototype configuration to be pressure modeled is illustrated by the schematics in Figures 1 and 2. A 2.4 m long, 0.46 m wide channel is formed by a replaceable ceiling and two permanent side-walls extending 0.23 m below the ceiling. At one end of the channel is a 0.9 m high PMMA wall separated from the ceiling by a 0.32 m high inert wall section.

Tests are initiated by ignition of the PMMA wall at the single point shown in the schematics. Use of a point ignition greatly enhances experimental reproducibility and simplifies the elevated pressure model tests. About 16 to 17 minutes after this ignition, there is steady flame impingement on the ceiling material and about 25 to 27 minutes after ignition, flames have spread laterally to almost the full, 0.305 m width of the PMMA wall. If the PMMA wall width were equal to the 0.46 m channel width, complete lateral flame spread would not occur during the time available for the experiment due to the point ignition and very low lateral flame spread rate. Some 35 to 40 minutes after ignition, safety considerations generally dictate a termination of the test by extinguishment of the PMMA wall fire.

The height and position of the PMMA wall and the depth of the channel and vertical side walls that are shown in Figures 1 and 2 were selected after a number of model experiments at elevated air pressure. These 20-atmosphere tests indicated that complete flame spread over an inert ceiling would occur within 30 minutes (at full-scale) solely as a result of the PMMA wall fire if a 1.22 m high wall in direct contact with the ceiling were used, as originally planned. In order to distinguish among different combustible ceilings on the basis of flame spread rate, the PMMA wall height was reduced to 0.9 m; a 0.32 m high inert wall was inserted between the top of the PMMA wall and the ceiling. With this final arrangement, it was found from the model experiments that flames from the PMMA wall fire would not extend along the complete length of an inert ceiling for the equivalent of more than 30-40 minutes (see Sections 2.3 and 2.4).

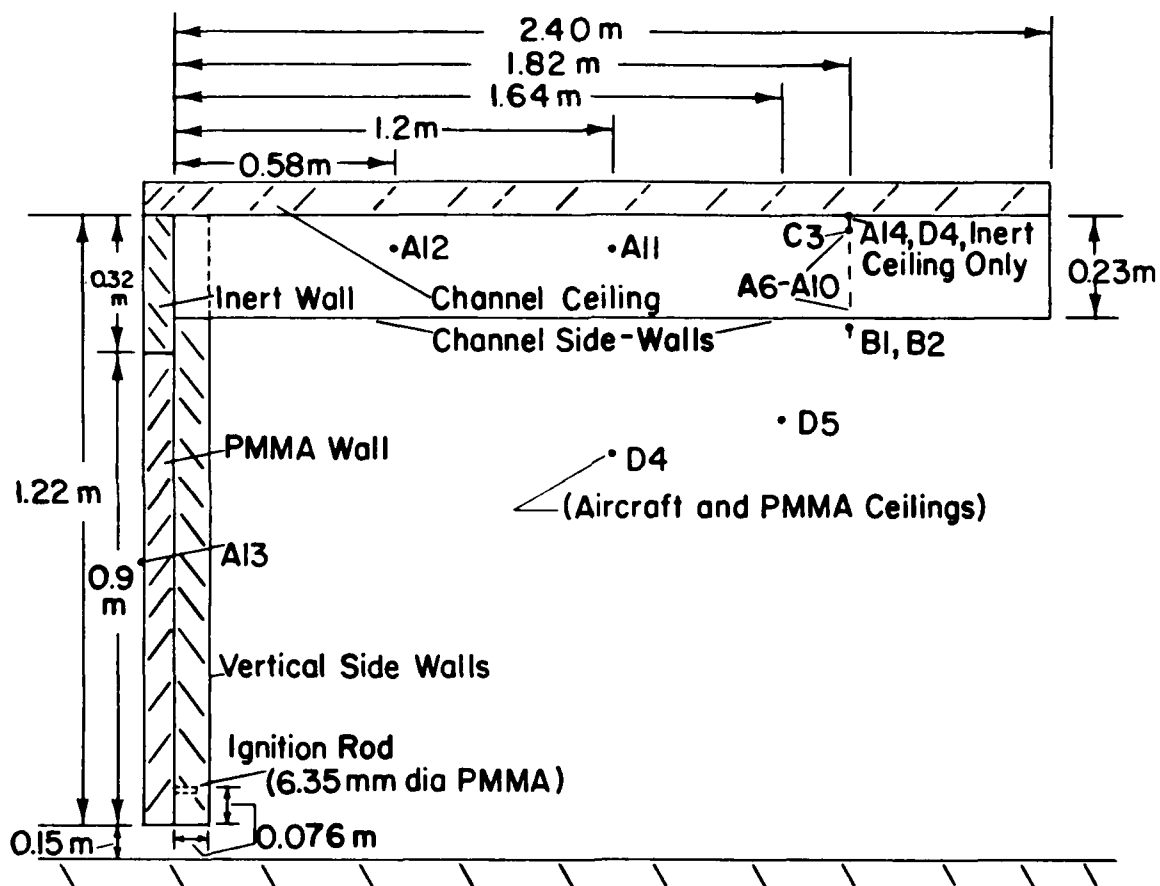


FIGURE 1 SIDE VIEW OF CHANNEL

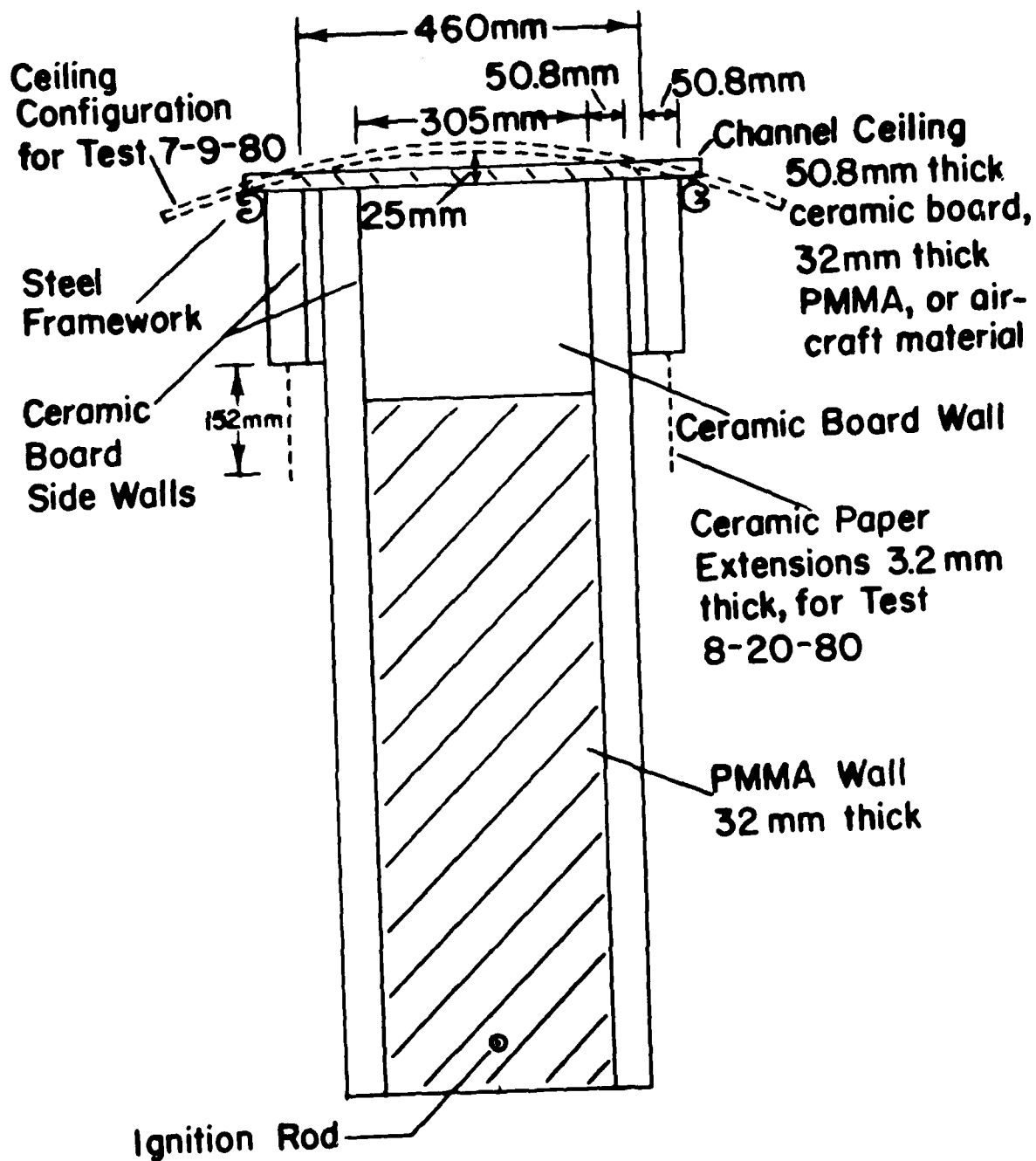


FIGURE 2 END VIEW OF CHANNEL

Model experiments were also used to determine the minimum channel depth (distance from ceiling to bottom of channel side-wall) required to contain the ceiling gas flow. Initial experiments with 0.15 m channel depth revealed an excessive amount of gas leakage with inert and combustible ceilings. Such leakage was virtually eliminated with the final selected depth of 0.23 m. This value is in good agreement with the predicted maximum thickness of a two-dimensional (planar) ceiling-jet, as obtained from the theory of reference 10 (Figure 6). For a ceiling height above the "point" fire source of 0.77 m (assume the point source is the mid-height of the PMMA wall) and a ceiling-jet length of 2.4 m, the predicted value of ceiling-jet thickness from reference 10 is 0.21 m.

The depth of the vertical, confining side-walls on the PMMA wall at the end of the channel were also selected from model experiments. It was found from model tests that a vertical side-wall depth of 0.05 m was inadequate for containing flames from the PMMA wall at a height of 1.22 m above the wall base. The minimum acceptable side-wall depth of 0.076 m, finally chosen, represents 1/16 of the total PMMA and inert wall height, a ratio obtained previously¹⁵ from full-scale tests.

2.1.3 FULL-SCALE TESTS. Full-scale experiments are performed with each of the five ceiling materials listed in Table 1. In addition, duplicate tests are run with the inert and PMMA ceilings for much longer durations than the initial tests. For the PMMA experiment, data are only obtained during a steady burning period of full ceiling involvement.

Each of the seven full-scale tests are instrumented according to the schematic in Figure 1, which contains instrument symbols explained in Table 2. All instrumentation is located as close as possible to the mid-plane of the channel. The main measurement station for these experiments is about 1.82 m from the PMMA wall. At this station are located two different narrow angle radiometers viewing the bottom of the smoke layer, an array of thermocouples, and a smoke absorption meter consisting of a radiometer viewing an optically-chopped, 725 C blackbody oven. Both narrow-angle radiometers utilize an optically chopped beam, amplifiers "locked-in" to the chopping frequency and right angle mirrors for viewing the layer with a horizontal radiometer axis. Calibration of the radiometers is performed with right angle mirrors installed. In addition, a thermocouple and a water-cooled Gardon-type heat flux gage are mounted flush with the surface of the inert ceiling in order to obtain surface temperature and total heat flux to the ceiling respectively. With combustible ceilings, the surface thermocouple is not used. Instead, a (180°) wide angle, radiant flux measurement is made by an upward facing Gardon gage at the center of the channel, 0.763 m below the ceiling surface.

Gas temperature distributions are obtained from thermocouples at the main measurement station and at three other locations. Radiation errors are minimized by use of 0.127 mm dia chromel-alumel wire and by thermocouple bead sizes which are less than twice the wire dimension. Conduction errors are also minimized by keeping thermocouple wires coincident with expected isotherms.

TABLE 1.-DESCRIPTION OF CEILING MATERIALS

Ceiling Material	Material Composition	Material Thickness
Inert	"Cotronics" type 360 ceramic board	50.8 mm: $p/p_o = 1.0$
		12.7 mm: $p/p_o = 11.2$
		6.35 mm: $p/p_o = 21.4$
		and $p/p_o = 31.6$
PMMA	Polymethyl methacrylate cast sheet ("Plexiglas" type G)	31.75 mm: $p/p_o = 1.0$
		6.35 mm: $p/p_o = 11.2$
		3.18 mm: $p/p_o = 21.4$
		and $p/p_o = 31.6$
No. B8811	Honeycomb Composite (solid face 0.64 mm thick)	6.99 mm overall
No. 223	Honeycomb Composite (perforated face, 0.38 mm thick, melts and sags, expos- ing honeycomb during fire spread)	12.45 mm overall
No. 234	Fiberglass Reinforced polyester (rigid solid sheet)	2.03 mm

TABLE 2.-MEASUREMENT INSTRUMENTS FOR FULL-SCALE TESTS

Instrument I.D.	Description
B1	Radiometer, 1.3° total view angle of smoke layer, optically chopped, orifice 0.23 m below* ceiling, sensor 0.79 m from ceiling (also used for pressure modeling measurements).
B2	Radiometer, 25.4 mm diameter parallel beam from smoke layer, optically chopped, orifice 0.23 m below ceiling. Uses nitrogen purged, right angle mirror.
C3	Smoke Absorption Radiometer. 25.4 mm diameter parallel beam views optically chopped radiation from 725°C oven, optical axis 70 mm below ceiling, 300 mm path length for smoke absorption. Nitrogen purged, honeycomb view ports define absorption path length.
D4	Gardon-type, Total Heat Flux Gauge, 180° view angle, 0-10 W/cm ² range, flush with surface of inert ceiling (facing down), 0.763 m below aircraft and PMMA ceilings (facing ceiling).
D5	Gardon-type Radiometer, 0-10 W/cm ² range, Nitrogen-purged Irtran II window, 90° total view angle of smoke layer, 0.61 m below ceiling.
A6	Thermocouple in smoke layer, 30 mm below ceiling
A7	Thermocouple in smoke layer, 63 mm below ceiling
A8	Thermocouple in smoke layer, 130 mm below ceiling
A9	Thermocouple in smoke layer, 191 mm below ceiling
A10	Thermocouple in smoke layer, 225 mm below ceiling
A11	Thermocouple in smoke layer, 70 mm below ceiling
A12	Thermocouple in smoke layer, 64 mm below ceiling
A13	Thermocouple on back surface, center of PMMA wall
A14	Thermocouple on surface of inert ceiling.

* Increase all below-ceiling distances by 25 mm (see Figure 2) for Test 7-9-80.
All instrumentation is mounted nearly equidistant from the two channel side-walls.

The flame spread process on the vertical PMMA wall and under the ceiling is photographed with two 35 mm cameras. One camera, located behind the transparent PMMA wall, views the advance up the wall of flame followed by the onset of surface bubbles which characterize the beginning of fuel pyrolysis. A clear view of this pyrolysis front and the upward spread process is obtained from behind the wall if the camera is in darkness and an illuminated white surface in front of the wall is used as a background. The second camera, which is motorized and equipped with a 250-exposure-capacity film back, views the ceiling from the side of the channel structure through a long, back surface mirror set at a shallow angle (about 25° to the horizontal) on the laboratory floor. Because the mirror has roughly the same dimensions as the ceiling, the side camera records flame lengths and position along the entire ceiling surface and on much of the upper portion of the vertical PMMA wall. A digital clock and a length grid appear in each camera view to facilitate data reduction and synchronization of photographs with all other measurements.

The entire full-scale ceiling channel is located under a large-capacity, water-cooled combustion hood. During the initial stages of the test, when upward fire spread on the PMMA wall is in progress, combustion products exit the end of the channel and flow up to the hood exhaust duct by natural convection. A fan in the hood exhaust duct is activated once the capacity of the hood is taxed by the volume of combustion products. This generally occurs well after flame impingement on the ceiling material.

2.1.4 MODEL TESTS. Experiments with geometrically scaled models of the full-scale ceiling channel are performed at elevated air pressures of 11.2, 21.4 and 31.6 atmospheres. These experiments are initiated in a facility consisting of a pressure vessel of 1.22 m inside diameter and 2.7 m^3 volume. Combustion products are well above the model ceiling channel for all experiments due to stratification and an adequate vessel interior volume. Further details about the pressure vessel and the remainder of the facility at the Factory Mutual Research Corporation (FMRC) may be found in reference 16.

The configuration and composition of the wall and ceiling channel shown in Figures 1 and 2 are also used for the model experiments. All full-scale dimensions given in Figures 1 and 2 are reduced by the factor, $(p/p_0)^{-2/3}$, where p is absolute air pressure and p_0 the reference, atmospheric pressure. One exception to this scaling rule is the thickness of the three aircraft material ceilings. Changing the thickness of complex, composite materials is generally not possible without total refabrication. As a result, the normal, full-scale aircraft material thickness is employed at all test pressures. However, the thickness of the inert and PMMA ceilings is scaled roughly as the required $p^{-2/3}$. Both these ceilings are thermally thick for the duration of the fire so that the exact ceiling thickness is unimportant.

Another exception to the geometric scaling at elevated pressures is the ignition mode shown in Figures 1 and 2. For all experiments at elevated pressure, a small wooden toothpick is used to ignite the PMMA wall, instead of a

scaled, PMMA rod. The energy applied by the burning toothpick or PMMA rod to the PMMA wall at all scales is probably close to the minimum amount needed for initiation of upward fire spread.

Instrumentation for the model experiments is necessarily limited by the space available in the vessel and the elevated pressure environment. As in the full-scale experiments, the flame position under the ceiling and the radiance of the bottom of the ceiling smoke layer are measured during the elevated pressure tests. In addition, the total mass loss rate of the combined wall-ceiling configuration is measured continuously by a load transducer coupled to the platform on which the ceiling channel is mounted.

The radiometer used to measure the radiance of the ceiling flames and ceiling surface for the pressure vessel experiments is fully described in reference 1. This instrument, which is also used for the full-scale tests, views the ceiling through a first surface, right-angle mirror. Although soot from the burning ceiling can be deposited on the mirror during a given experiment, cleaning of the mirror with acetone and cotton after each test prevents significant buildup of residue. Calibration of the radiometer-mirror system with a blackbody oven has shown that such mirror cleaning does not adversely affect infrared reflectivity.

Flame position under the model ceilings is obtained by a motorized 35 mm camera viewing the ceiling through a pressure vessel window and a long back surface mirror set at a shallow angle on the load platform. Because of limited space under the model ceiling, the viewing mirror only extends from the PMMA wall to near the right-angle mirror of the radiometer. Flame position measurements are thus limited to about 2/3 the total channel length, except that the existence of flame at the end of the channel can be viewed directly by the camera for the two smallest model structures used at 21.4 and 31.6 atmospheres.

2.2 EXPERIMENTAL RESULTS: FULL-SCALE TESTS

Measurements from all seven full-scale tests are tabulated in the Appendix, generally as a function of time (in seconds) after ignition of the PMMA wall. The tabulated measurements can be used in conjunction with the schematics of Figures 1 and 2 and with the instrument descriptions in Table 2.

2.2.1 UPWARD FLAME SPREAD ON PMMA WALL. Measurements of flame height and pyrolysis height above the ignition point on the PMMA wall are given in Tables A-1 and A-2. These data represent the results of two separate experiments with an inert ceiling on the channel. Although the flame and pyrolysis fronts reach the top of the PMMA wall in about 750 and 900 s, respectively, the tear-shaped flame zone does not occupy the full, 0.305 m width of the PMMA wall at any height until roughly 1500 s after ignition.

A least squares, exponential regression fit to the upward spread data yields consistent, pyrolysis height growth factors for the two experiments but

significantly different flame height growth factors. The inconsistency in the latter case is likely due to rapid flame height fluctuations and the indistinct nature of the flame tip in photographs. In both cases, results compare favorably with measurements made in the previous study¹ for a 1.83 m high PMMA wall in the open: average exponential growth factors for pyrolysis and flame heights of 0.0027 s^{-1} and 0.0026 s^{-1} , respectively, in the present study and 0.0024 s^{-1} and 0.0023 s^{-1} in the previous¹ study. The somewhat higher growth factors for a PMMA wall beneath a ceiling channel could be due to radiative feedback from the ceiling, heated by combustion products in the channel flow.

2.2.2 MASS LOSS RATE OF PMMA WALL. An average mass loss rate per unit area of the burning PMMA wall is obtained from the known burning time at a given wall height (the extinguishment time after ignition minus the pyrolysis spread time to that height minus an 80 s transient (see reference 15) before quasi-steady burning), from the weight of burned wall segments cut along the vertical wall centerline after the test, and from the initial wall thickness. The resultant, centerline fuel mass flux is given in Table A-3 for the two experiments with an inert ceiling on the channel. As expected, average fuel mass flux is much higher for the longer duration test because of the gradual buildup of thermal radiation to the wall from both the channel hot gas layer and the channel ceiling. Thermal radiation from the ceiling channel is also the reason that the mass fluxes above a 0.6 m height for the shorter duration test are about 25% higher and for the longer duration test about 45% higher than those measured by Orloff et al¹⁵ for a PMMA wall in the open. Below a 0.6 m wall height, fuel mass flux for the shorter duration test is about the same as that given in reference 15 but, for the longer duration test, about 24% higher than the reference 15 values.

2.2.3 CEILING FIRE GROWTH. The extent of flames under each tested ceiling of the channel structure is given in Figure 3. Flame lengths, also listed in Tables A-4 to A-9, refer to the horizontal distance between the inert section of the channel end wall (above the PMMA) and the average position of the flame tip. Segments of flame which are detached from the main body of visible flame are disregarded in making the flame length determination.

2.2.3.1 Inert Ceiling. With an inert, ceramic board ceiling on the channel, flames from the PMMA wall fire gradually increase in length under the ceiling due to lateral fire spread on the PMMA wall. Such spread is essentially complete by 25 minutes after ignition, when flames extend out 30-40 cm along the ceiling. Subsequent flame lengthening to about 1 m some 42 minutes after ignition (see Figure 3) is due to the gradual increase in temperature of the ceiling surface, with a consequent increase in radiative flux to the wall fire. This thermal radiation feedback from the ceiling surface and ceiling layer gases leads to higher wall burning rates and greater flame lengths as shown in Section 3.3.3. Although flame lengths are still increasing at 44 minutes after ignition due to this coupling of the wall fire with ceiling-induced thermal radiation, data on ceiling layer radiative properties in Table A-11 indicate that a quasi-steady condition has been achieved.

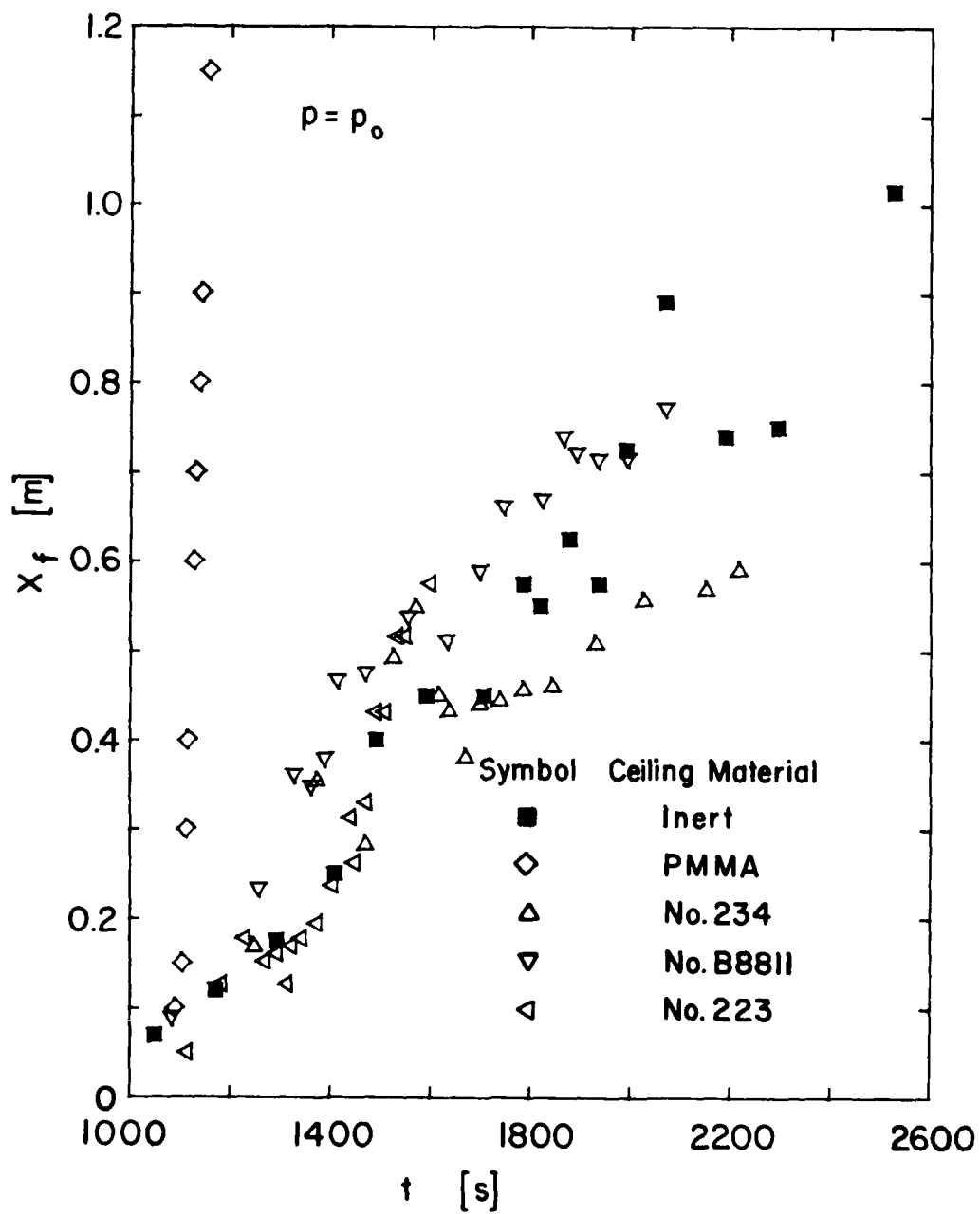


FIGURE 3 FLAME LENGTHS UNDER FULL-SCALE CEILINGS

During fire development, the white, ceramic board side-walls of the 2.4 m long ceiling channel are blackened wherever there is contact with hot combustion products or flame. Such markings clearly indicate a characteristic thickness of the hot gas layer in the channel. Measurements of the blackened zone dimensions on the channel side walls after the tests with an inert ceiling show layer thickness to be a nearly constant 178 mm from near the inert end wall (above the PMMA) to within 610 mm of the outflow end of the channel. Closer to the channel outflow end, these measurements show the layer thickness decreasing as follows:

Distance from End [mm]	Layer Thickness [mm]
610	178
305	154
178	132
0	88

2.2.3.2 Aircraft Material No. 234. This ceiling consists of five curved panels of fiberglass-reinforced polyester, oriented as shown in the Figure 2 schematic. No backing or insulation is applied to the panels. The horizontal width of the ceiling exposed to flame is maintained at the normal 460 mm through the use of ceramic sealants and gaskets which are also used to close any gaps between adjacent panels. Maximum ceiling height above the top of the PMMA wall is 25 mm greater than that for the other ceilings, due to the panel curvature.

During fire impingement on the ceiling panels, pyrolysis products are observed above the ceiling, presumably from decomposition of the ceiling material. This ceiling vaporization is obvious by 18.5 minutes after ignition and by 20 minutes after ignition, decomposition has resulted in buckling of the ceiling panel closest to the PMMA wall fire. However, flame spread due to ceiling combustion is not evident. As shown in Figure 3, flame lengths at equivalent times are comparable to those for the inert ceiling. There is some shortening of flames, in fact, due to the slightly increased ceiling height of the curved panels.

2.2.3.3 Aircraft Material No. B8811. This flat ceiling consists of a solid-faced, honeycomb composite. No backing or insulation is applied above the ceiling. Ceramic paste seals the single joint between panels, about 2 m from the wall fire. As a result of fire impingement, the ceiling blackens and blisters significantly but there is no flame spread due to ceiling combustion. Nearly the entire length of the ceiling is blackened and blistered by about 22 to 25 minutes after ignition, while flaming combustion extends only 35 to 45 cm out from the end wall. At later times, flame lengths under the B8811 ceiling are about the same as for the inert ceiling (see Figure 3).

2.2.3.4 Aircraft Material No. 224. Hot combustion products from the PMMA wall fire cause tearing and separation of the perforated face of this material from the underlying honeycomb. By 18 minutes after ignition, when wall fire flames are just impinging on the ceiling, the perforated face is torn across the full

width of the channel for a distance of 61 cm from the end wall and blisters in the face material appear for a distance of 116 cm. Separation of the face material from the honeycomb occurs over the entire, 2.4 m ceiling length by about 24 minutes after ignition, when flame length is only some 30 cm. However, flame spread due to ceiling combustion does not occur for this ceiling material. Flame lengths under the ceiling are roughly the same as for the other flat aircraft materials or for the inert ceiling (see Figure 3).

2.2.3.5 PMMA Ceiling. The flame spread process under a PMMA ceiling, with the usual, PMMA wall fire initiation, is described by measured flame lengths provided in Table A-9 as a function of time after ignition. It is evident from Table A-9 that about 18.4 minutes after ignition, self-sustained flame spread begins to occur over the PMMA ceiling surface. Flame lengths then grow almost linearly with time (see Figure 3) at a rate of about 1.95 cm/s (regression coefficient of 0.92) until flame reaches the outlet-end of the channel less than 20 minutes after ignition. During this spread process, a leading portion of flame appears to be quite thin, with detached, weakly luminous flamelets well downstream from this thin flame region. Upstream of the thin flame region, cellular combustion takes place, resulting in a much thicker flame zone. This cellular flame reaches the outlet-end of the channel 7 to 12 s after the arrival of the leading portion of flame. A cellular flame zone then fills the entire ceiling channel. Spillage of some flame from below the 0.23 m deep side-walls of the channel necessitates fire extinguishment about 21 minutes after ignition.

It was found that during the 164 s period from the onset of ceiling combustion (as evidenced by increased flame length compared to the inert case) until fire extinguishment, the ceiling pyrolysis zone propagated a distance of only 115 cm from the end wall. The average pyrolysis zone spread rate during this interval was thus about 0.7 cm/s, compared to a flame spread rate of 1.95 cm/s. Clearly, there was significant flame extension beyond the pyrolysis zone for this case of ceiling fire spread.

The problem of fire spillage from the ceiling channel was solved for a final experiment with a steadily burning PMMA ceiling by the addition of a 0.152 m ceramic paper extension to the 0.23 m deep ceiling side-walls, as shown in Figure 2. During this experiment, the cellular flame zone was observed to be about 76 mm above the bottom edge of the ceramic paper, which coincided with the extent of ceramic paper blackening seen after the fire. Total flame zone thickness during the steady burning process was, thus, about 0.305 m.

2.2.4 TEMPERATURE AND RADIATION MEASUREMENTS. Data on ceiling and gas temperatures, thermal radiation and heat flux obtained during the full-scale tests appear in Tables A-10 through A-16. Measurements are provided as a function of time from ignition for thermocouples (prefix "A"), narrow angle radiometers (prefix "B"), an infrared absorption meter (prefix "C") and wide angle heat flux gages (prefix "D"). In Table A-16, the time-averaged values of instrument outputs are given for the period of steady burning. Further details on instrument locations appear in Table 2. Instruments which malfunction during an experiment are shown with invalid outputs deleted.

Examination of Table A-11 shows that the peak heat flux to the inert ceiling at a horizontal distance of 1.82 m from the PMMA exposure fire is about 2 W/cm² a little more than 43 minutes after ignition. This flux is reduced to about 1.2 W/cm² at 30 minutes after ignition. As shown in Table A-10, the ceiling heat flux gage (D4) is not initially zeroed for the first test but the corrected measured flux to the ceiling 30 minutes after ignition is in good agreement with that from the subsequent test.

2.3 EXPERIMENTAL RESULTS: MODEL TESTS

Results from the elevated pressure experiments are presented in Figures 4 through 18. These figures contain correlations of data on a given material for all pressures, including one atmosphere when relevant. Corrections for the test pressure are made in accordance with pressure modeling requirements^{1,2}, so that good correlation of data is an indication of modeling success. It should be noted, however, that the time origin for many elevated pressure experiments has been shifted to yield the best possible data correlation during the initial stages of ceiling fire spread.

2.3.1 CEILING FIRE SPREAD. Because all characteristic lengths are reduced as $(p/p_0)^{-2/3}$ and all characteristic solid phase burning times are reduced as $(p/p_0)^{-4/3}$ in the pressure modeling scheme,^{1,12} the quantities $x_f(p/p_0)^{2/3}$ and $t(p/p_0)^{4/3}$ should be independent of air pressure and result in correlation of data on ceiling flame length, x_f , at any absolute pressure, p (where p_0 is the ambient atmospheric pressure) as a function of time, t , after ignition. Figures 4 through 8 demonstrate this correlation technique for the five different ceiling materials. In Figures 4 and 8, the results from the full-scale experiments are seen to be in reasonable agreement with model results for the lowest air pressures of 11.2 and 21.4 atmospheres. A clear divergence from full-scale behavior is seen to occur, however, when the highest air pressure of 31.6 atmospheres is utilized in the model experiments.

The maximum value of $x_f(p/p_0)^{2/3}$ for complete fire spread to the end of the ceiling is 2.4 m, the length of the full-scale channel. This value is attained for all the elevated pressure, model experiments with PMMA as well as with the three aircraft materials. However, measurements of $x_f(p/p_0)^{2/3}$ are not always available at elevated pressure, due to obstruction of the camera mirrored field of view by a radiometer. This radiometer interference begins at $x_f(p/p_0)^{2/3}$ equal to about 1.8 m. In Figure 8, measurements of flame tip position at the end of the channel are shown for tests at 31.6 atmospheres. These data correspond to direct camera views of the beginning of flame outflow from the channel structure.

Use of the pressure modeling correction for the three aircraft materials, as shown in Figures 5, 6 and 7, results in a good correlation of model results for materials No. 223 and 234 but only a rough correlation for the B8811 material. It should be noted that complete flame spread over the full-scale aircraft ceilings does not occur. The complete flame spread over the model ceilings is

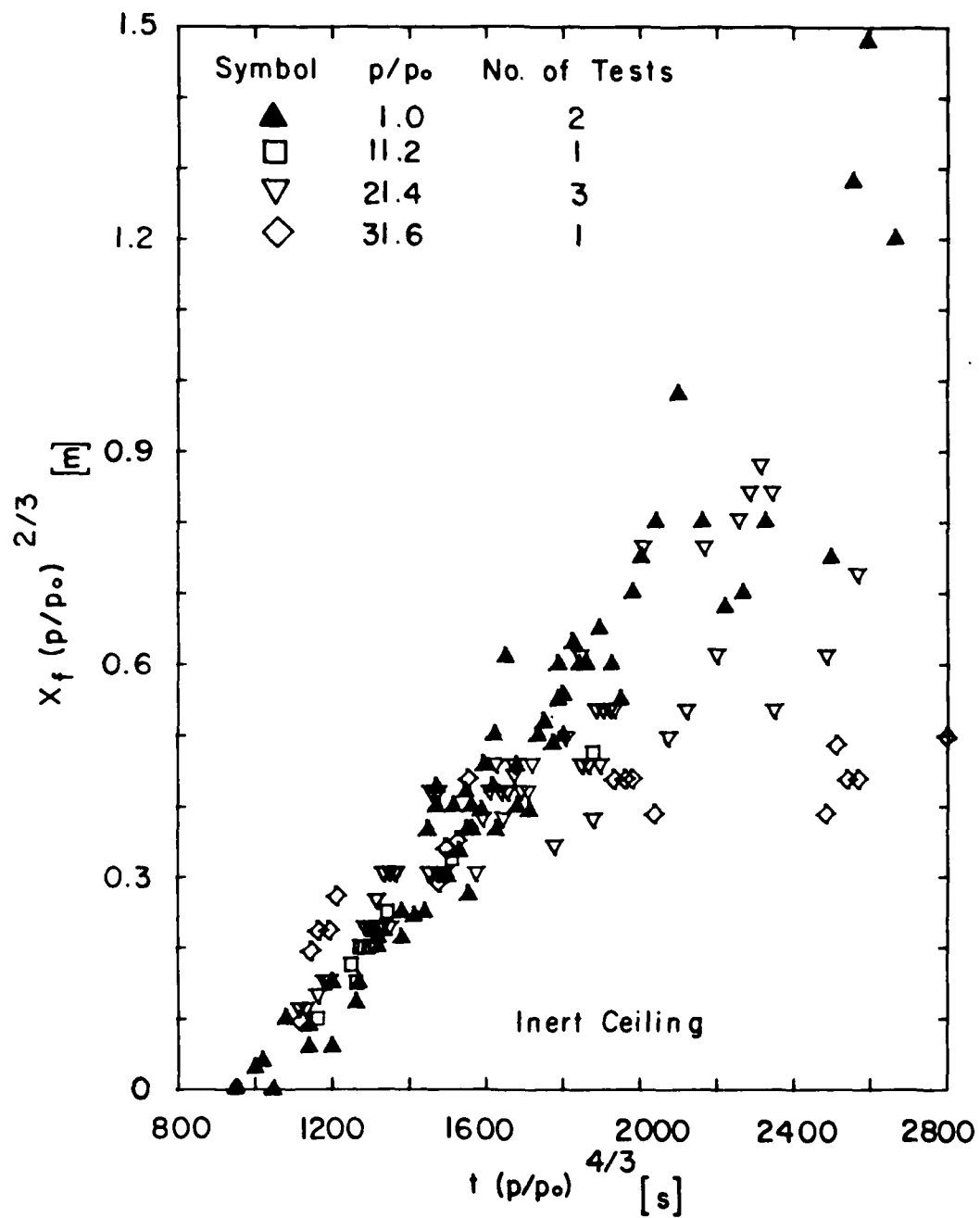


FIGURE 4 CORRELATION OF FLAME LENGTH UNDER INERT CEILINGS

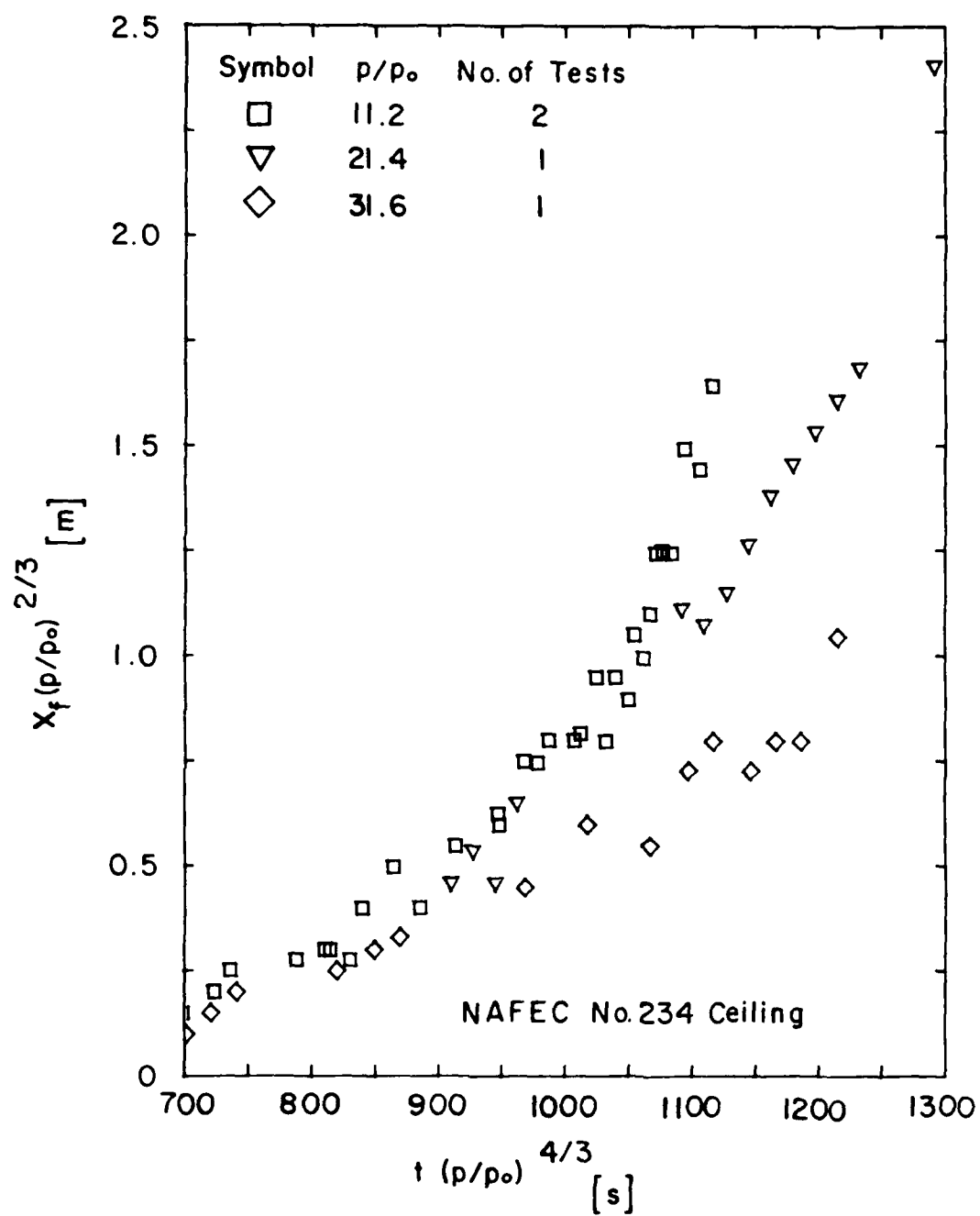


FIGURE 5 CORRELATION OF FLAME LENGTH UNDER NO. 234 MODEL CEILINGS

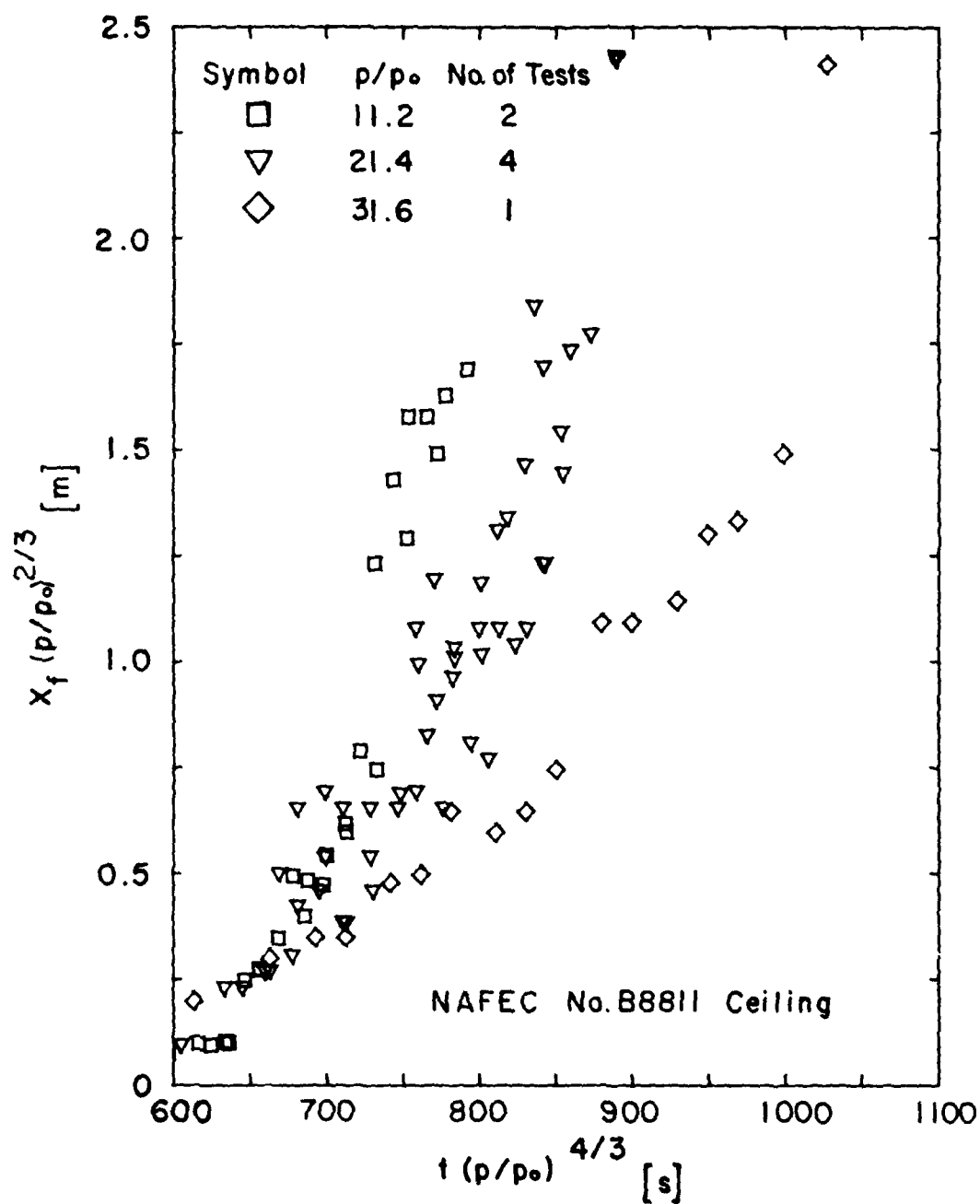


FIGURE 6 CORRELATION OF FLAME LENGTH UNDER NO. B8811 MODEL CEILINGS

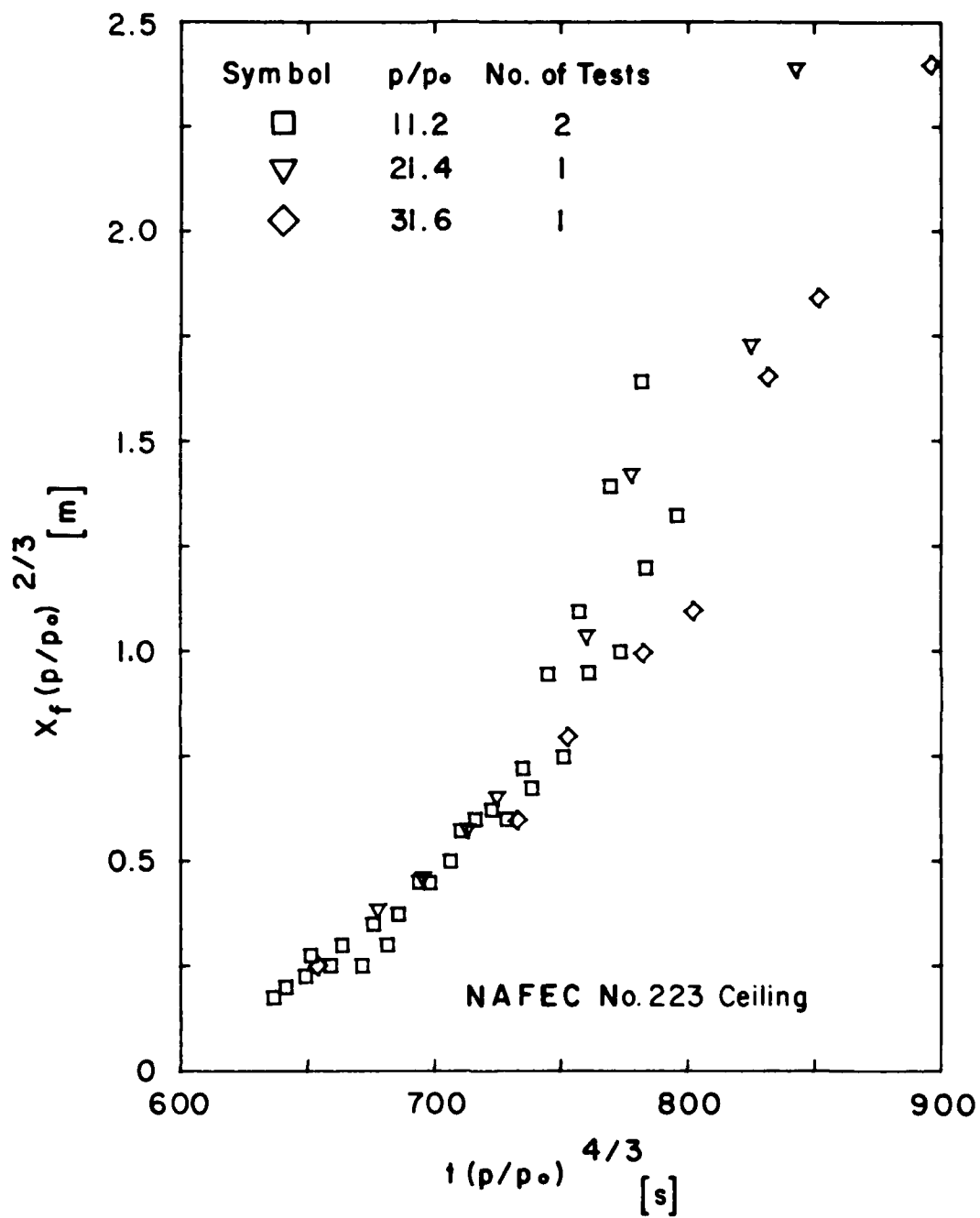


FIGURE 7 CORRELATION OF FLAME LENGTH UNDER NO. 223 MODEL CEILINGS

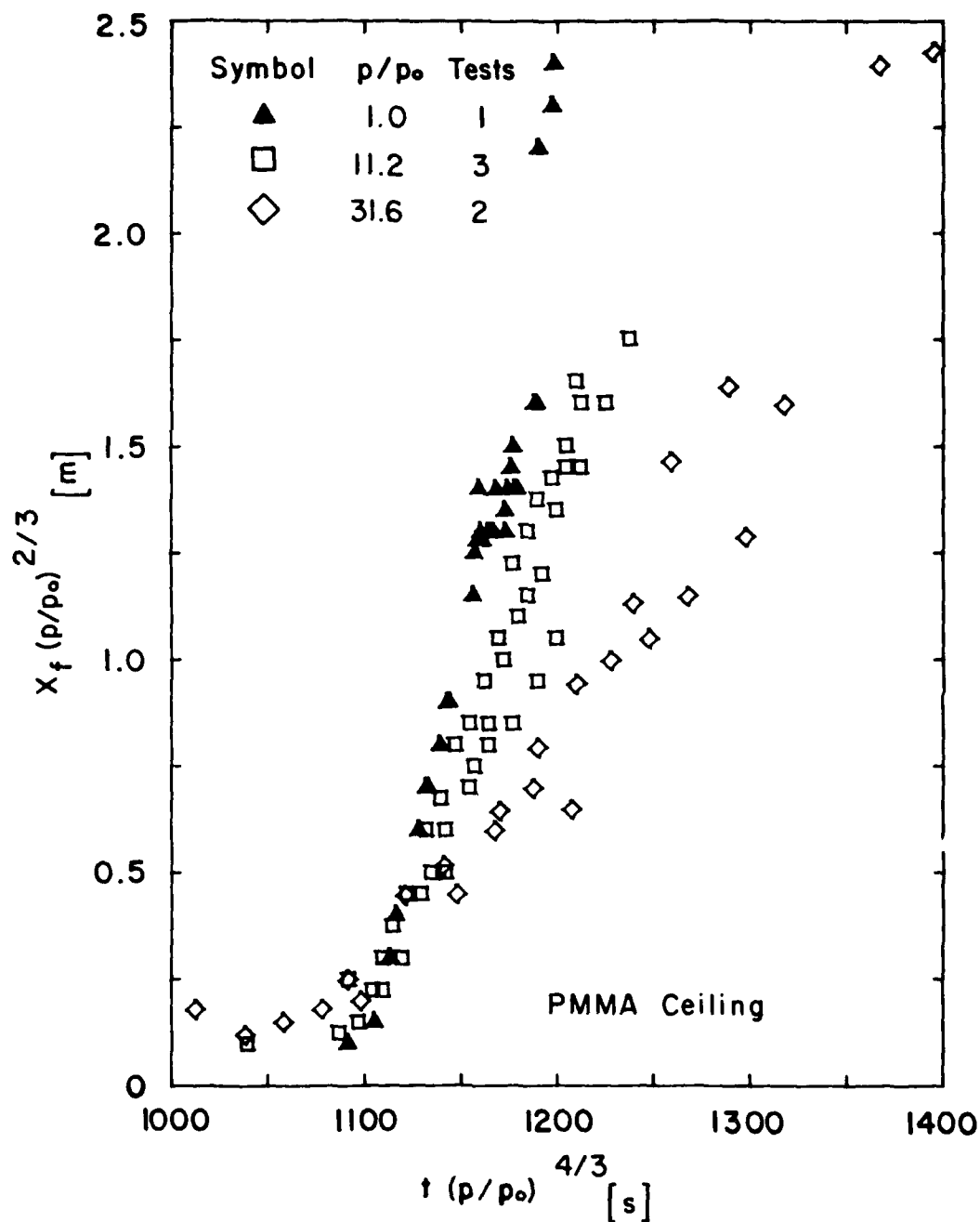


FIGURE 8 CORRELATION OF FLAME LENGTH UNDER PMMA CEILINGS

enhanced by the unimportance of radiative heat loss from hot char layers at elevated pressure and by the use of full-scale ceiling thickness in the models, which provides more fuel than required by the modeling scheme.

For aircraft material No. 223, complete flame spread at elevated pressure occurs only after the perforated surface layer melts and sags, allowing the underlying honeycomb to be exposed.

2.3.2 CEILING FIRE RADIANCE. As explained in references 1 and 12, the pressure modeling scheme results in the preservation of the product of convective heat flux and length-scale (proportional to Nusselt Number since gas temperatures are preserved). With all length scales proportional to $p^{-2/3}$, this means that the product, $p^{-2/3}$, times convective heat flux, should be independent of air pressure. All heat fluxes, whether convective or radiative, must be consistent with this requirement to insure complete modeling success. Since solid angles and geometric view factors are preserved when all length scales are reduced as $p^{-2/3}$, the radiance, N , of ceiling layer gas and ceiling surface should exhibit the same behavior as convective flux. As a result, $N(p/p_0)^{-2/3}$ should be independent of air pressure.

The pressure corrections derived above for radiance, N , as a function of time, t , from ignition are applied in Figures 9 through 13 to measurements for the five ceiling materials. Agreement with full-scale results is satisfactory for tests at 11.2 atmospheres with inert and PMMA ceilings. At higher ambient pressures for these two ceiling materials, there is clearly not good correlation with transient, one-atmosphere data.

Radiance measurements from model tests with inert ceilings at pressures of 21.4 and 31.6 atmospheres diverge from the one-atmosphere and 11.2-atmosphere results as the ceiling surface temperature increases with increasing test time. The radiance of the hot ceiling, which is nearly independent of pressure, dominates the radiometer output in the absence of flame or dense smoke. Pressure modeling of this ceiling surface radiance is not possible since $N(p/p_0)^{-2/3}$, not N , should be independent of pressure.

Table A-16 shows that the steady-state value of ceiling layer radiance for a full-scale test with a PMMA ceiling is $6.43 \text{ kW/m}^2\text{sr}$. Comparison of this full-scale measurement with the model results in Figure 13 indicates excellent agreement for test pressures of 11.2 and 21.4 atmospheres. For the steadily burning PMMA ceiling, success in modeling ceiling layer radiance is probably due to the dominant effect of flame radiation over ceiling surface radiation, although even flame radiation will cease to be modeled at a sufficiently high pressure. The measured radiance at 31.6 atmospheres does not, in fact, model the full-scale value, apparently due to radiant saturation of the flame, since the peak radiance at this pressure is identical to that at 21.4 atmospheres. A similar behavior characteristic of radiant saturation is exhibited by all the aircraft materials at 31.6 atmospheres (see Table 4 in Sec. 2.5).

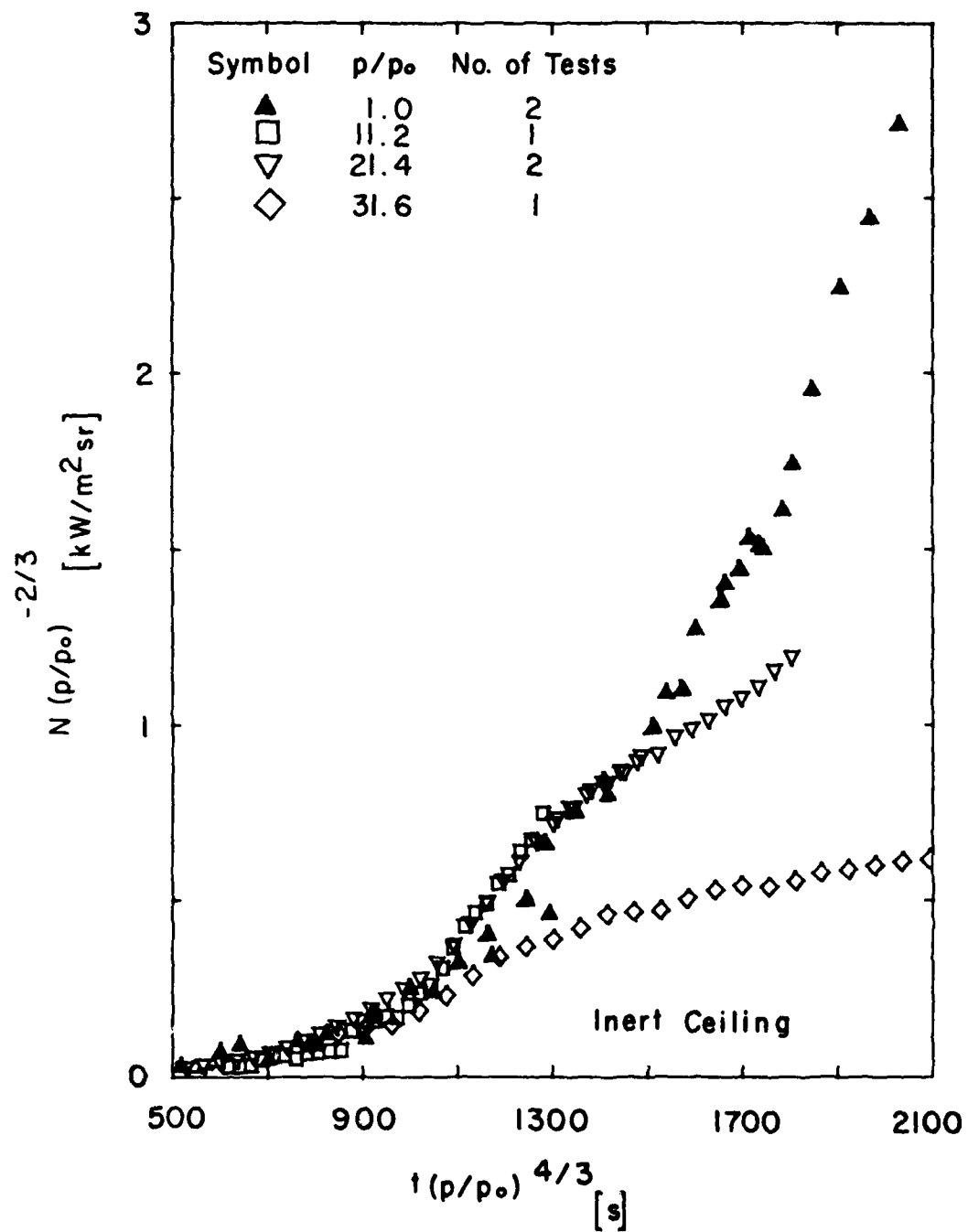


FIGURE 9 CORRELATION OF FLAME AND INERT CEILING RADIANCE

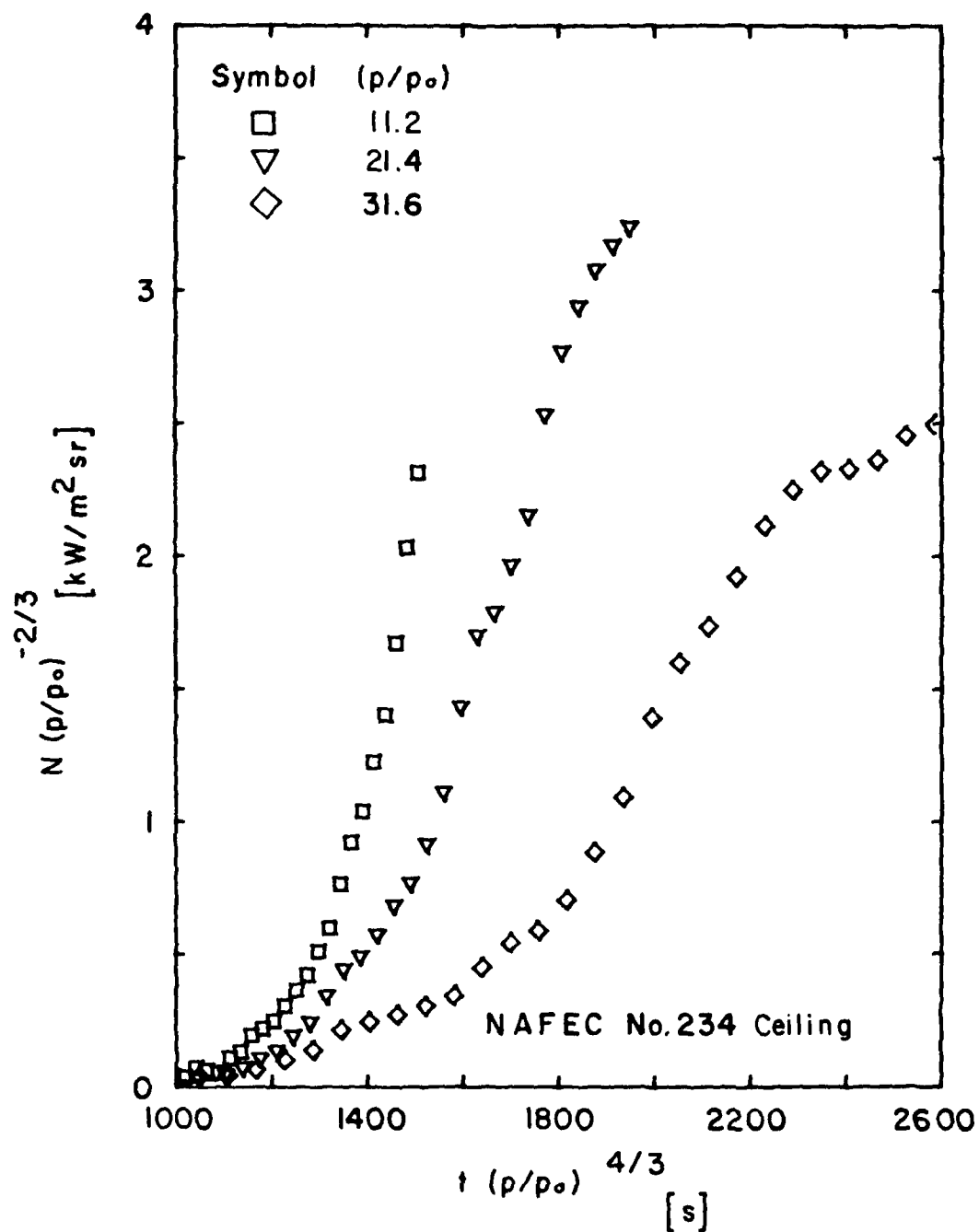


FIGURE 10 CORRELATION OF FLAME AND NO. 234 MODEL CEILING RADIANCE

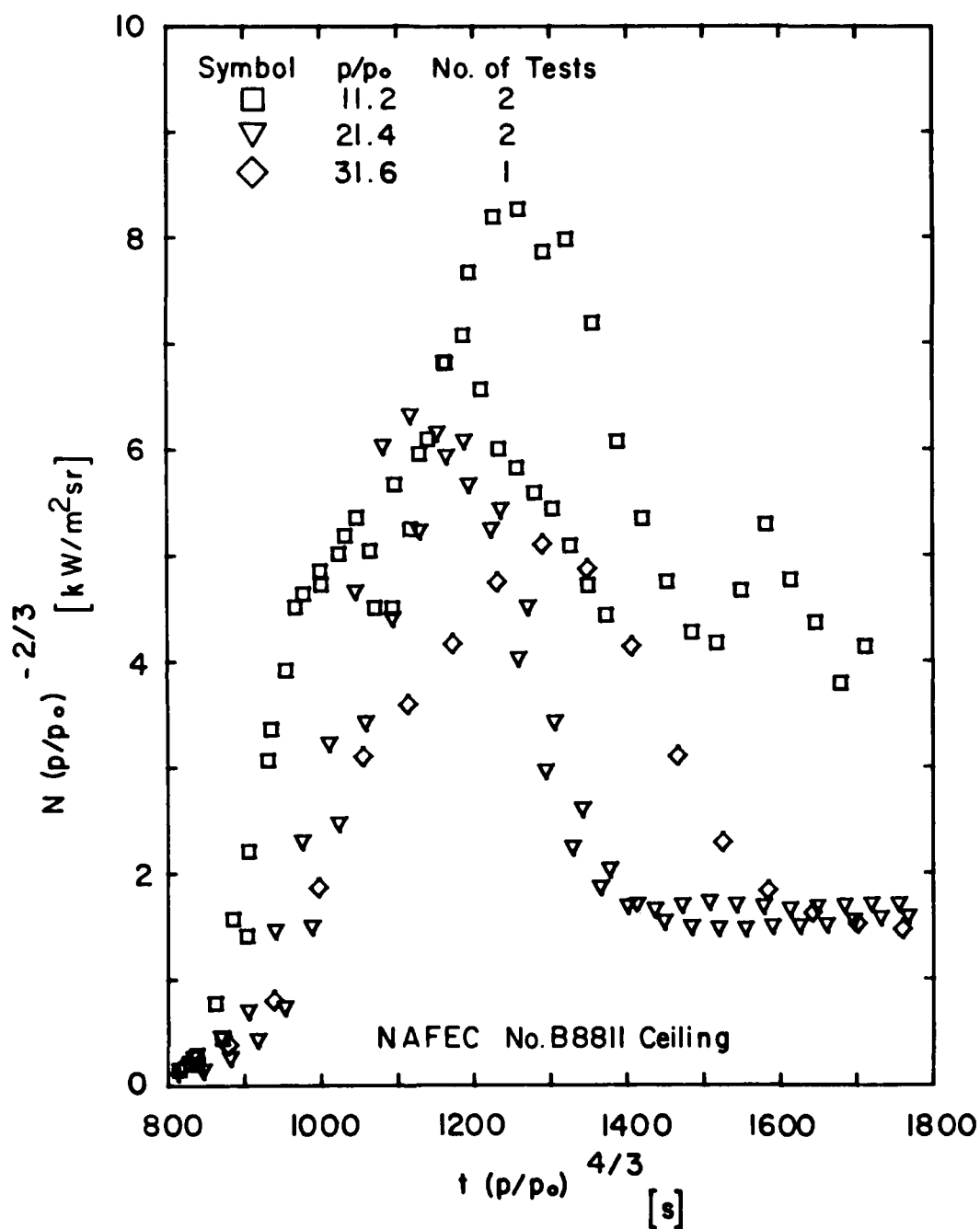


FIGURE 11 CORRELATION OF FLAME AND NO. B8811 MODEL CEILING RADIANCE

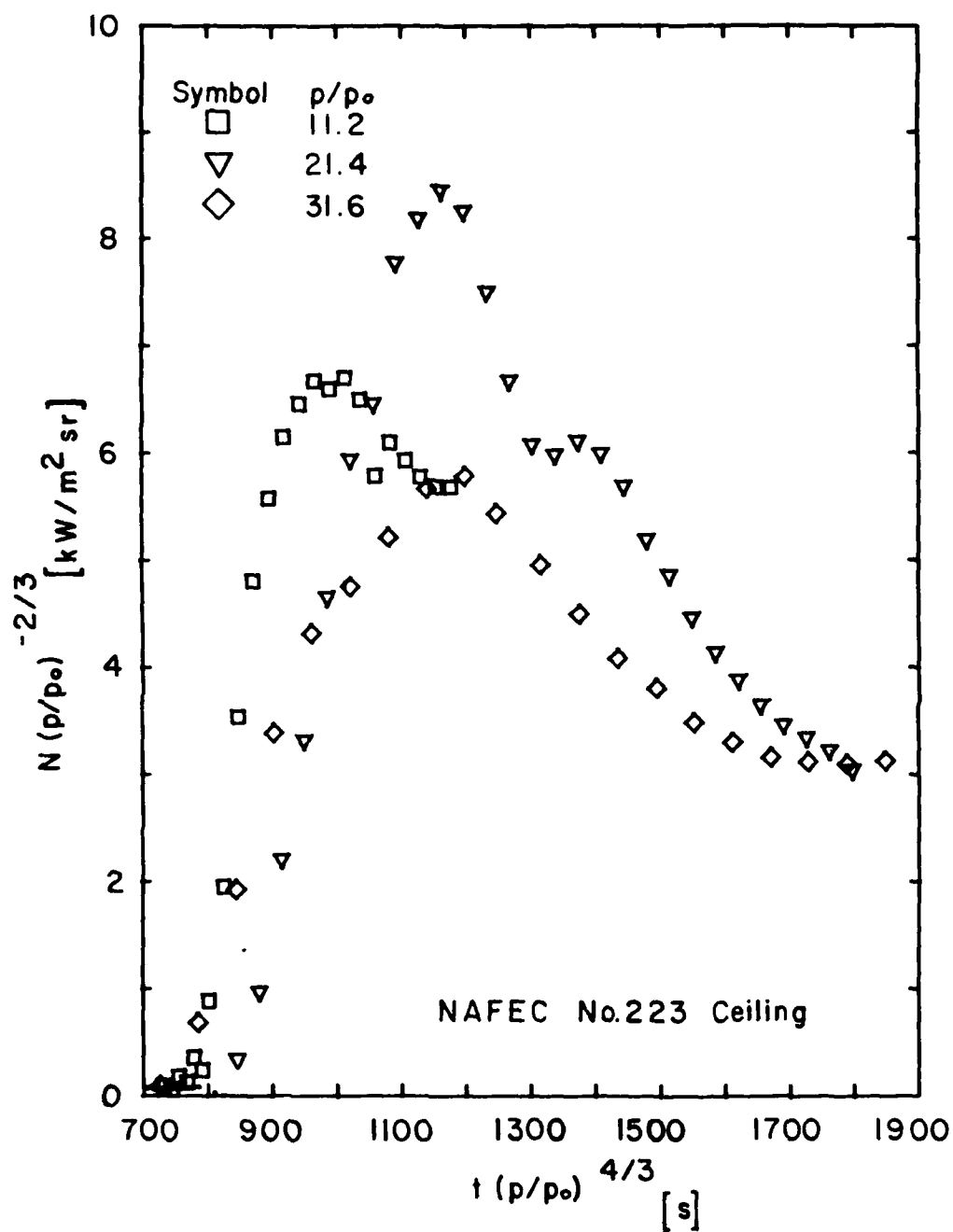


FIGURE 12 CORRELATION OF FLAME AND NO. 223 MODEL CEILING RADIANCE

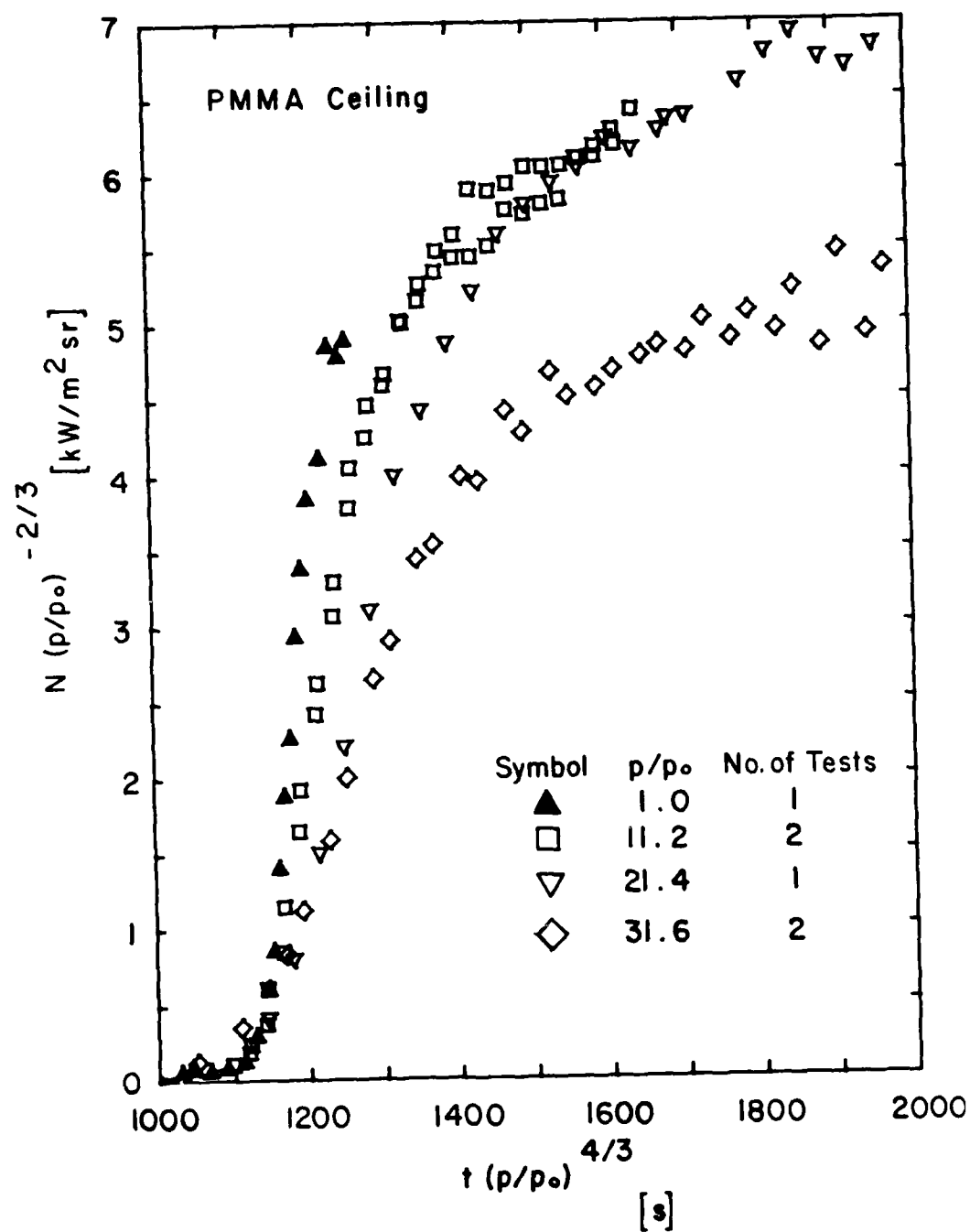


FIGURE 13 CORRELATION OF FLAME AND PMMA CEILING RADIANCE

Correlation of radiance measurements for the three aircraft materials is affected by three factors: 1) the lack of modeling of the flame spread process; 2) the use of a constant material thickness, which leads to an improperly modeled total fire duration; and 3) the limited radiometer response time of about 1.5-2 s. The last factor, which is also relevant for the PMMA ceiling, means that the increase in radiant output cannot be followed accurately during flame front transit at elevated pressure across the roughly 1.3 cm sensing area of the radiometer. Flame transit times at elevated pressures will typically be from 0.1 to 1.0 s.

2.3.3 WALL-CEILING BURNING RATE. By replacing the Nusselt Number with the Sherwood Number, it can be shown^{12,14} that the product of fuel mass flux and a characteristic length scale should be preserved by the pressure modeling scheme. With all length scales proportional to $p^{-2/3}$, the fuel mass flux will be proportional to $p^{4/3}$ times the total mass loss rate, \dot{m} . The product of fuel mass flux and length scale is then proportional to $\dot{m} p^{2/3}$, which should be independent of air pressure.

The pressure-corrected mass-loss rate, $\dot{m}(p/p_0)^{2/3}$, is shown in Figures 14 through 18 as a function of pressure-corrected time from ignition. Tests at all three elevated ambient pressures with each of the five ceiling materials are included. In these figures, \dot{m} represents the mass loss rate of both the channel end-wall and the ceiling, as obtained from a fourth order polynomial regression to the load-cell readings.

The mass loss rate (equal to burning rate in the absence of soot production) shown in Figure 14 corresponds to a measurement for the burning PMMA wall alone, since the ceiling is inert. Correlation of the mass loss rate data in Figure 14 leads to prediction of a steady, full-scale wall burning rate of 4-6 g/s at 1200-1600 s after ignition. Measured wall burning rates, given in Table A-3, of 1.44 to 2.55 g/s are far less than the above steady values predicted by modeling. However, a steady-state condition is not achieved until 2640 s at full scale and measurements correspond to only about 1/3 to 1/2 of this test time. At equivalent times in the model, full-scale burning rates are predicted to be 2 to 4 g/s.

Good correlation of data is obtained for the case of a PMMA ceiling in Figure 18. As noted previously, use of a constant thickness for the aircraft materials results in improper modeling of total fuel quantities, which affects the modeling of peak burning rates. For this reason, burning rates and fire durations at the highest ambient pressures are greater than expected, as shown in Figures 15-17.

2.4 ANALYSIS OF MODELING RESULTS

The significance of the preceding data correlations can be better understood by analyzing the dependence of flame heat transfer rates on ambient air pressure. Such an analysis will clarify the problems involved in pressure modeling ceiling flame spread and ceiling fire radiant heat loss.

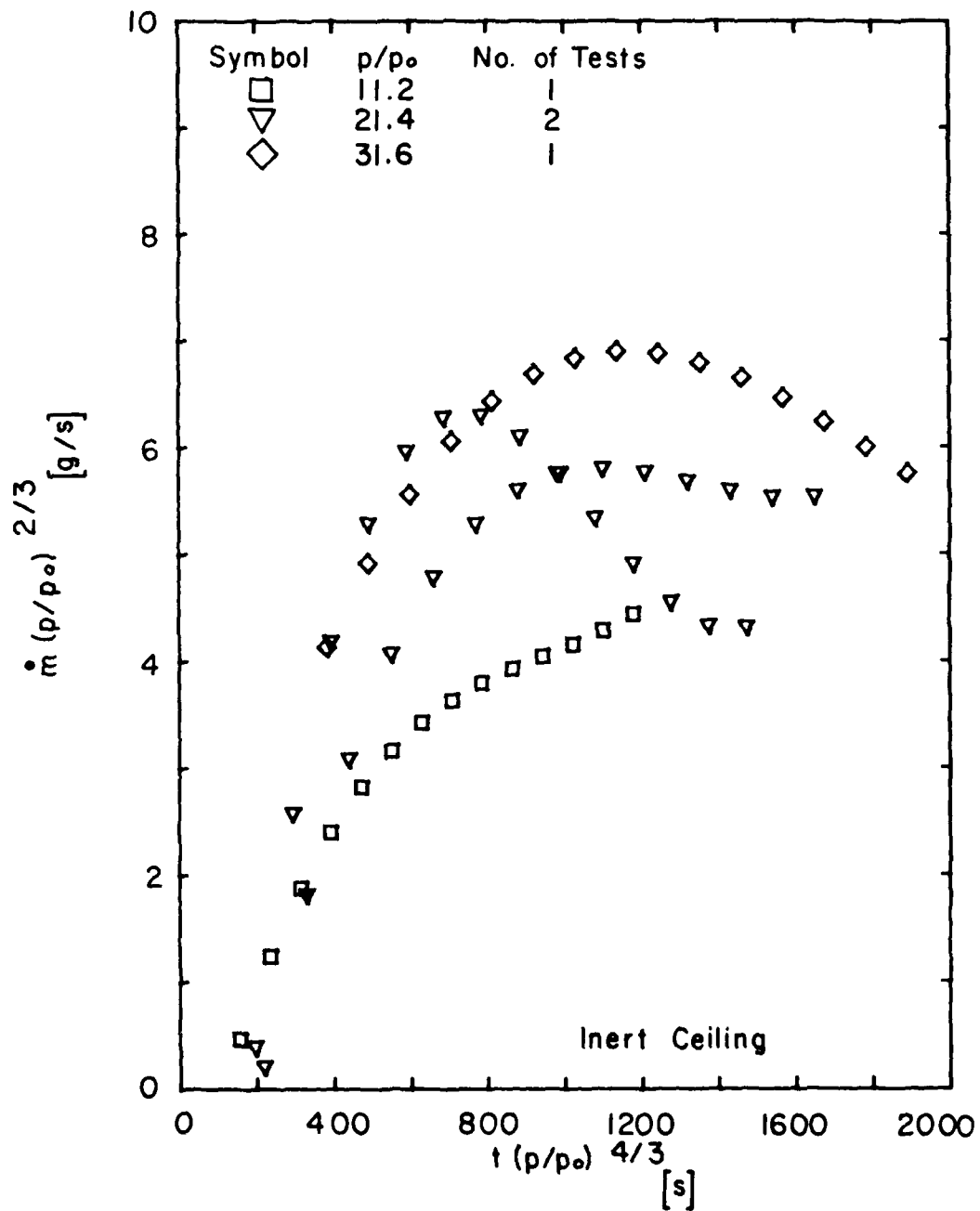


FIGURE 14 CORRELATION OF MASS LOSS RATE FOR INERT MODEL CEILINGS

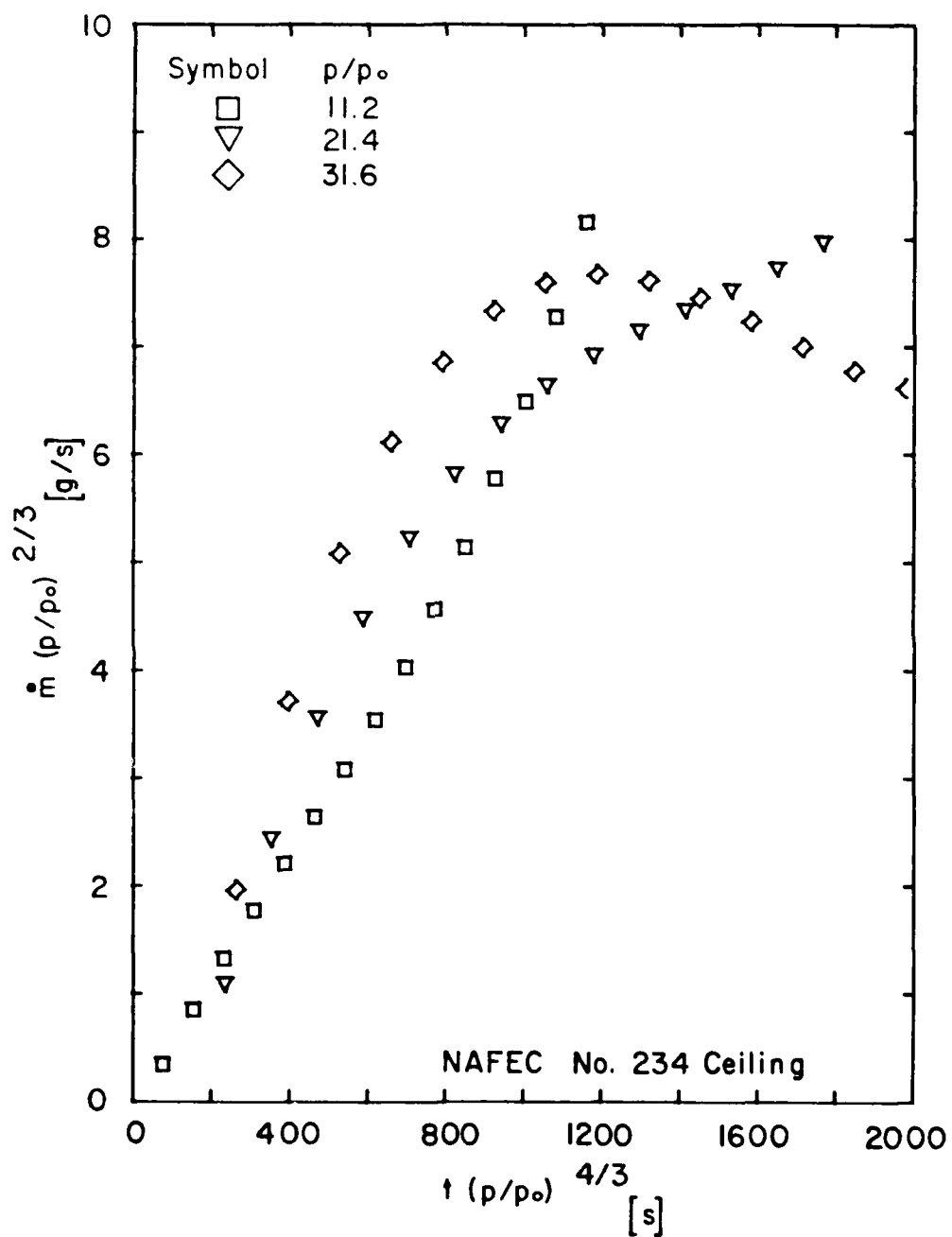


FIGURE 15 CORRELATION OF MASS LOSS RATE FOR NO. 234 MODEL CEILINGS

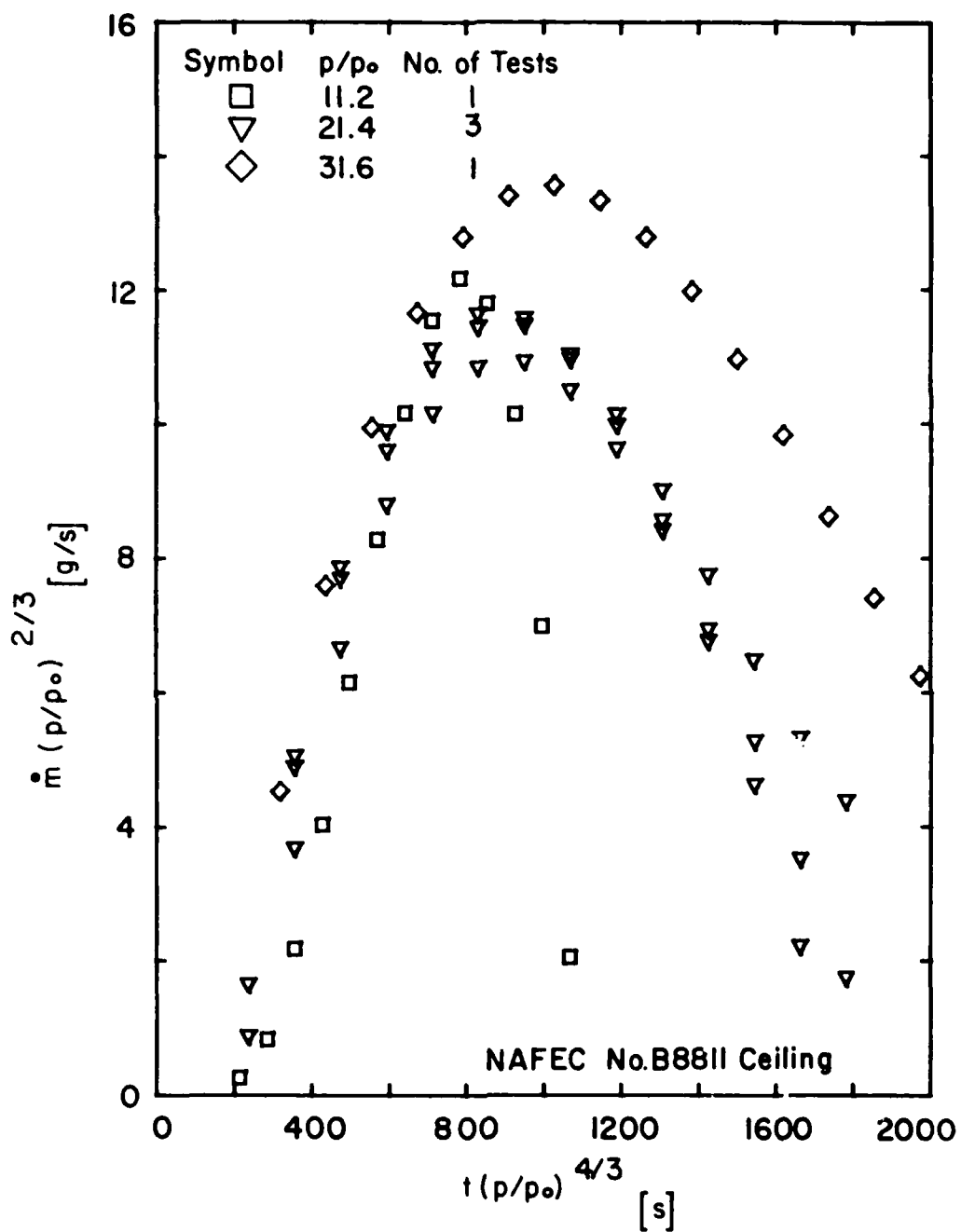


FIGURE 16 CORRELATION OF MASS LOSS RATE FOR NO. B8811 MODEL CEILINGS

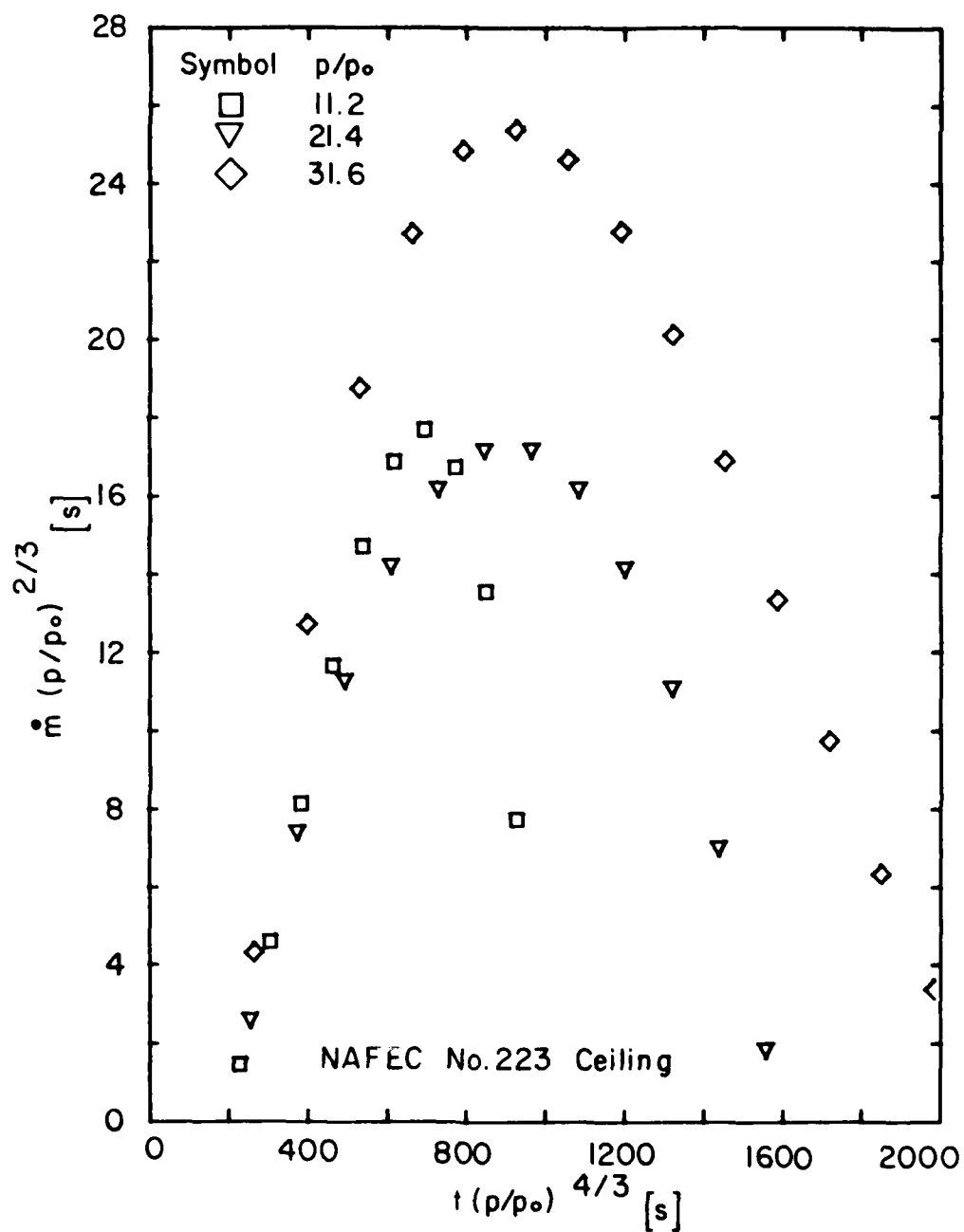


FIGURE 17 CORRELATION OF MASS LOSS RATE FOR NO. 223 MODEL CEILINGS

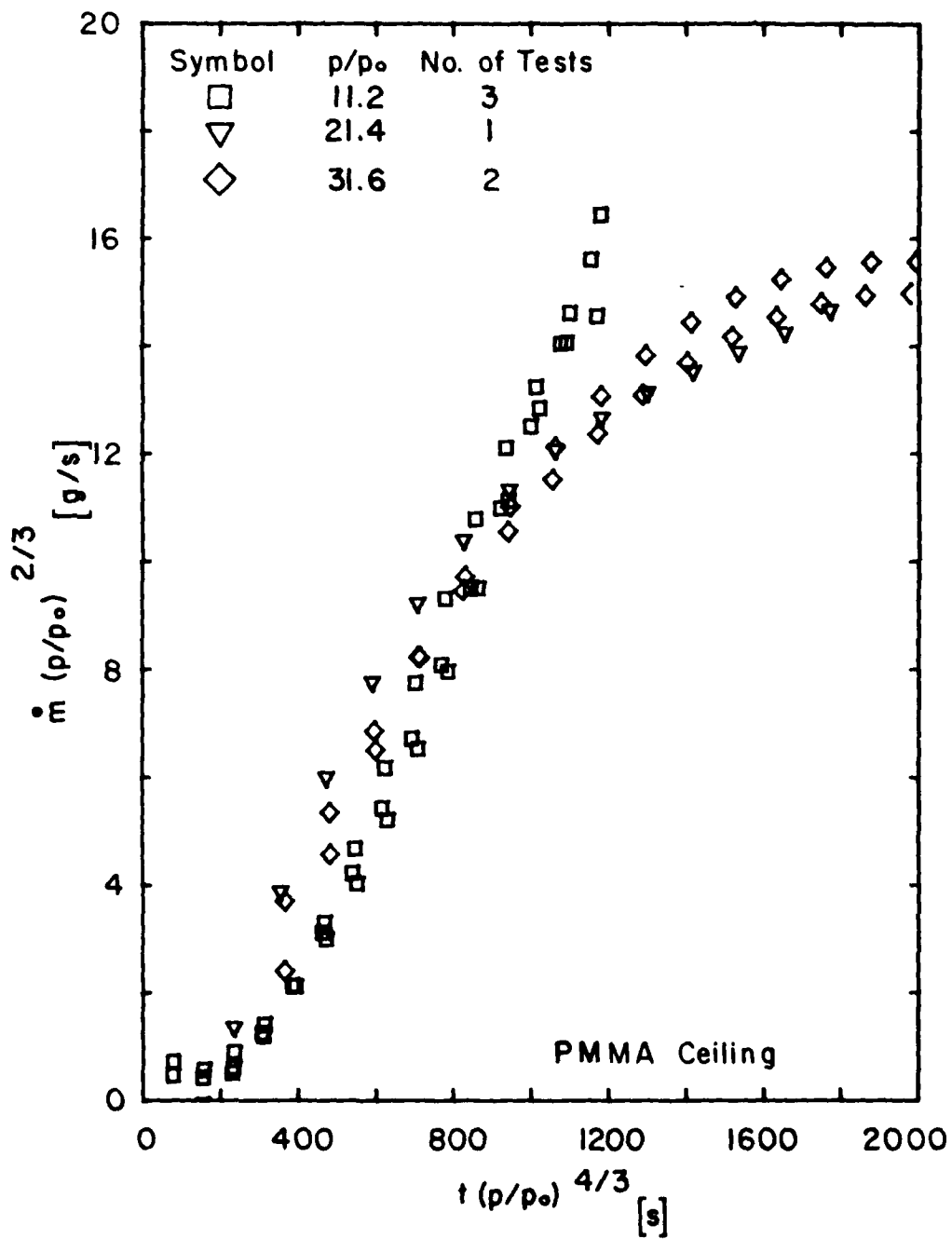


FIGURE 18 CORRELATION OF MASS LOSS RATE FOR PMMA MODEL CEILINGS

2.4.1 HEAT FLUX TO CEILING. The net heat flux, \dot{q}'' , to an inert or fuel ceiling is given by the following expression, previously derived by Orloff et al¹⁵ for the case of a steadily burning wall fire and used by Alpert¹ for the case of upward fire spread:

$$\dot{q}'' = \sigma T_g^4 [1 - \exp(-kL_m')] - \alpha \sigma T_s^4 + \dot{q}_c'' \quad (1)$$

where L_m' is the actual mean beam length at absolute pressure, p , and the remaining symbols are defined in the nomenclature. The constant, α , is taken to be 1.0 for steady burning and 0.5 for a spreading fire when T_s is the pyrolysis temperature of the ceiling material. During fire spread across the channel ceiling, the convective heat flux, \dot{q}_c'' , as well as the flame radiative properties are influenced by external factors such as the imposed flow from the PMMA wall fire, the conditions at the channel exit and by thermal radiation from the channel side-walls. These factors will be ignored here to simplify the analysis. Instead, conditions typical of PMMA wall fires will be assumed in order to obtain approximations for T_g , k and \dot{q}_c'' during the ceiling fire.

As shown in reference 17, gas temperature, T_g , is found to be preserved at elevated pressure while absorption coefficient, k , is found to increase in wall fires as the $4/3$ power of pressure. An increase in k at least proportional to pressure is expected if the ratio of fuel mass fraction converted to soot to the density of a soot particle is independent of pressure. Small increases in soot fraction with pressure could then give the result, $k = k_0(p/p_0)^{4/3}$. The convective heat flux in PMMA wall fires is found¹⁵ to be about 5.5 kW/m^2 at one atmosphere. It is assumed here that this flux is accurately pressure modeled, leading to the quantity, $\dot{q}_c'' p^{-2/3}$, being independent of ambient pressure. As a result, $\dot{q}_c'' \approx 5.5 (p/p_0)^{2/3} \text{ kW/m}^2$.

The radiation mean beam length, L_m' , in the ceiling channel, will be reduced as $p^{-2/3}$, together with all other length scales. This quantity can, therefore, be expressed as $L_m' = L_m (p/p_0)^{-2/3}$, where L_m is the mean beam length at one atmosphere.

With the preceding assumptions used in equation (1), the heat flux to the channel ceiling becomes:

$$\dot{q}'' = \sigma T_g^4 [1 - \exp(-k_0 L_m (p/p_0)^{2/3})] - \alpha \sigma T_s^4 + 5.5 (p/p_0)^{2/3} \quad (2)$$

2.4.2 FLAME SPREAD. The rate of flame spread under a combustibile ceiling should be inversely proportional to the time, Δt , required to heat the ceiling to its pyrolysis temperature, T_s , from an initial temperature of T_∞ . For a thermally thick fuel,

$$\Delta t \approx \rho C \lambda (T_s - T_\infty)^2 / \dot{q}''^2 \quad (3)$$

where $\rho C \lambda$ is the product of fuel density, specific heat and thermal conductivity and where \dot{q}''^2 is given by equation (1).

Thus, spread rates across thermally thick fuels are directly proportional to the square of the net heat flux to the fuel. The pressure dependence of this quantity is examined in Figure 19. In this figure, $\dot{q}''^2(p/p_o)^{-4/3}$ should be independent of ambient air pressure, according to the modeling scheme, and equal to the value, $\dot{q}_o''^2$, at one atmosphere, or full-scale. Clearly, such is not always the case. The variation of pressure-corrected heat flux is especially large for $k_o L_m$ greater than about 0.17.

An estimate of the mean beam length for a fire in the ceiling channel can be obtained from reference 18, where it is shown that

$$L_m \approx 1.75 Wd/(W+d) \quad (4)$$

In equation (4), W is the width of the flame volume (the channel width of 0.46 m) and d is the flame depth (at most the 0.23 m depth of the channel side-walls). The maximum value of L_m for a ceiling channel filled with flame is then, from equation (4), $L_m = 0.267$ m. If the flame absorption coefficient is typical of PMMA, then $k_o = 1.3$ to 1.5 m^{-1} from references 19 and 20. The resultant value for $k_o L_m$, about 0.4, is seen in Figure 19 to lead to significant errors in pressure modeling in the 20- to 30-atmosphere range, since the squared net heat flux to the ceiling after pressure correction will be only about 20% of that at one atmosphere. On the other hand, $k_o L_m$ at a 1 m elevation on a 0.3 m wide PMMA wall fire (flame thickness about 0.07 m) is only 0.13 to 0.15, leading to a pressure-corrected, squared net heat flux to the wall nearly 80% of the full-scale value. Pressure modeling of fire spread should, thus, be more successful for 1 m high walls than for ceilings in a long, channel configuration. This explains why correlation of fire spread data for a PMMA ceiling in Figure 8 is not as good as the correlations for PMMA wall fire spread in reference 1.

Figure 19 also shows that the occurrence of fuel charring, which tends to elevate surface temperatures, can result in squared heat fluxes to the fuel at 10 to 30 atmospheres which are much greater than those at one atmosphere, even after the appropriate pressure corrections are applied. These increased heat fluxes can explain why complete fire spread occurs for all aircraft ceilings at elevated pressures but not at one atmosphere. Such behavior is basically due to the fact that radiant heat loss from fuel surfaces at elevated pressure (but not at one atmosphere) is generally insignificant compared to flame radiative feedback to the fuel. This same insignificance of solid surface radiant heat loss at elevated pressures is probably responsible for the lack of modeling of flame lengths under the inert ceiling, as shown in Figure 4. It is radiant heating of the PMMA wall fire by the hot ceiling which causes the increases in flame length under the ceiling.

2.4.2 RADIANCE. The radiance, N , of both the hot gases in the ceiling channel and the ceiling surface itself along a ray normal to the ceiling is given by

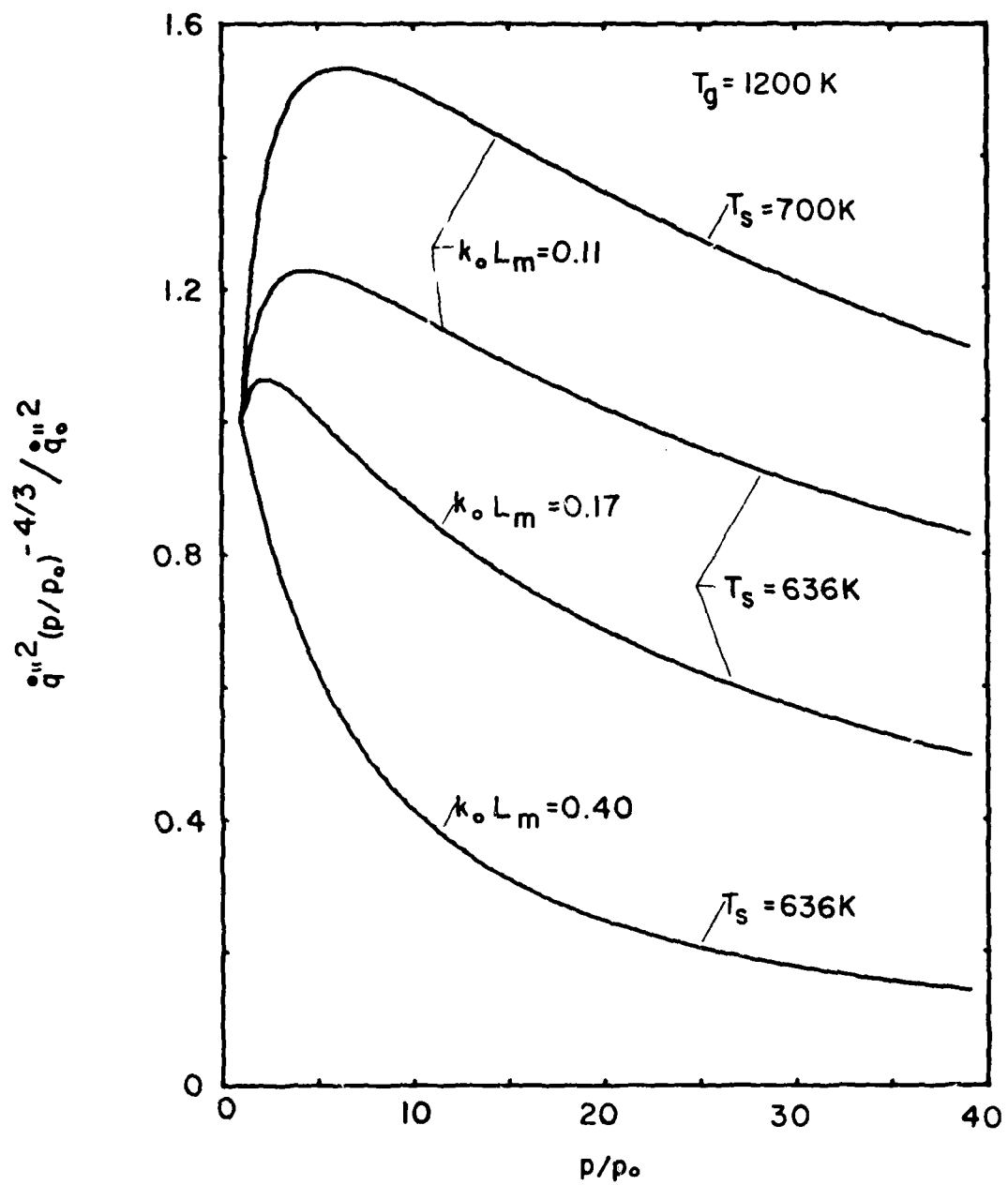


FIGURE 19 PREDICTED BEHAVIOR OF SQUARE OF NET HEAT FLUX TO THERMALLY THICK FUEL SURFACE.

the following expression:

$$N = \frac{\sigma T_g^4}{\pi} [1 - (1 - T_s^4/T_g^4) \exp(-kd')] \quad (5)$$

where d' is the actual depth of ceiling layer gases at any absolute pressure, p . Equation (5) is applicable to wall fires as well as ceiling fires. In terms of quantities at one atmosphere, or full-scale, equation (5) becomes:

$$N = \frac{\sigma T_g^4}{\pi} [1 - (1 - T_s^4/T_g^4) \exp(-k_0 d (p/p_0)^{2/3})] \quad (6)$$

As noted previously, the quantity, $N(p/p_0)^{-2/3}$, should be independent of air pressure in the modeling scheme. The plots of ceiling layer radiance in Figure 20, which are obtained from equation (6), show that this modeling condition is not satisfied, even after the pressure correction, $(p/p_0)^{-2/3}$ is applied. In this figure, $k_0 d = 0.076$ is typical of a 5 cm layer thickness or a 0.81 m elevation on a PMMA wall fire, while $k_0 d = 0.34$ is the maximum value expected for a PMMA ceiling above a 23 cm deep channel filled with flame.

Clearly, the radiance of either a burning wall or a burning ceiling at elevated pressure will be far less than the equivalent value at one atmosphere. On the basis of the plots in Figure 20, ceiling layer radiance measured at 10 to 30 atmospheres will be only 1/2 to 1/3 the respective values predicted by modeling theory for a given, full-scale radiance measurement. Such errors are reduced somewhat, as shown in Figure 20, if the radiance measurement is due mainly to the hot gas layer and not a hot ceiling surface. This effect can be seen in Figure 9, where radiance measurements obtained at elevated pressure diverge from the corresponding, full-scale values as the inert ceiling surface heats up and becomes an important factor in the ceiling layer radiance.

2.5 COMPARISON OF CEILING FIRE GROWTH

The data obtained at elevated pressures on flame length, radiance, and fuel mass loss for all five ceiling materials have been matched to both exponential and linear, (least squares) regression fits. Generally, exponential and linear data fits are about equally good, with regression coefficients ranging between 0.88 and 0.96.

Table 3 lists the exponential growth factors resulting from regression fits to the flame length, fuel mass loss and ceiling layer radiance. A fit for the data on x_f proportional to $e^{\gamma t}$ implies a flame spread velocity, V_f , given by

$$V_f = \frac{dx_f}{dt} = \gamma x_f$$

The exponential growth factor, γ , is thus the ratio, V_f/x_f . Similarly, exponential fits to the mass loss, \dot{m} , and radiance data yield $\dot{m}/\Delta m$ and \dot{N}/N .

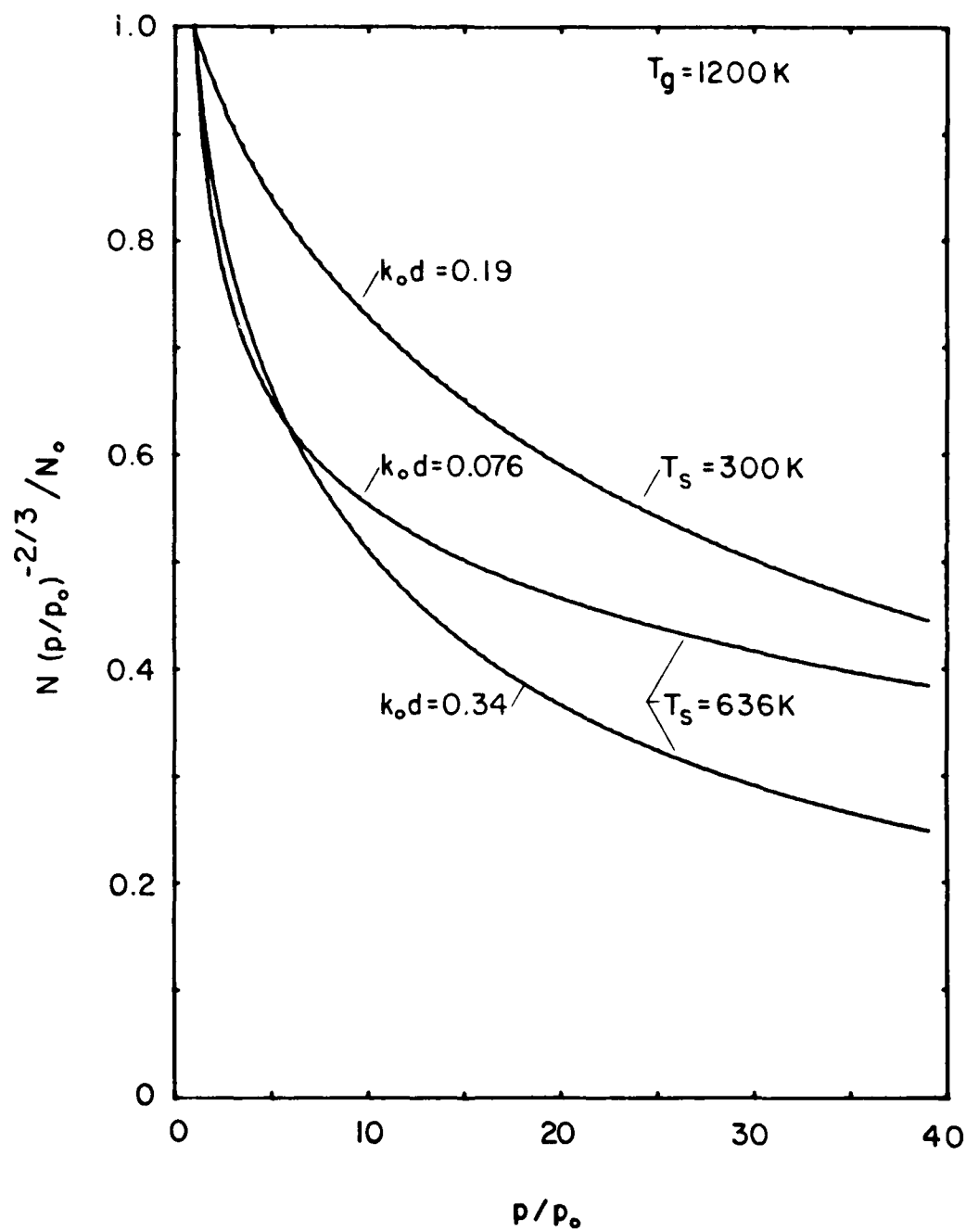


FIGURE 20 PREDICTED BEHAVIOR OF FLAME AND FUEL SURFACE RADIANCE

TABLE 3.-CEILING FIRE EXPONENTIAL GROWTH FACTORS

Ceiling Material	Flame Spread V_f/x_f [s^{-1}]	Mass Loss $\dot{m}/\Delta m$ [s^{-1}]	Radiance \dot{N}/N [s^{-1}]
$p/p_o = 11.2$			
Inert	0.046	0.056	0.12
PMMA	0.40	0.079	0.36
No. B8811	0.44	0.082	0.53
No. 223	0.34	0.10	0.74
No. 234	0.13	0.057	0.195
$p/p_o = 21.4$			
Inert	0.073	0.0745	0.25
PMMA	N.A.	0.099	0.66
No. B8811	0.54	0.12	0.75
No. 223	0.645	0.15	0.85
No. 234	0.245	0.082	0.31
$p/p_o = 31.6$			
Inert	0.032	0.062	0.32
PMMA	0.82	0.10	1.13
No. B8811	0.52	0.14	0.86
No. 223	0.92	0.22	1.77
No. 234	0.38	0.071	0.50

N.A. = not available due to camera malfunction

Table 3 shows that aircraft material No. 234 behaves similarly to the inert material as far as mass loss and radiance are concerned but has a flame spread rate about three times that of the inert material. The remaining three materials, including PMMA, have much larger growth factors than material No. 234 at all elevated pressures. Of the three materials with the higher growth factors, values of γ are nearly always largest for aircraft material No. 223 with respect to flame spread, mass loss, and radiance.

Peak values of mass loss rate and radiance are listed in Table 4 for the elevated pressure experiments. Peak flame lengths are not listed since flame spread is complete to the end of the channel for all except the inert material. As with the growth factors in Table 3, the materials can be roughly ranked in the following order of increasing peak mass loss rate or peak radiance at all elevated pressures:

1. Inert
2. No. 234
3. No. B8811
4. PMMA
5. No. 223

with the last three materials exhibiting very similar peak mass loss and radiance behavior.

TABLE 4.-MAXIMUM MASS LOSS RATE AND RADIANCE OF CEILING FIRES

Ceiling Material	Peak Mass Loss Rate \dot{m}_{\max} [g/s]	Peak Radiance N_{\max} [W/cm ² sr]
		$p/p_o = 11.2$
Inert	>0.9	>0.37
PMMA	>3.2	3.0
No. B8811	2.5	4.1
No. 223	3.5	3.3
No. 234	>1.6	>1.15
		$p/p_o = 21.4$
Inert	0.77	>0.69
PMMA	1.9	5.5
No. B8811	1.5	4.8
No. 223	2.25	6.5
No. 234	1.0	2.5
		$p/p_o = 31.6$
Inert	0.71	0.64
PMMA	1.55	5.5
No. B8811	1.4	5.1
No. 223	2.55	5.75
No. 234	0.77	2.56

> = experiment time insufficient to determine maximum value

III ANALYTICAL MODELING OF THERMAL RADIATION FROM LONG CEILING CHANNELS

Flows of flaming gases or combustion products in a long ceiling channel, such as that in an aircraft cabin, can undergo significant temperature variations with distance from one end of the ceiling to the other. Such variations in gas temperature along the length of the channel can be due to radiant heat loss to the cooler floor area or to conduction losses to the ceiling surface. If there are ventilation openings in the channel configuration permitting hot gas outflow and cool air inflow, mixing of outflow with inflow may occur, leading to reduced gas temperatures near the opening. On the other hand, combustible ceilings or wall fire impingement on the ceiling will lead to elevated gas temperatures.

A mathematical formulation is developed here to calculate thermal radiation from ceiling layers with temperatures and absorption coefficients nonuniform in three dimensions. This is a generalization of the methods described for uniform ceiling layers²¹ and for ceiling layers with properties varying in the vertical direction only²². Some simplified methods of calculating the problem are then tried and compared with the exact numerical procedure to evaluate the accuracy of various approximations.

3.1 MATHEMATICAL FORMULATION

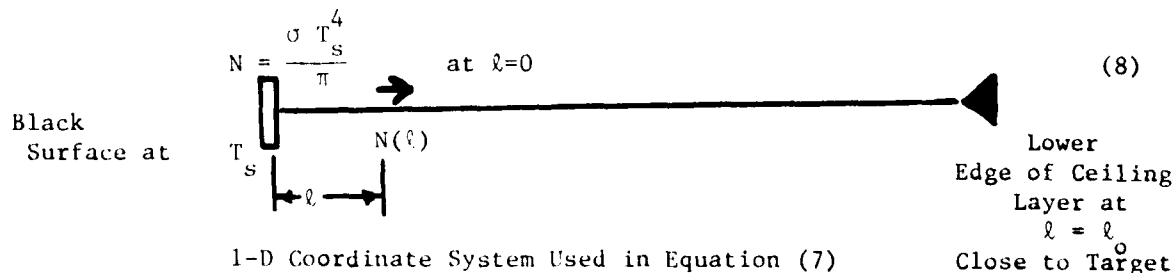
Temperatures and absorption coefficients in the ceiling layer are assumed to be known functions of the three spatial coordinates x , y and z :

$$\begin{aligned} T &= T(x, y, z) \\ k &= k(x, y, z) \end{aligned}$$

The one dimensional equation of radiative transfer for the radiance, N , (power per unit area per unit solid angle) along a ray of path length, ℓ , in the ceiling layer which is in thermodynamic equilibrium is,

$$\frac{dN(\ell)}{d\ell} = \frac{k(\ell) \sigma T(\ell)^4}{\pi} - k(\ell) N(\ell) \quad (7)$$

where σ is the Stefan-Boltzmann constant. For rays viewing the enclosure surfaces bounding the ceiling layer, the boundary condition is:

$$N = \frac{\sigma T_s^4}{\pi} \quad \text{at } \ell=0 \quad (8)$$


1-D Coordinate System Used in Equation (7)

Integrating equation (7) using (8) over the path length ℓ_0 through the ceiling layer yields

$$N(\ell_0) = \exp\left[-\int_0^{\ell_0} k(\ell)d\ell\right] \left\{ \int_0^{\ell_0} \frac{\sigma T^4(\ell)k(\ell)}{\pi} \exp\left[\int_0^{\ell} k(u)du\right]d\ell + \frac{\sigma T_s^4}{\pi} \right\} \quad (9)$$

This can be re-written as

$$N(\ell_0) = \frac{\sigma}{\pi} \int_0^{\ell_0} T^4(\ell)k(\ell) \exp\left[-\int_{\ell}^{\ell_0} k(u)du\right]d\ell + \frac{\sigma T_s^4}{\pi} \exp\left[-\int_0^{\ell_0} k(\ell)d\ell\right] \quad (10)$$

The radiative flux \dot{q}'' , from the ceiling layer and enclosure surfaces to a differential target surface element is given by:

$$\dot{q}'' = \int_{\Omega} \frac{N(\vec{n} \cdot \vec{r}_0)}{r_0} d\Omega \quad (11)$$

where $(\vec{n} \cdot \vec{r}_0) \geq 0$ and \vec{n} is the unit normal to the target element with direction cosines u , v and w ; \vec{r}_0 is the radius vector along the line of sight (ray) to the far edge of the ceiling layer; $(\vec{n} \cdot \vec{r}_0)$ represent the dot product (≥ 0) of the two vectors; and $d\Omega$ is the elemental solid angle subtended at the target element. The integration is performed over all solid angles with $(\vec{n} \cdot \vec{r}_0) \geq 0$ which includes the ceiling layer.

The path length ℓ can be written in cylindrical coordinates as

$$\ell = \frac{z_0 - z}{\cos\theta} \quad \text{for all } \phi, H_1 \leq z \leq z_0 \leq H_2$$

where z_0 is the vertical coordinate of the ray at the far edge of the ceiling layer; H_1 and H_2 are the vertical coordinates of the lower and upper edges of the ceiling layer respectively; θ and ϕ are the polar and azimuthal angles respectively; z is the vertical coordinate at ℓ . The origin $z=0$ is at the target. It is assumed that the region below the ceiling layer is transparent. To transform equation (11) into cylindrical coordinates we use the following three relationships:

$$0 \leq \ell \leq \ell_0 \quad z_0 \geq z \geq H_1 \quad ,$$

for any function f ;

$$\int_0^{\lambda_0} f(\lambda) d\lambda = \int_{z_0}^{H_1} f(z, \theta, \phi) \frac{d\lambda}{dz} dz = \int_{z_0}^{H_1} - \frac{f(z, \theta, \phi)}{\cos \theta} dz = \int_{H_1}^{z_0} \frac{f(z, \theta, \phi)}{\cos \theta} dz ;$$

and in particular

$$\int_{\lambda}^{\lambda_0} k(u) du = \int_{H_1}^z \frac{k(s, \theta, \phi)}{\cos \phi} ds$$

and also $d\Omega = \sin \theta d\phi d\theta$.

So the flux received by the target can be written as

$$\begin{aligned} \dot{q}'' &= \frac{\sigma}{\pi} \int_{\theta=0}^{\pi/2} \int_{\phi=0}^{2\pi} \frac{(\vec{n} \cdot \vec{r}_o)^*}{r_o} \sin \theta \int_{z=H_1}^{z_0} \frac{T^4(z, \theta, \phi) k(z, \theta, \phi)}{\cos \theta} \exp \left[- \int_{H_1}^z \frac{k(s, \theta, \phi)}{\cos \theta} ds \right] dz d\phi d\theta \\ &+ \frac{\sigma T_s^4}{\pi} \int_{\theta=0}^{\pi/2} \sin \theta \int_{\phi=0}^{2\pi} \frac{(\vec{n} \cdot \vec{r}_o)^*}{r_o} \exp \left(- \int_{H_1}^z \frac{k(s, \theta, \phi)}{\cos \theta} ds \right) d\phi d\theta \end{aligned}$$

where "*" indicates that $(\vec{n} \cdot \vec{r}_o) \geq 0$.

Now $(\vec{n} \cdot \vec{r}_o)/r_o = u \sin \theta \cos \phi + v \sin \theta \sin \phi + w \cos \theta$

as $\vec{n} = \vec{i} u + \vec{j} v + \vec{k} w$

$\vec{r}_o = r_o (\vec{i} \sin \theta \cos \phi + \vec{j} \sin \theta \sin \phi + \vec{k} \cos \theta)$.

In order to simplify the preceding computations, it is convenient to divide the enclosure into box-like sections as in Figures 21A and 21B such that the target is located at a corner of each section. The flux reaching the target will be the sum from all sections and each section flux is computed independently of others. Limits of integration are found for a typical section in the following discussion.

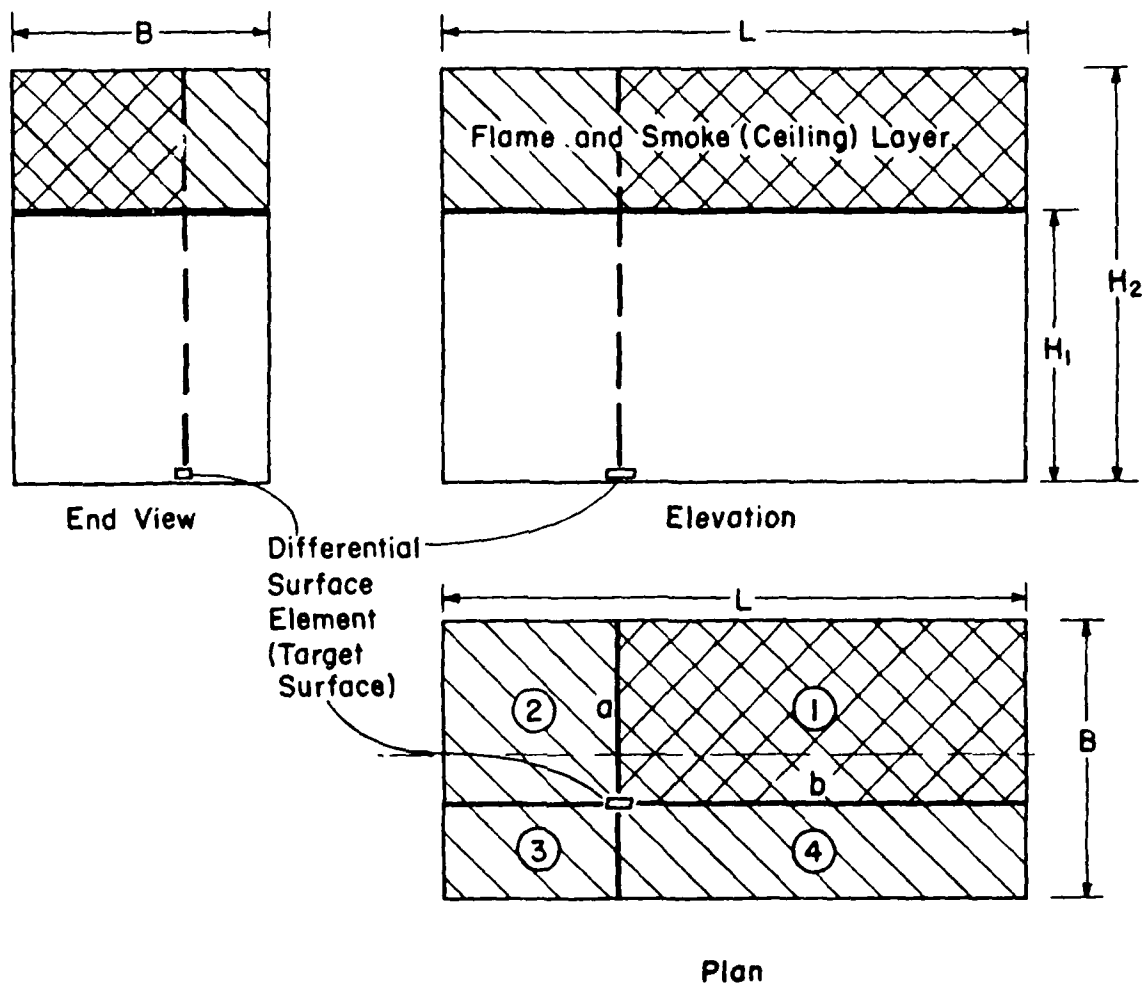


FIG. 21A Elevation, end and plan views of enclosure of length- L x breadth- B x height- H_2 . The target is located on the floor of the enclosure. The lower edge of the ceiling layer is at a height H_1 above the target surface. Also shown are the four rectangular parallelepipeds (boxes) used to calculate the radiative flux from the ceiling layer to the target element. The target is at one corner of each rectangular parallelepiped. The ceiling layer in rectangular parallelepiped No. 1 of length- b x breadth- a x height- H_2 is shown by the cross-hatched region in each view, ($b \geq a$). This figure is from reference 21.

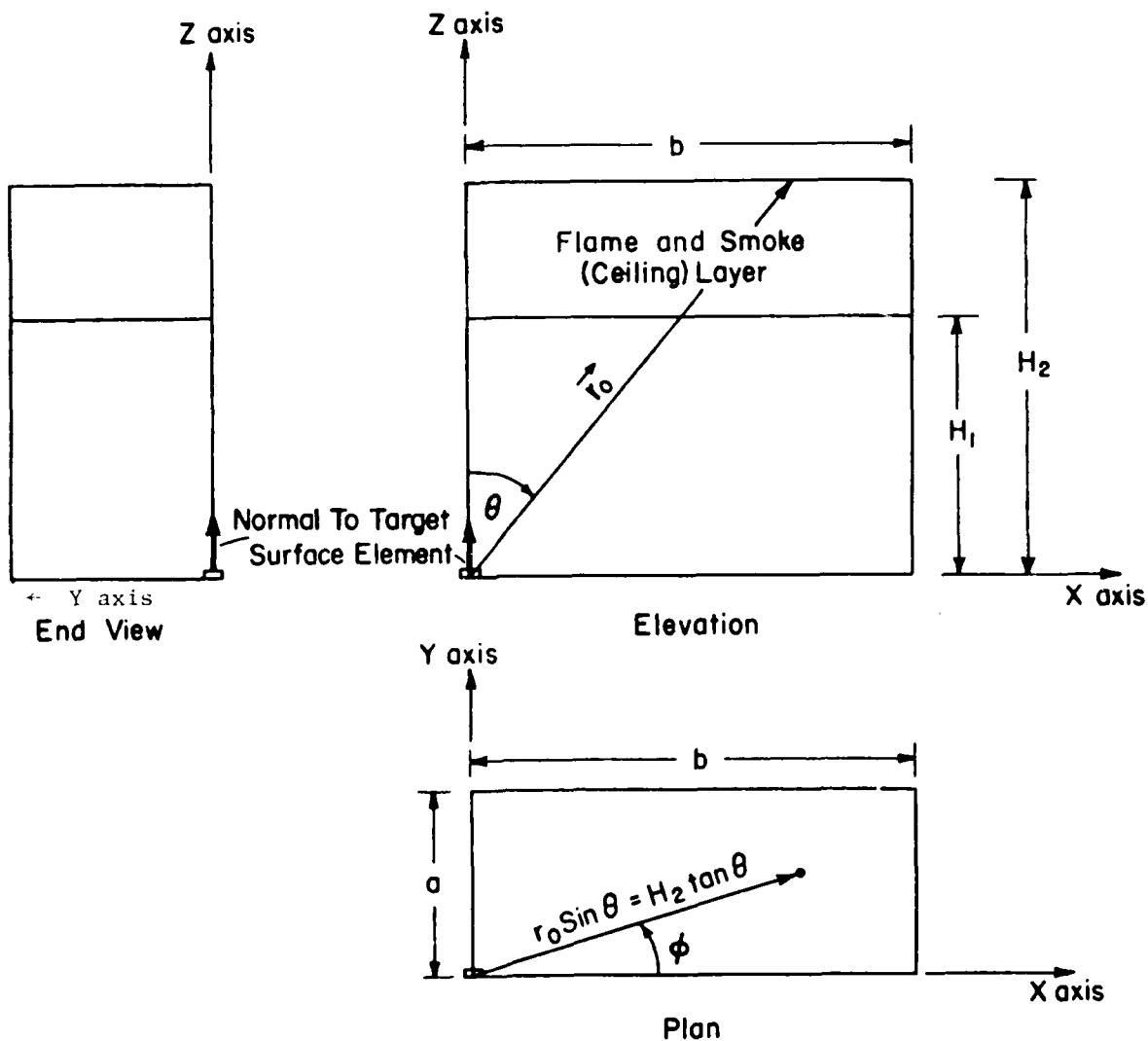


FIG.21B Detail of elevation, end and plan views of rectangular parallelepiped No. 1 of length- b x breadth- a x height- H_2 . The lower edge of the ceiling layer is at a height H_1 above the target surface. The target is at one corner of the rectangular parallelepiped. In this particular case the target normal is shown to coincide with the z -axis. The origin of a Cartesian and a spherical polar coordinate system is located at the target element. θ and ϕ are the polar and azimuthal angles respectively for the spherical polar coordinate system. The rectangular coordinate axes are selected such that $b \geq a$. This figure is from reference 21.

It is assumed that the absorption coefficient below the ceiling layer is zero, so that contributions from this region do not influence the results. This fact, together with the target direction and the section boundaries, determine the limits. Since each section flux is computed independently, direction cosines of target normal are to be redefined for each section, according to the section coordinate setup.

The flux from one section is given by:

$$\begin{aligned} \dot{q}_1'' = \frac{\sigma}{\pi} \int_{\theta=0}^{\tan^{-1}(\frac{\sqrt{a^2+b^2}}{H_1})} \sin\theta \int_{\phi=\phi_\ell(\theta)}^{\phi_u^*(\theta)} (u \sin\theta \cos\phi + v \sin\theta \sin\phi + w \cos\theta) \\ \int_{z=H_1}^{z_0} \frac{T^4(a, \theta, \phi) k(z, \theta, \phi)}{\cos\theta} \exp(-\int_{H_1}^z \frac{k(s, \theta, \phi)}{\cos\theta} ds) dz d\phi d\theta + \frac{\sigma T_s^4}{\pi} \tan^{-1}(\frac{\sqrt{a^2+b^2}}{H_1}) \phi_u^*(\theta) \\ \exp(-\int_{H_1}^{z_0} \frac{k(s, \theta, \phi)}{\cos\theta} ds) \sin\theta (u \sin\theta \cos\phi + v \sin\theta \sin\phi + w \cos\theta) d\phi d\theta \quad (12) \end{aligned}$$

where "*" indicates θ and ϕ such that $(u \sin\theta \cos\phi + v \sin\theta \sin\phi + w \cos\theta) \geq 0$.

and where a is the width of the section

b is the length of the section

H_1 the lower edge of the ceiling layer measured up from the height of the target

H_2 the upper edge of the ceiling layer or the height of the enclosure measured up from the target

$$\phi_\ell(\theta)=0 \quad \phi_u(\theta)=\pi/2 \quad \text{for } 0 \leq \theta \leq \tan^{-1}(a/H_1)$$

$$\phi_\ell(\theta)=0 \quad \phi_u(\theta)=\sin^{-1}(\frac{a}{H_1 \tan\theta}) \quad \text{for } \tan^{-1}(\frac{a}{H_1}) \leq \theta \leq \tan^{-1}(b/H_1)$$

$$\phi_\ell(\theta)=\cos^{-1}(\frac{b}{H_1 \tan\theta}), \quad \phi_u(\theta)=\sin^{-1}(\frac{a}{H_1 \tan\theta}) \quad \text{for } \tan^{-1}(\frac{b}{H_1}) \leq \theta \leq \tan^{-1}(\frac{\sqrt{a^2+b^2}}{H_1})$$

$$z_0 = H_2 \quad \text{for } 0 \leq \theta \leq \tan^{-1}(a/H_2)$$

$$z_0 = \text{minimum of } (\frac{b}{\tan\theta \cos\phi}, H_2) \quad \text{for } \tan^{-1}(\frac{a}{H_2}) < \theta \leq \tan^{-1}(\frac{\sqrt{a^2+b^2}}{H_1})$$

$$\phi_\ell \leq \phi \leq \tan^{-1}(\frac{a}{b})$$

$$z_0 = \text{minimum of } \left(\frac{a}{\tan \phi \sin \theta}, H_2 \right)$$

$$\text{for } \tan^{-1}\left(\frac{a}{H_2}\right) < \theta < \tan^{-1}\left(\frac{\sqrt{a^2+b^2}}{H_1}\right),$$

$$\tan^{-1}\left(\frac{a}{b}\right) < \phi \leq \phi_u(\theta).$$

3.2 APPROXIMATE SOLUTION

An analytic approximation for the above numerical formulation is available when the enclosure bounding the gas layer is a rectangular parallelepiped, temperature and absorption coefficient are uniform and the target surface is parallel to the ceiling layer, as shown in reference 21. When properties change only in the vertical (z) direction, this analytic technique is modified somewhat by use of an equivalent layer temperature, \bar{T}^4 , and absorption coefficient, \bar{k} , defined in reference 22 as follows:

$$\bar{T}^4 = \frac{H_2 \int_0^{H_2} T^4(z) k(z) E_2 \left(\int_0^z k(z) dz \right) dz}{1 - e E_3 \left(\int_0^{H_2} k(z) dz \right)} \quad (13)$$

$$\bar{k} = \frac{H_2 \int_0^{H_2} k(z) dz / \int_0^{H_2} (T(z) - T_\infty) dz}{H_2} \quad (14)$$

where $\bar{T} = (\bar{T}^4)^{1/4}$ and E_2, E_3 are the second and third exponential integrals, respectively.

A layer depth, $H_2 - H_1$ is defined by:

$$H_2 - H_1 = \int_0^{H_2} (T(z) - T_\infty) dz / (\bar{T} - T_\infty) \quad (15)$$

The equivalent radiant properties, defined above, can then be used to compute the radiative flux, \dot{q}'' , to a target at the corner of one of the four rectangular parallelepipeds in the enclosure (see Figure 21) by means of the following analytic approximation developed in reference 21:

$$\dot{q}'' = \frac{\sigma \bar{T}^4}{2\pi} \left\{ 1 - \left(1 - \frac{\bar{T}^4}{T^4} \right) \exp(-\bar{k} L_m) \right\} V \quad (16)$$

$$\text{where } L_m = \frac{2ab(H_2 - H_1)}{(H_2 - H_1)(a+b) + ab}$$

$$\text{and } V = \frac{a}{\sqrt{H_1^2 + a^2}} \tan^{-1} \left(\frac{b}{\sqrt{H_1^2 + a^2}} \right) + \frac{b}{\sqrt{H_1^2 + b^2}} \tan^{-1} \left(\frac{a}{\sqrt{H_1^2 + b^2}} \right)$$

and layer depth, $H_2 - H_1$ is given by equation (15).

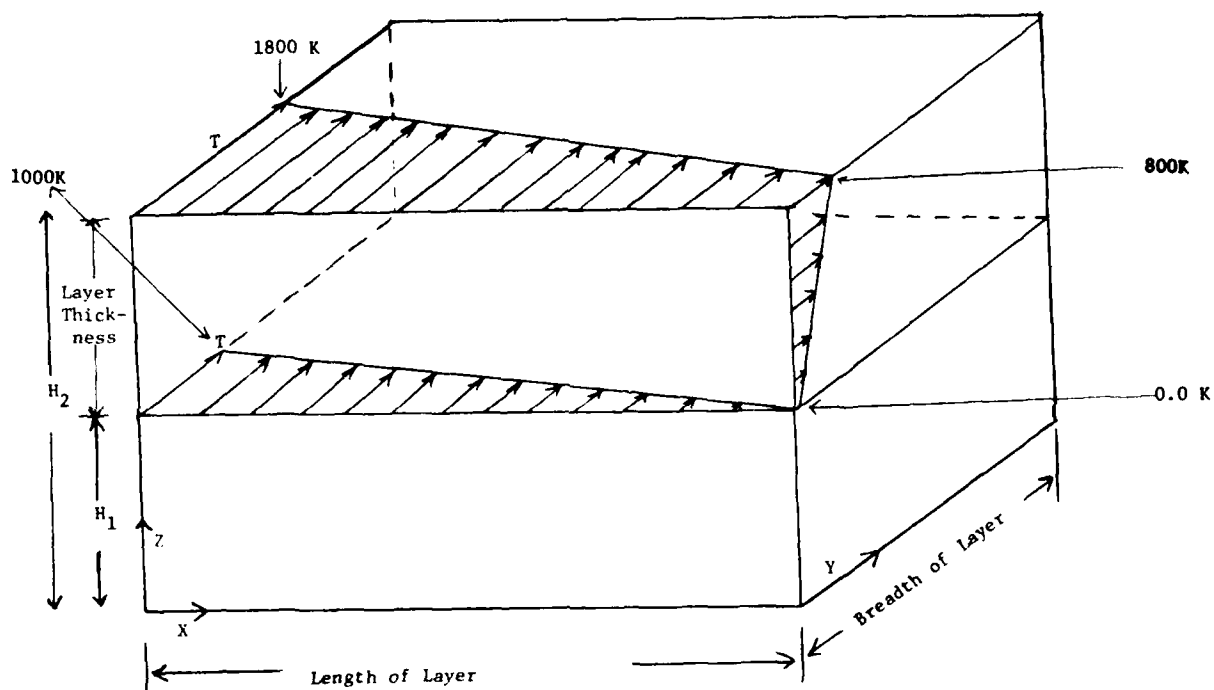
An approximation technique would be valuable in the case of a smoke layer with three-dimensional variations in both temperature and absorption coefficient, since huge amounts of computation time are needed to calculate radiative flux with purely numerical methods. To determine the accuracy of such a simplified calculation procedure, a specific ceiling layer with the largest temperature gradients which might exist (during an aircraft cabin fire) is examined. As shown in Figure 22, the temperature distribution assumed for the gas layer is a linear function with respect to height, z , and length, x , and constant with respect to width, y . Radiation from the ceiling surface is neglected and the absorption coefficient is taken as constant to see effects of gas temperature more clearly.

Results of several calculation procedures with the assumed temperature profile are shown in Table 5 for an upward facing target 1 m below the bottom of a 1 m thick layer at the mid-length point while Table 6 pertains to a target at one end of the layer. In the first row of Tables 5 and 6 are the exact numerical solutions for absorption coefficients of 1.2 m^{-1} and 0.5 m^{-1} . The second row of Table 5 gives a simplified numerical result obtained by assuming that the vertical distribution of temperature at the target location (x_T, y_T) is the same distribution in z at all x, y locations in the gas layer. Results in the third and last rows of Table 5 are obtained by the analytic method^{21,22} discussed above, with the equivalent temperature, T^4 , derived from the vertical temperature distribution at the target location alone.

For the present example, the analytic method is seen to be very accurate when the target is below the center of the layer. However, Table 6 shows that the analytic method overestimates the radiant flux by 13 to 15% when the target is below one end of a layer. The latter case is a rather stringent test of the analytic approximation since a real gas layer would not normally have an abrupt end, with no further contribution to the target radiant flux from a burning end-wall or outflow region. It is also seen from Tables 5 and 6 that the accuracy of the approximation technique will not be significantly affected by the magnitude of the gas absorption coefficient.

3.3 APPLICATION TO FULL-SCALE TEST RESULTS

The preceding techniques can be used to examine the self-consistency of the temperature and heat flux measurements made during the full-scale ceiling channel tests. Measured values of radiance and of radiant flux are compared



Temperature profile is assumed to be uniform along breadth of layer.

FIGURE 22 BASIC TEMPERATURE DISTRIBUTION USED FOR CALCULATED RESULTS IN TABLES 5 AND 6

TABLE 5.-RADIANT FLUX TO TARGET LOCATED BELOW CENTER OF LAYER

Layer Dimensions [m]	Kind of Approximation	Temp. Distn. $T(x,y,z)$ [K]	Kind of Computation	Flux in $[W/cm^2]$ for	
				Absorption Coefficient	
				$k=1.3 [m^{-1}]$	$k=0.5 [m^{-1}]$
1) 30x4x1 $H_1 = 1$	None	200-33.33x +800z	Numerical	2.11	1.7
2) "	Local Vertical Distribution for all x,y	-300+800z	Numerical	2.08	1.68
3) "	For all $\underline{x,y,z}$ $T^4 = \bar{T}^4$ $\bar{k} = 1.3$ Temperature Distribution of Line 2	844.4	Analytical	2.09	
4) "	For all $\underline{x,y,z}$ $T^4 = \bar{T}^4$ $\bar{k} = 0.5$ Temperature Distribution of Line 2	916.45	Analytical		1.69

TABLE 6.-RADIANT FLUX TO TARGET LOCATED BELOW END OF LAYER

Layer Dimensions [m]	Kind of Approximation	Temp. Distn. T(x,y,z) [K]	Kind of Computation	Flux in [W/cm ²] for	
				Absorption Coefficient	
				k=1.3 [m ⁻¹]	k=0.5 [m ⁻¹]
1) 30x4x1 H ₁ = 1	None	200-33.33x + 800z	Numerical	5.44	3.90
2) "	For all <u>x,y,z</u> T ⁴ = T ⁴ $\bar{k} = 1.3$ using local vertical distribution	1311.93	Analytical	6.13	
3) "	For all <u>x,y,z</u> T ⁴ = T ⁴ k=0.5 using local vertical distribution	1386.7	Analytical		4.49
4) 10x4x1 H ₁ = 1	None	200-100x + 800z	Numerical	4.54	3.18

with values computed from temperature distributions inferred and extrapolated from the experimental data. Three cases are examined: tests with an inert ceiling; a spreading fire under a PMMA ceiling and a steadily burning PMMA ceiling. Data for the inert ceiling are obtained from Table A-11 for a quasi-steady period just before extinguishment at 2700 s. Table A-15 is used for the spreading PPMA fire, at a time after ignition of 1257.6 s (extinguishment about 5 s thereafter), while Table A-16 contains the data on the steadily burning PMMA fire.

3.3.1 DISTRIBUTION OF PROPERTIES. The positions of the thermocouples, absorption coefficient instrument and radiometers are shown in Figure 2. With the data from these instruments and the following assumptions, temperature and absorption coefficient distributions for the whole ceiling layer are found.

Assumption 1. All properties do not vary along the width (y direction); i.e., $P(x, y_1, z) = P(x, y_2, z)$ for all y_1 and y_2 .

Assumption 2. Properties vary along the length (x direction) exactly the same way at all heights. Similarly the variation along the height is the same at all lengths;

i.e., $P(x_1, y, z_1) - P(x_1, y, z_2) = P(x_2, y, z_1) - P(x_2, y, z_2)$
for all x_1, x_2, z_1, z_2 .

So, if $P_{x_1}(z) = b_0 + b_1 z + b_2 z^2 + b_3 z^3$ at $x = x_1$

and $P_{z_1}(x) = a_0 + a_1 x + a_2 x^2 + a_3 x^3$ at $z = z_1$,

a two dimensional distribution satisfying the requirements is

$$P(x, z) = C_0 + a_1 x + a_2 x^2 + a_3 x^3 \\ + b_1 z + b_2 z^2 + b_3 z^3$$

where $C_0 = P^* + (b_0 - P_{x_1}(z_1)) + a_0 - P_{z_1}(x_1)$.

$P^* = \text{Actual Property } P \text{ at } (x_1, z_1) \text{ (ideal or observed value).}$

Since there is only one set of thermocouples along the height and another set along the length, polynomial fits of the observed temperatures are made along height and along length and combined as above to give a two-dimensional fit. This temperature distribution is evaluated at extreme points to make sure that the range of temperature is realistic.

As there is only one location where an absorption coefficient is measured, information on absorption coefficient is limited. The measured value is ob-

tained very near the ceiling. For both cases where the ceiling is burning PMMA, the absorption coefficient, which is influenced by the PMMA fuel vapor, is found to be 3.5 m^{-1} . Since the absorption coefficient for a PMMA flame is known to be about 1.55 m^{-1} (from reference 19), an average value of 2.5 m^{-1} is used in one calculation. A fit for absorption coefficient over z , varying from 1.5 (where temperature is maximum) to 3.5 (where k is observed) is used in a second calculation. The absorption coefficient is assumed to be constant with respect to x and y .

3.3.2 ENCLOSURE APPROXIMATIONS. As shown in Figure 2, the burning part of the end-wall does not extend to the ceiling and is narrower than the ceiling. However, the calculations are done assuming the whole .46 m wide end-wall is black, and is at 636 K (the PMMA vaporization temperature). There is no wall at the channel outlet. It is assumed that the ceiling is a black surface at a measured temperature or at 636 K (for PMMA) above the layer and that a 300 K temperature exists below the ceiling layer. There are side walls and they are also assumed to be black and at the ceiling temperature inside the ceiling layer and at 300 K (ambient) below it.

When the flux to the 90° angle Gardon radiometer is computed, only the 1.2-m length of ceiling which is visible to the radiometer is used. This layer section is taken as a parallelepiped and not as a cone, which is actually seen by the radiometer. The general numerical program can handle the cone structure but the analytic approximation does not.

3.3.3 COMPUTATION RESULTS. Fluxes to the total heat flux gage and the 90° angle radiometer are computed using the numerical scheme described above and the analytical scheme of reference 21. Results are listed in Tables 7 to 9 for the three separate experiments. The computed fluxes are on the whole slightly lower than the measured values, probably due to thermocouple radiation errors giving somewhat lower than actual gas temperatures. On the other hand, computed radiance is much higher than the observed value for the two PMMA ceiling fires, perhaps due to changes in radiometer calibration. Although the measured outputs of both narrow angle radiometers (B1, B2) are generally self-consistent, the slightly higher output of the parallel beam instrument (B2) is used for comparison with the calculations in Tables 7 to 9.

Calculations have also been performed to determine if the measured PMMA wall mass flux is consistent with the radiant flux level from the ceiling surface and gas layer. For a vertical target on the burning PMMA wall surface during the quasi-steady period of the second inert ceiling test (Table A-11), calculated radiant fluxes transmitted through the PMMA flame¹⁵ vary from 0.31 W/cm^2 at 23 cm to 0.8 W/cm^2 at 69 cm above the ignition point. This radiant feedback should result in a 31% to 62% increase, at these respective locations, in the total heat flux to the fuel (see reference 15) compared to that for a wall burning in the open. Corresponding increases in measured wall mass flux are somewhat lower, 23% to 44% (see Section 2.2.2) since the mass flux measurements represent a time-average over the entire period of fire growth.

TABLE 7. COMPUTED AND OBSERVED HEAT LOSSES, FULL-SCALE TEST 6-19-80, INERT CEILING

Target	Location of Target in Enclosure x, z_1 [m]	Size of Area used for Computation x, y, z_1 [m]	Kind of Computation	Properties T [K] k_1 [m^{-1}]	Heat Flux [W/cm ²]		Radiance [W/cm ² /sr]	
					Computed	Observed	Computed	Observed
90° Cardon radiometer	1.6, 0.61	1.2x0.46x0.61	Numerical	$T(x, y, z_1)$ 1.5	0.78	0.79	0.56	-
90° Cardon radiometer	1.6, 0.61	1.2x0.46x0.61	Analytical	849	0.74	0.79	-	-
Total Cardon gage	1.8, 0.0	2.4x0.46x0.18	Numerical	$T(x, y, z_1)$ 1.5	2.04*	1.99	-	-
Total Cardon gage	1.8, 0.0	2.4x0.46x0.18	Analytical	830	1.79*	1.99	-	-
Ray Radiometer	1.8, 0.23	-	Numerical	$T(x, y, z_1)$ 1.5	-	-	0.54	0.47

$$T(x, y, z_1) = 1.130 \times 10^3 + 6.378 z_1 - 61.34 z_1^2 + 166.020 z_1^3 - 202.540 z_1^4 - 578.72 x + 350.68 x^2 - 89.42 x^3$$

Ceiling temperature 703 K

Temperature of walls in contact with ceiling layer 703 K

Wall temperature below ceiling layer:

PMMA wall 636 K

All other walls 300K

Thickness of layer .18 m

x is distance from PMMA end-wall [m]
 y is distance from ceiling side-wall [m]
 z_1 is distance from ceiling [m]

* Includes 0.55 W/cm^2 for convective heat flux, based on a heat transfer coefficient of $10 \text{ W/m}^2\text{K}$ (see ref. 20)

TABLE 8. COMPUTED AND OBSERVED RADIANT HEAT LOSSES, FULL-SCALE TEST 8-5-80, PMMA CEILING

Target	Location of Target in Enclosure x, y, z_1 [m]	Size of Area used for Computation x_1, y_1, z_1 [m]	Kind of Computation	Properties		Radiant Flux		Radiance	
				T [K]	z_1 [m]	Computed [W/cm ²]	Observed [W/cm ²]	Computed [W/cm ² /sr]	Observed [W/cm ² /sr]
90° carbon radiometer	1.6, 0.23, 0.61	1.2x0.46x0.61	Numerical	1(x,y,z ₁)	k(x,y,z ₁)	1.27	1.30	0.89	-
90° carbon radiometer	1.6, 0.23, 0.61	1.2x0.46x0.61	Analytical	997	2.5	1.29	1.30	-	-
Total carbon gage	1.2, 0.23, 0.76	2.4x0.46x0.76	Numerical	1(x,y,z ₁)	k(x,y,z ₁)	1.41	1.49	1.17	-
Total carbon gage	1.2, 0.23, 0.76	2.4x0.46x0.76	Analytical	1069	2.5	1.41	1.49	-	-
Rav radiometer	1.6, 0.23, 0.23	-	Numerical	1(x,y,z ₁)	k(x,y,z ₁)	2.77	-	0.78	0.54

$$1(x,y,z_1) = 971$$

$$= 30.144 x + 209.107 x^2 - 71.04506 x^3$$

$$+ 11.761.903 z_1 - 145.600z_1^2 + 868.631 z_1^3$$

$$= 1,985,434 z_1^4 \text{ [K]}$$

$$k(x,y,z_1) = 3.53 - 10.2062 z_1 [\text{m}^{-1}]$$

Ceiling temperature 636 K

Temperature of walls in contact with ceiling layer 636 K

Temperature of walls below ceiling layer:

PMMA wall 636 K

All other walls 300 K

Thickness of layer .23 m

x is distance from PMMA end-wall [m]

y is distance from ceiling side-wall [m]

z₁ is distance from ceiling [m]

TABLE 9. COMPUTED AND OBSERVED RADIANT HEAT LOSSES, FULL-SCALE TEST 8-20-80, PMMA CEILING BURNING STEADILY

Target	Location of Target in Enclosure x, y, z_1 [m]	Size of Area used for Computation x, y, z_1 [m]	Kind of Computation	Gas Properties		Radiant Flux		Radiance	
				T [K]	k_1 [m]	Computed [W/cm ²]	Observed [W/cm ²]	Computed [W/cm ² /sr]	Observed [W/cm ² /sr]
90° Gardon radiometer	1.6, 0.23, 0.61	1.2x0.46x0.61	Numerical	$T(x, y, z_1)$	$k(x, y, z_1)$	1.89	1.88	1.21	-
90° Gardon radiometer	1.6, 0.23, 0.61	1.2x0.46x0.61	Analytical	1047	2.5	1.93	1.88	-	-
Total Gardon gage	1.2, 0.23, 0.76	2.4x0.46x0.76	Numerical	$T(x, y, z_1)$	$k(x, y, z_1)$	1.67	2.12	1.30	-
Total Gardon gage	1.2, 0.23, 0.76	2.4x0.46x0.76	Analytical	1067	2.5	1.71	2.12	-	-
Ray radiometer	1.8, 0.23, 0.23	-	Numerical	$T(x, y, z_1)$	$k(x, y, z_1)$	3.85	-	1.06	0.64

$$T(x, y, z_1) = 1127 - 50.0 x$$

$$k(x, y, z_1) = 3.628 - 19.068 z_1 + 80.8038 z_1^2 - 140.898 z_1^3$$

Temperature of ceiling and walls in contact with ceiling layer 636 K

Wall temperature below ceiling layer:

PMMA wall 636 K

All other walls 300 K

Thickness of layer .305 m

x is distance from PMMA end-wall [m]

y is distance from ceiling side-wall [m]

z_1 is distance from ceiling [m]

3.4 USE OF THE APPROXIMATE RADIATION MODEL

When there are significant longitudinal and vertical gradients of temperature and/or absorption coefficient in a ceiling layer, the radiant flux to floor level can be computed reliably from the analytic model, as demonstrated by the previous examples. An average temperature and absorption coefficient for use in the analytic model are computed from equations (13) and (14) for the axial location in the enclosure corresponding to that of the target.

Normally, data on gas and surface temperatures are readily available but not complete information on infrared absorption coefficient as a function of axial position, x , and height z . It is noted in reference 22 that because the radiative flux calculation is relatively insensitive to the exact value of absorption coefficient, neglecting the molecular radiators, CO_2 and H_2O , introduces little error. Consequently, it should be sufficient to assume that the spacial variation of absorption coefficient within the layer is primarily due to the dilution by ambient temperature air of constant density soot particles. This dilution effect on absorption coefficient can be related simply to gas temperatures by the following relation, explained in reference 22:

$$k(x,z) = \left(\frac{T_o}{T(x,z)} \right) \left(\frac{T(x,z) - T_\infty}{T_o - T_\infty} \right) k_o \quad (17)$$

where k_o and T_o are the measurements of gas absorption coefficient and gas temperature at a single, reference location and $k(x,z)$ and $T(x,z)$ are the corresponding quantities at any other axial or vertical position in the layer. This relation will only be valid if total gas pressure is constant (the enclosure is ventilated), gas specific heat is constant and the observed temperature distribution is due to entrainment of cold ambient air into the layer. Significant convective or radiative heat losses to the ceiling, side-walls, or to floor level from the bottom of the layer will thus tend to introduce errors in the $k(z)$ obtained from equation (17). Use of equation (17) allows the distribution, $k(z)$, to be calculated from a single measurement of infrared absorption coefficient and plentiful measurements of gas temperature.

IV SUMMARY OF RESULTS

Experiments with full-scale and model ceiling channels exposed to a developing PMMA wall fire yield three primary results:

1. Pressure modeling predictions of flame spread rates under a PMMA ceiling, flame lengths under an inert ceiling and radiant heat loss from the gas layer under both types of ceilings, based on the results of model tests at elevated pressure, are in reasonable agreement with measurements obtained at one atmosphere (full-scale). The behavior of three aircraft material ceilings is not pressure modeled well since fire spread is complete at elevated pressure but does not occur at one-atmosphere.
2. A simplified heat transfer analysis of the fire spread process shows that pressure modeling is likely to be more successful when applied to thin flame zones. For this reason, modeling predictions of fire growth will be less accurate when applied to deep ceiling channels than to vertical walls. One possible cause of modeling inaccuracy for the aircraft ceiling materials is shown by the heat transfer analysis to be the elevated surface temperatures associated with char formation. Another possible cause is shown to be the excess of fuel and thermal insulation available at elevated pressures due to the use of the same material thickness as at full-scale. In contrast, the PMMA and inert ceiling thicknesses are able to be properly scaled in accordance with the modeling requirements.
3. Exponential growth factors characterizing fire spread rates, mass loss rates and radiant heat loss are determined for all model ceiling configurations at each of three elevated air pressures. Ceiling materials can be readily grouped according to fire growth hazard with these exponential factors, with such grouping being roughly independent of pressure level.

A comprehensive analysis of radiation heat transfer from near-ceiling gas layers yields three main results:

1. An exact, numerical solution technique is formulated for computing the radiant flux toward the floor from hot gas layers generated by an aircraft cabin fire. Arbitrary variations in gas temperature and absorption coefficient in all three dimensions are permitted and radiation from the bounding wall and ceiling surfaces is taken into account.
2. Simplified analytic and numerical approximations are developed by assuming that only gas radiation properties along a vertical ray directly above the floor-level target are important. A single gas temperature and absorption coefficient for use in an analytic radiant flux expression are obtained from a suitable spatial average of this vertical property distribution. Such an approximation is tested and found to be capable of closely reproducing the exact numerical results, even when sharp, unrealistic changes in gas layer properties are assumed.
3. The radiation analyses are generally consistent with the experimental data on full-scale ceiling layer temperature, absorption coefficient and radiant heat loss. Predicted radiative enhancement of the full-scale PMMA wall fire by ceiling layer heat is also consistent with the measured PMMA mass flux distribution.

V CONCLUSIONS

1. The pressure modeling technique can be used to make conservative predictions of fire growth on walls or under ceilings as long as full scale flame zones are sufficiently thin. The product of absorption coefficient and mean beam length at one atmosphere should be less than about 0.2.
2. Tests at elevated air pressure can be used to rank materials according to rate of fire growth in wall or ceiling configurations as determined from measurements of flame spread rate, mass loss rate and radiant heat loss. Such ranking should be valid as long as results are reasonably independent of absolute air pressure in the range of 10⁻¹ to 10¹ atmospheres.
3. A simplified, analytic approximation involving the use of a suitable averaged gas temperature and absorption coefficient should be adequate for the calculation of radiant flux to floor level from ceiling gas layers with large streamwise gradients in gas radiation properties.

REFERENCES

1. Alpert, R.L., "Pressure Modeling of Vertically Burning Aircraft Materials," U.S. Dept. of Transportation, Final Report No. FAA-RD-78-139, January, 1979.
2. Babrauskas, V., "Flame Lengths Under Ceilings," Fire and Materials, 4, 3, p. 119, (1980).
3. Annamalai, K. and Sibulkin, M., "Flame Spread over Combustible Surfaces," Combustion Science and Technology, 19, p. 167, (1979).
4. Delichatsios, M., "The Flow of Fire Gases under a Beamed Ceiling," to be published in Combustion and Flame, (1981).
5. Carrier, G., Fendell, F., and Feldman, P., "Wind-Aided Flame Spread Along a Horizontal Fuel Slab," Combustion Science and Technology, 23, p. 41, (1980).
6. Fernandez-Pello, A.C., "Flame Spread in a Forward Forced Flow," Combustion and Flame, 36, p. 63, (1979).
7. You, H.Z., and Faeth, G.M., "Ceiling Heat Transfer during Fire Plume and Fire Impingement," Fire and Materials, 3, 3, p. 140, (1979).
8. Zukoski, E.E. and Kubota, T., "Two-Layer Modeling of Smoke Movement in Building Fires," Fire and Materials, 4, 1, p. 17, (1980).
9. Hwang, C.C., Chaiken, R.F., Singer, J.M. and Chi, D.N.H., "Reverse Stratified Flow in Duct Fires: A Two-Dimensional Approach," Sixteenth Symposium (International) on Combustion, The Combustion Institute, p. 1385, 1977.
10. Alpert, R.L., "Fire Induced Turbulent Ceiling-Jet," Factory Mutual Research Corp., Technical Report Serial No. 19722-2, May 1971.
11. Hinkley, P.L., Wraight, H.G.H., and Theobald, C.R., "The Contribution of Flames Under Ceilings to Fire Spread in a Compartment," Fire Research Note 712, Fire Research Station, Borehamwood, England, (1968).
12. de Ris, J. Kanury, A.M., Yuen, M.C., "Pressure Modeling of Fires," Fourteenth Symposium (International) on Combustion, The Combustion Institute, p. 1033, 1973.
13. Alpert, R.L., "Pressure Modeling of Transient Crib Fires," Combustion Science and Technology, 15, p. 11, (1976).
14. Alpert, R.L., "Pressure Modeling of Fires Controlled by Radiation," Sixteenth Symposium (International) on Combustion, The Combustion Institute, p. 1489, 1977.
15. Orloff, L., Modak, A.T., Alpert, R.L., "Burning of Large-Scale Vertical Surfaces," Sixteenth Symposium (International) on Combustion, The Combustion Institute, p. 1345, 1977.

16. Alpert, R.L., "Pressure Modeling of Transient Crib Fires," Factory Mutual Research Corp., Technical Report Serial No. 22360-2, 1975.
17. Alpert, R.L., "The Role of Radiation in Pressure Modeling of Upward Fire Spread," American Society of Mechanical Engineers, Heat Transfer Division paper No. 79-HT-28, 18th National Heat Transfer Conference, 1979.
18. Hottel, H.C., Sarofim, A.F., "Radiative Transfer," McGraw-Hill Book Company, New York, p. 278, 1967.
19. Markstein, G.H., "Radiative Properties of Plastics Pool Fires," Seventeenth Symposium (International) on Combustion, The Combustion Institute, p. 1053, 1979.
20. Orloff, L., "Simplified Radiation Modeling of Pool Fires," Eighteenth Symposium (International) on Combustion, The Combustion Institute, to be published, 1981.
21. Modak, A.T. and Mathews, M.K., "Radiation Augmented Fires Within Enclosures," Proceedings of the ASME, Journal of Heat Transfer, 100, p. 544, (1978)
22. Orloff, L., Modak, A.T., and Markstein, G.H., "Radiation from Smoke Layers," Seventeenth Symposium (International) on Combustion, The Combustion Institute, p. 1029, 1979.

TABLE A-1. UPWARD FLAME SPREAD ON PMMA WALL
TEST 6-10-80, INERT CEILING

Time [s]	Pyrolysis Height [cm]	Flame Height [cm]
192	10.5	21.0
292	14.5	23.5
345	16.0	31.0
380	20.0	33.0
461	26.0	37.0
476	28.0	46.0
505	30.0	46.0
531	32.0	53.5
561	38.0	48.0
615	38.0	53.0
661	44.0	62.3
668	44.0	65.3
696	42.0	60.3
724	46.0	66.3
761	53.7	77.3
767	55.3	72.3
781	55.8	71.3
791	60.3	82.4
797	61.3	82.4
808	62.3	82.4
819	63.3	82.4
826	65.3	78.3
844	67.3	82.4
854	66.3	82.4
859	69.3	
863	70.5	
869	72.3	
874	71.3	
899	75.3	
906	76.3	
927	79.3	

Exponential Growth Factors: Pyrolysis Height $2.651 \times 10^{-3} \text{ [s}^{-1}\text{]}$
Flame Height $2.100 \times 10^{-3} \text{ [s}^{-1}\text{]}$

TABLE A-2. UPWARD FLAME SPREAD ON PMMA WALL

TEST 6-19-80, INERT CEILING

Time [s]	Pyrolysis Height [cm]	Flame Height [cm]
61	9.5	13.5
129	11.5	14.5
180	14.0	16.5
214	16.5	18.5
242	17.5	23.0
289	20.0	24.5
301	21.5	26.5
338	24.0	27.5
390	28.0	34.5
440	32.5	41.5
480	35.5	43.5
510	39.0	51.5
540	42.5	55.3
575	46.0	60.3
601	49.0	68.8
634	55.3	67.3
647	55.3	71.8
659	57.3	71.3
682	60.3	78.3
700	63.3	82.7
721	66.3	82.7
738	68.5	
764	72.3	
780	75.3	
825	80.3	
867	82.7	

Exponential Growth Factors: Pyrolysis Height $2.759 \times 10^{-3} \text{ [s}^{-1}\text{]}$
 Flame Height $3.001 \times 10^{-3} \text{ [s}^{-1}\text{]}$

TABLE A-3.-MASS LOSS RATE OF PMMA WALL
TEST 6-10-80, INERT CEILING

Height Above Ignition [cm]	Mass Flux [g/m ² s]
7.6	5.75
23	6.37
38	6.88
53	8.13
69	10.20
84	10.77

Extinguishment 1890 s after ignition.

From preceding mass flux data, average mass loss rate per unit width of wall at 945 s after ignition is 7.22 g/ms

Assuming an average width of burning wall of 0.2 m, total wall mass loss rate is 1.44 g/s

MASS LOSS RATE OF PMMA WALL
TEST 6-19-80, INERT CEILING

Height Above Ignition [cm]	Mass Flux [g/m ² s]
7.6	7.21
23	7.66
38	8.23
53	9.37
69	11.60
84	12.70

Extinguishment 3577 s after ignition.

From preceding mass flux data, mass loss rate per unit width of wall at 1788 s after ignition is 8.52 g/ms

Assuming an average width of burning wall of 0.3 m, total wall mass loss rate is 2.55 g/s

TABLE A-4. FLAME EXTENT UNDER INERT CEILING

TEST 6-10-80

Time [s]	Flame Length [cm]
954	0.0
1000	3.0
1050	0.0
1140	6.0
1200	6.0
1262	12.2
1319	21.4
1380	21.4
1413	24.4
1449	36.6
1470	42.7
1500	30.0
1530	33.6
1546	42.0
1549	36.6
1554	27.5
1564	36.6
1587	39.4
1594	45.8
1617	42.7
1627	36.6
1650	61.0
1680	45.8
1713	39.4
1750	51.9
1774	48.8
1800	55.7
1825	63.0

TABLE A-5. FLAME EXTENT UNDER INERT CEILING

TEST 6-19-80

Time [s]	Flame Length [cm]
1020	4.0
1080	10.0
1142	9.0
1200	15.0
1269	15.0
1320	20.0
1380	25.0
1440	25.0
1470	40.0
1514	40.0
1560	40.0
1622	50.0
1680	40.0
1735	50.0
1786	60.0
1788	55.0
1800	50.0
1841	60.0
1861	60.0
1894	65.0
1925	60.0
1950	55.0
1980	70.0
2003	75.0
2040	80.0
2100	98.0
2160	80.0
2221	68.0
2267	70.0
2325	80.0
2498	75.0
2556	128.0
2594	148.0
2664	120.0

TABLE A-6. FLAME EXTENT UNDER NAFEC #234 CEILING

TEST 7-9-80

Time [s]	Flame Length [cm]	Time [s]	Flame Length [cm]
1143	0.0	1759	52.0
1232	18.0	1760	62.0
1271	18.0	1761	42.0
1272	24.0	1801	42.0
1324	24.0	1802	42.0
1358	30.0	1803	40.0
1359	35.0	1804	42.0
1360	35.0	1846	42.0
1394	35.0	1849	62.0
1398	42.0	1859	42.0
1461	20.0	1860	42.0
1462	35.0	1928	50.0
1463	32.0	1929	55.0
1464	28.0	1930	49.0
1502	26.0	1931	43.0
1503	42.0	1932	57.0
1528	30.0	1992	57.0
1529	65.0	2002	42.0
1531	42.0	2003	67.0
1533	67.0	2004	55.0
1543	67.0	2132	57.0
1567	67.0	2133	60.0
1568	42.0	2134	56.0
1582	54.0	2156	56.0
1589	44.0	2137	55.0
1606	50.0	2198	57.0
1609	67.0	2199	60.0
1617	32.0	2200	56.0
1619	42.0	2201	67.0
1628	34.0	2240	55.0
1629	42.0	2242	57.0
1630	44.0	2287	56.5
1631	54.0	2288	60.0
1632	42.0	2290	67.0
1663	34.0		
1664	35.0		
1665	37.0		
1666	42.0		
1667	34.0		
1690	42.0		
1691	48.0		
1692	42.0		
1693	44.0		
1694	44.0		
1724	42.0		
1725	42.0		
1726	44.0		
1727	42.0		
1758	42.0		

TABLE TABLE A-7. FLAME EXTENT UNDER NAFEC #B8811 CEILING

TEST 7-22-80

Time [s]	Flame Length [cm]	Time [s]	Flame Length [cm]
960	0.0	1727	65.0
1063	10.0	1730	77.0
1127	5.0	1750	70.0
1135	15.0	1751	70.0
1140	15.0	1752	68.0
1200	15.0	1753	46.0
1225	15.0	1803	77.0
1264	25.0	1805	65.0
1297	30.0	1807	65.0
1307	32.0	1853	58.0
1315	45.0	1854	70.0
1321	30.0	1855	77.0
1336	46.0	1856	80.0
1337	30.0	1874	77.0
1338	30.0	1875	71.0
1353	32.0	1876	65.0
1354	32.5	1877	77.0
1366	35.0	1878	80.0
1367	30.0	1879	82.0
1378	45.0	1916	60.0
1380	35.0	1917	62.0
1382	39.0	1918	63.0
1383	33.0	1919	77.0
1405	45.0	1948	70.0
1406	38.0	1949	75.0
1407	49.0	1950	72.5
1407	46.0	1951	77.0
1420	46.0	1987	58.0
1421	44.0	1988	93.0
1422	49.0	1989	65.0
1432	46.0	2059	65.0
1446	48.0	2060	77.0
1447	52.0	2061	90.0
1505	46.0	2062	65.0
1525	46.0	2085	77.0
1548	55.0	2086	77.0
1551	48.0	2087	77.0
1552	58.0	2088	65.0
1553	50.0		
1577	58.0		
1580	46.0		
1619	58.0		
1634	58.0		
1667	48.0		
1668	46.0		
1691	50.0		
1692	58.0		
1693	60.0		
1694	62.0		

TABLE A-8. FLAME EXTENT UNDER NAFEC #223 CEILING

TEST 7-30-80

Time	Flame Length	Time	Flame Length
[s]	[cm]	[s]	[cm]
1089	0.0	1550	50.8
1118	7.6	1551	50.8
1140	7.6	1572	58.4
1175	15.2	1613	61.0
1176	10.2	1614	53.3
1199	12.7	1615	50.8
1201	15.2	1632	50.8
1246	17.8		
1247	20.3		
1248	12.7		
1281	17.8		
1282	15.2		
1284	17.8		
1299	15.2		
1301	15.2		
1313	7.6		
1314	15.2		
1315	15.2		
1321	17.8		
1323	20.3		
1328	12.7		
1332	15.2		
1335	17.8		
1366	20.3		
1368	20.3		
1369	17.8		
1388	20.3		
1389	22.9		
1390	17.8		
1439	30.5		
1440	27.9		
1441	30.5		
1442	35.6		
1448	17.8		
1449	30.5		
1450	30.5		
1451	27.9		
1483	27.9		
1484	43.2		
1485	43.2		
1494	45.7		
1495	40.6		
1509	40.6		
1510	45.7		
1511	43.2		
1512	45.7		
1545	61.0		
1546	48.3		
1549	53.3		

TABLE A-9. FLAME SPREAD UNDER PMMA CEILING

TEST 8-5-80

Time [s]	Flame length [cm]
971	0.0
1091	10.0
1105	15.0
1115	30.0
1116	40.0
1128	60.0
1132	70.0
1133	70.0
1139	80.0
1143	90.0
1144	90.0
1156	115.0
1157	125.0
1158	128.0
1159	140.0
1160	130.0
1161	128.0
1164	130.0
1165	130.0
1167	130.0
1168	140.0
1173	130.0
1173	135.0
1174	140.0
1176	145.0
1177	150.0
1178	140.0
1179	140.0
1188	160.0
1189	160.0
1190	220.0
1197	230.0
1198	240.0

Flame Length Exponential Growth Factor = $0.0249 \text{ [s}^{-1}\text{]}$ (Regression Coefficient = 0.89)

Flame Length Linear Growth Rate = 1.95 [cm/s] (Regression Coefficient = 0.92)

TABLE A-10. TEMPERATURE AND RADIATION MEASUREMENTS

FULL-SCALE TEST 6-10-80, INERT CEILING

TIME SEC	A13 DEG C	A14 DEG C	A6 DEG C	A7 DEG C	A8 DEG C	A9 DEG C	A10 DEG C	A11 DEG C	A12 DEG C	E1 W/CMSR	E2 W/CMSR	C3 1/M	D4 W/C CM	D5 W/C CM
6.4	21.3	24.8	22.1	22.1	22.2	21.4	20.0	25.6	21.7	0.001	0.005	0.11	-0.502	-0.000
26.9	21.8	24.7	21.6	21.1	20.1	19.6	19.4	23.1	21.9	-0.001	0.001	0.11	-0.524	-0.000
49.3	21.8	24.6	21.5	21.4	20.9	20.2	19.9	23.5	21.8	0.002	-0.001	0.09	-0.573	-0.000
69.6	21.7	24.6	22.0	22.3	22.1	21.8	20.5	24.2	22.9	0.002	-0.000	0.13	-0.533	-0.001
89.9	21.7	24.5	22.3	22.9	22.9	19.5	19.3	24.2	23.4	0.002	0.001	0.14	-0.554	-0.001
110.2	21.7	24.7	23.2	23.5	22.7	21.1	19.3	23.4	24.1	0.002	-0.003	0.15	-0.535	-0.000
130.6	21.8	24.3	22.7	24.1	23.5	21.0	19.4	25.7	23.7	0.003	0.005	0.12	-0.534	-0.000
151.0	21.7	24.9	22.2	24.8	24.3	22.1	19.8	27.2	25.4	0.005	0.005	0.03	-0.532	-0.000
171.4	21.7	25.1	23.6	26.4	26.3	20.5	19.6	27.3	26.3	-0.003	-0.003	0.03	-0.534	-0.000
191.3	21.7	25.5	23.5	26.8	26.5	21.9	21.1	22.7	27.3	0.001	0.012	0.05	-0.531	-0.001
212.6	21.7	25.5	27.7	27.9	27.0	21.4	19.7	23.2	29.7	0.001	0.003	0.00	-0.534	-0.001
232.6	21.7	25.7	28.0	28.4	27.4	21.7	19.3	31.0	30.1	0.007	0.012	0.03	-0.532	-0.000
252.9	21.7	26.0	27.5	30.1	28.9	20.8	19.6	31.9	32.7	-0.002	0.001	0.05	-0.502	0.001
273.3	21.8	26.4	31.1	31.8	29.2	22.2	19.5	30.9	35.3	-0.001	0.005	0.01	-0.532	-0.000
293.7	21.8	26.7	32.6	33.1	30.7	24.4	19.7	35.6	35.4	0.002	0.003	0.02	-0.531	-0.000
314.1	21.8	27.1	34.9	35.6	32.0	22.4	19.6	35.9	37.0	0.004	0.005	0.04	-0.530	-0.000
334.4	21.8	27.5	35.6	36.2	33.7	20.2	19.7	38.6	40.2	0.003	0.012	0.02	-0.579	0.001
354.7	21.8	28.0	37.3	37.9	35.3	22.9	19.7	39.7	41.1	0.002	0.013	0.01	-0.577	0.000
375.0	21.8	28.6	38.8	39.1	37.7	31.1	21.0	41.2	42.3	0.001	0.004	-0.00	-0.576	-0.000
395.5	21.8	29.2	40.3	41.3	34.0	26.2	21.7	43.6	43.3	0.003	0.018	-0.01	-0.575	0.001
415.9	21.9	30.0	43.2	44.5	37.4	27.3	20.8	46.5	45.5	0.005	0.005	0.02	-0.573	0.001
436.3	21.9	30.6	45.0	45.9	43.1	29.9	19.6	48.1	43.2	0.003	0.002	0.03	-0.571	0.001
456.6	21.9	31.2	47.1	47.9	45.3	30.2	20.2	48.9	51.8	0.003	0.009	0.02	-0.570	0.002
476.9	21.9	31.8	48.4	49.4	47.6	30.0	20.1	52.3	52.0	0.002	-0.007	0.03	-0.570	0.002
497.2	21.9	32.5	49.7	51.0	48.0	29.7	20.9	54.6	54.3	0.005	0.010	0.01	-0.563	0.002
517.5	22.0	33.3	53.1	54.8	53.7	30.8	20.1	55.1	54.7	0.002	-0.001	0.01	-0.564	0.002
537.8	22.1	35.2	54.8	56.7	56.3	33.4	19.7	59.2	54.3	0.007	-0.004	0.02	-0.561	0.002
558.1	22.1	35.2	59.5	60.5	56.7	37.3	20.2	63.2	57.7	-0.000	0.004	0.03	-0.568	0.003
578.4	22.2	36.1	62.9	64.1	61.7	38.4	20.4	65.9	62.1	0.006	0.014	0.02	-0.565	0.003
598.8	22.2	36.1	65.9	66.5	61.5	40.1	20.4	68.1	71.2	0.003	0.007	0.01	-0.564	0.003
619.1	22.3	39.4	68.6	64.7	63.3	44.0	22.5	73.0	74.1	0.001	-0.001	0.05	-0.547	0.005
639.5	22.4	40.7	70.7	73.2	63.6	30.3	22.0	75.8	77.0	0.006	0.000	0.06	-0.544	0.005
659.8	22.4	42.1	73.6	77.3	71.4	40.3	23.5	78.0	84.0	0.001	0.011	0.02	-0.540	0.005
679.1	22.5	43.6	75.6	80.6	73.9	41.8	22.9	82.1	83.0	0.004	0.009	0.05	-0.530	0.005
699.4	22.5	45.2	75.6	85.1	77.6	58.5	24.1	87.3	95.7	0.007	0.005	0.07	-0.532	0.005
720.8	22.7	47.1	82.5	91.2	81.7	46.0	21.3	93.0	93.4	0.007	0.004	0.05	-0.529	0.005
741.2	22.8	49.9	89.1	93.2	85.4	55.3	22.9	97.6	100.1	0.005	0.010	0.07	-0.524	0.008
761.6	22.9	52.9	91.2	102.3	89.6	59.5	21.5	102.0	105.5	0.001	0.009	0.10	-0.512	0.008
782.1	23.0	53.2	103.7	108.1	93.6	53.6	21.5	105.6	112.9	0.007	0.005	0.03	-0.510	0.009
802.5	23.2	55.4	113.2	111.5	108.5	60.9	20.0	113.2	115.1	0.010	0.009	-0.01	-0.502	0.009
822.8	23.3	57.6	116.2	113.5	108.5	56.6	23.5	122.3	127.1	0.007	0.019	0.05	-0.497	0.005
843.2	23.5	60.4	121.7	123.5	115.0	72.5	22.1	128.6	135.8	0.006	0.009	0.05	-0.493	0.003
863.6	23.7	63.3	130.8	130.8	119.3	65.0	21.7	136.4	139.0	0.006	0.014	0.08	-0.482	0.010
884.0	23.9	65.4	136.5	141.4	127.3	63.8	21.9	144.2	152.9	0.009	0.010	0.04	-0.471	0.012
904.3	24.1	69.8	146.2	149.3	136.9	70.1	23.4	152.6	154.3	0.008	0.013	0.04	-0.456	0.013

TIME SEC	A13 DEG C	A14 DEG C	A6 DEG C	A7 DEG C	A8 DEG C	A9 DEG C	A10 DEG C	A11 DEG C	A12 DEG C	W/K MIN	A22 W	C3 T.M	D4 W/K	D5 W/K
324.7	21.4	72.	155.6	159.2	140.8	50.6	21.8	101.4	172.3	0.014	0.009	0.09	-0.435	0.014
345.0	24.7	77.4	164.7	161.3	149.7	54.6	22.8	103.2	171.2	0.009	0.003	0.08	-0.427	0.016
365.4	24.9	81.3	174.2	155.8	155.8	84.3	21.9	174.8	137.9	0.010	0.003	0.05	-0.473	0.018
385.7	25.2	83.0	172.3	150.4	150.4	58.1	23.3	132.8	197.6	0.015	0.000	0.09	-0.458	0.019
405.0	25.5	80.4	193.5	141.8	130.2	60.6	24.0	100.9	193.5	0.009	0.003	0.10	-0.398	0.022
425.4	25.8	87.3	190.9	140.4	120.7	80.5	23.9	202.8	210.7	0.009	0.000	0.09	-0.398	0.023
445.7	26.3	83.1	200.9	141.9	110.8	72.2	23.7	215.6	221.9	0.018	0.000	0.08	-0.377	0.025
465.0	26.6	103.4	213.7	142.0	100.3	75.6	24.2	219.5	223.5	0.017	0.000	0.13	-0.359	0.028
485.4	27.0	103.4	218.5	143.0	100.8	75.7	23.4	243.6	231.5	0.014	0.000	0.11	-0.355	0.029
505.7	27.4	112.0	183.7	143.0	207.9	65.6	25.3	241.1	231.4	0.027	0.000	0.12	-0.319	0.033
526.0	27.4	120.0	200.0	143.0	207.9	65.6	25.3	241.1	231.4	0.027	0.000	0.12	-0.319	0.033
546.3	27.9	117.4	204.1	143.0	212.7	70.5	24.5	243.5	233.4	0.015	0.000	0.23	-0.315	0.037
566.6	28.4	121.3	204.1	143.0	212.7	70.5	24.5	243.5	233.4	0.015	0.000	0.23	-0.315	0.037
586.9	28.9	125.1	204.1	143.0	212.7	70.5	24.5	243.5	233.4	0.015	0.000	0.23	-0.315	0.037
607.2	29.3	130.7	204.1	143.0	212.7	70.5	24.5	243.5	233.4	0.015	0.000	0.23	-0.315	0.037
627.5	29.8	136.1	204.1	143.0	212.7	70.5	24.5	243.5	233.4	0.015	0.000	0.23	-0.315	0.037
647.8	30.3	141.4	204.1	143.0	212.7	70.5	24.5	243.5	233.4	0.015	0.000	0.23	-0.315	0.037
668.1	30.8	146.8	204.1	143.0	212.7	70.5	24.5	243.5	233.4	0.015	0.000	0.23	-0.315	0.037
688.4	31.3	151.3	204.1	143.0	212.7	70.5	24.5	243.5	233.4	0.015	0.000	0.23	-0.315	0.037
708.7	31.8	156.7	204.1	143.0	212.7	70.5	24.5	243.5	233.4	0.015	0.000	0.23	-0.315	0.037
729.0	32.3	162.1	204.1	143.0	212.7	70.5	24.5	243.5	233.4	0.015	0.000	0.23	-0.315	0.037
749.3	32.8	167.5	204.1	143.0	212.7	70.5	24.5	243.5	233.4	0.015	0.000	0.23	-0.315	0.037
769.6	33.3	173.0	204.1	143.0	212.7	70.5	24.5	243.5	233.4	0.015	0.000	0.23	-0.315	0.037
789.9	33.8	178.4	204.1	143.0	212.7	70.5	24.5	243.5	233.4	0.015	0.000	0.23	-0.315	0.037
810.2	34.3	183.8	204.1	143.0	212.7	70.5	24.5	243.5	233.4	0.015	0.000	0.23	-0.315	0.037
830.5	34.8	189.2	204.1	143.0	212.7	70.5	24.5	243.5	233.4	0.015	0.000	0.23		

TEST 6-10-80

TIME SEC	A13 DEG C	A14 DEG C	A6 DEG C	A7 DEG C	A8 DEG C	A9 DEG C	A10 DEG C	A11 DEG C	A12 DEG C	B1 W/CMMR	E2 W/CMMR	C3 1/M	D4 W/CMMR	D5 W/CMMR
1842.0	50.2	239.2		513.8	423.1	200.3	76.3	531.1	503.1	0.144	0.182	0.80	0.485	0.270
1842.4	51.0	294.1		510.6	431.6	241.3	67.3	543.6	572.6	0.153	0.134	0.53	0.477	0.293
1842.8	51.5	299.2		513.1	433.3	200.0	100.5	513.6	492.7	0.151	0.203	0.92	0.599	0.224
1843.2	51.9	270.1		521.2	132.9	50.9	38.9	513.5	215.4	0.036	0.154	0.83	-0.188	0.118
1843.5	52.6	222.4	571.3	113.8	65.8	36.8	36.2	103.1	167.1	0.039	0.055	0.53	-0.302	0.030
1843.9	52.8	231.2		114.2	51.4	29.8	31.8	103.7	154.8	0.027	0.087	0.43	-0.351	0.037
1844.1	53.0	192.6		123.9	50.7	33.7	36.9	103.3	130.2	0.027	0.034	0.32	-0.379	0.027
1844.5	53.0	103.1		123.4	51.3	30.3	36.3	103.5	134.0	0.023	0.037	0.27	-0.422	0.038
1844.9	53.5	156.7		114.2	37.9	29.4	23.5	94.5	123.1	0.020	0.030	0.23	-0.422	0.038
1845.3	55.2	147.6		114.6	53.7	33.3	29.1	93.2	110.1	0.022	0.034	0.19	-0.441	0.030
1845.7	56.0	132.3		104.9	43.0	30.4	30.6	82.8	112.4	0.071	0.037	0.27	-0.431	0.035
1846.1	56.2	127.2		94.6	43.6	29.7	26.5	80.5	103.8	0.073	0.037	0.22	-0.455	0.033
1846.5	57.2	122.1	110.3	94.6	33.0	27.2	26.5	83.5	99.2	0.070	0.031	0.16	-0.400	0.030
1846.9	57.2	117.4	97.8	74.3	45.5	27.5	26.5	87.3	95.3	0.035	0.025	0.13	-0.434	0.029
1847.3	57.3	112.9		76.9	30.3	25.5	23.4	74.5	94.8	0.035	0.018	0.11	-0.484	0.023
1847.7	58.0	108.6	99.6	83.3	31.1	26.6	26.9	80.1	93.8	0.033	0.024	0.03	-0.491	0.022
1848.1	58.0	105.2	95.6	82.5	34.8	24.3	24.9	82.1	88.5	0.033	0.024	0.03	-0.491	0.022
1848.5	58.0	101.8	97.5	80.5	27.9	23.7	24.5	70.1	81.9	0.030	0.024	0.04	-0.494	0.019
1848.9	58.5	95.0	87.1	87.0	25.2	24.8	24.5	67.3	81.6	0.035	0.016	0.04	-0.499	0.018
1849.3	58.3	86.3	85.9	85.3	24.6	24.6	23.2	58.2	70.7	0.033	0.015	0.04	-0.502	0.017
1849.7	58.9	93.7	85.1	74.3	23.9	23.7	23.0	58.2	69.9	0.037	0.011	0.06	-0.502	0.016
1850.1	59.4	84.5	84.5	65.4	25.7	24.5	23.9	72.0	83.0	0.035	0.013	0.01	-0.507	0.013
1850.5	59.2	89.2	74.5	60.2	24.3	24.9	23.0	73.1	83.2	0.030	0.010	0.01	-0.511	0.012
1850.9	59.1	87.1	63.2	58.0	23.3	24.1	23.2	69.2	83.3	0.033	0.005	-0.02	-0.509	0.014
1851.3	59.1	80.1	60.1	62.6	24.7	25.0	24.4	67.4	83.9	0.039	0.009	-0.02	-0.511	0.012
1851.7	59.7	84.0	64.1	64.1	24.0	23.8	23.2	63.3	82.2	0.061	0.009	-0.02	-0.513	0.012
1852.1	59.3	81.9	72.9	57.3	23.5	23.6	23.3	63.9	75.3	0.059	-0.000	-0.03	-0.516	0.014
1852.5	59.3	80.3	73.9	50.1	23.0	23.4	22.7	51.2	80.0	0.066	0.010	-0.05	-0.516	0.012
1852.9	59.8	78.8	72.2	55.7	25.3	24.4	24.4	58.2	71.5	0.066	0.011	-0.02	-0.521	0.010

TABLE A-11. TEMPERATURE AND RADIATION MEASUREMENTS
FULL-SCALE TEST 6-19-80, INERT CEILING

TIME SEC	A 13 DEG C	A 14 DEG C	A 6 DEG C	A 7 DEG C	A 5 DEG C	A 9 DEG C	A 10 DEG C	A 11 DEG C	A 12 DEG C	B 1 W/CVCHSR	B 2 W/CVCHSR	C 3 1/M	D 4 W/CVCHSR	D 5 W/CVCHSR
8.4	22.8	27.3	23.2	23.7	23.9	23.4	22.2	24.9	23.5	-0.003	0.003	0.01	0.006	0.001
28.9	22.8	26.9	23.1	23.6	23.7	22.3	21.8	25.0	23.7	-0.001	0.005	0.01	0.006	-0.001
49.3	22.8	26.7	23.5	23.8	22.0	21.3	21.2	25.5	24.4	0.001	-0.009	0.02	0.006	-0.001
69.6	22.7	26.7	23.7	24.3	24.6	23.8	22.5	25.9	25.2	0.001	-0.000	0.04	0.006	-0.001
90.0	22.7	26.8	25.2	25.4	25.0	24.1	23.7	26.7	26.4	0.002	-0.003	0.04	0.008	0.000
110.5	22.9	27.1	25.2	25.2	25.0	23.8	22.7	27.3	26.2	-0.001	0.002	0.06	0.007	0.001
130.9	22.7	27.6	26.4	27.7	26.5	23.4	22.0	28.6	27.7	0.002	0.002	0.06	0.007	-0.000
151.3	22.8	27.9	27.6	27.9	26.8	23.7	21.2	29.7	28.6	-0.001	-0.009	0.06	0.008	-0.001
171.8	22.8	28.4	28.4	29.1	27.5	23.1	21.7	30.6	29.2	-0.001	-0.009	0.07	0.009	0.001
192.2	22.8	28.6	29.6	29.5	28.9	25.2	23.8	31.3	30.9	-0.004	0.005	0.06	0.008	0.000
212.7	22.8	29.0	31.1	31.3	29.8	25.2	21.3	32.8	32.2	0.003	0.003	0.07	0.009	0.000
233.1	22.8	29.3	31.9	32.3	31.0	26.1	22.5	34.0	34.1	0.006	0.005	0.08	0.009	0.000
253.5	22.8	29.6	33.7	33.9	32.6	26.3	22.1	35.9	35.0	0.001	0.001	0.06	0.011	0.001
273.9	22.8	30.0	34.8	35.3	33.6	26.4	23.6	37.4	37.1	0.001	-0.008	0.07	0.011	0.001
294.3	22.8	30.4	36.0	36.2	34.4	28.3	23.0	39.5	38.4	-0.000	-0.003	0.09	0.011	0.002
314.7	22.8	30.7	38.5	38.5	34.9	25.9	21.7	39.9	39.8	0.001	-0.002	0.11	0.012	0.001
335.1	22.8	31.2	40.7	41.1	38.9	31.9	21.8	42.1	42.0	0.001	-0.000	0.11	0.013	0.002
355.5	22.8	31.7	42.7	42.9	40.1	28.6	21.9	43.4	44.2	-0.001	0.001	0.07	0.015	0.001
375.0	22.9	32.4	43.6	44.3	42.8	30.1	23.8	45.3	45.5	0.005	-0.001	0.06	0.016	0.002
395.4	22.9	33.0	44.5	45.2	44.1	35.2	24.0	47.8	48.6	0.002	0.009	0.07	0.018	0.001
416.9	22.9	33.7	47.3	47.4	45.8	32.5	23.5	51.0	51.5	0.007	0.007	0.07	0.018	0.002
437.3	22.9	34.4	48.7	49.4	47.8	37.1	25.9	53.6	53.2	0.001	0.000	0.09	0.020	0.002
457.7	22.9	35.1	53.7	54.3	51.1	35.6	23.8	55.5	57.4	0.001	0.001	0.08	0.023	0.002
478.1	22.9	35.9	55.6	55.7	52.3	41.3	25.6	59.2	59.2	0.007	0.007	0.11	0.027	0.003
498.5	22.9	36.8	57.4	58.8	55.8	34.4	23.9	61.2	61.7	0.003	0.013	0.08	0.028	0.003
518.9	22.9	37.8	61.2	62.2	58.1	32.5	23.5	64.0	66.8	0.003	0.004	0.09	0.033	0.002
539.3	23.0	38.9	66.1	66.3	61.6	39.5	22.5	67.9	71.2	0.005	-0.010	0.07	0.034	0.003
559.8	23.0	40.1	68.3	68.6	62.9	40.1	23.5	72.8	75.0	0.008	0.006	0.12	0.038	0.003
580.2	23.0	41.4	72.9	73.4	68.5	41.8	23.1	77.3	77.3	0.002	0.006	0.10	0.042	0.002
600.7	23.0	42.9	77.1	77.6	72.4	33.7	24.7	79.7	84.4	0.007	0.006	0.11	0.047	0.003
621.1	23.0	44.4	80.0	80.5	75.2	37.8	22.6	83.0	84.7	0.006	0.008	0.11	0.054	0.003
641.6	23.0	45.9	84.7	86.6	77.8	39.7	23.9	86.7	92.2	0.009	-0.003	0.10	0.057	0.005
662.0	23.0	47.7	90.3	90.6	82.5	50.7	23.0	91.8	97.5	0.009	0.017	0.10	0.067	0.005
682.4	23.0	49.6	96.5	96.2	85.7	36.1	21.7	98.1	100.7	0.006	0.004	0.13	0.068	0.005
702.9	23.0	51.9	103.2	103.3	91.7	36.3	22.4	103.7	112.0	0.005	0.002	0.10	0.073	0.005
723.4	23.0	54.3	108.0	108.7	100.5	38.6	23.0	113.1	124.6	0.006	0.012	0.11	0.080	0.005
743.8	23.0	57.1	113.3	115.4	104.1	51.6	27.4	120.0	120.6	0.010	0.009	0.11	0.090	0.006
764.3	23.0	59.9	122.9	125.2	114.9	44.7	23.1	128.8	137.3	0.010	0.013	0.15	0.108	0.008
784.6	23.0	63.0	132.4	134.5	119.9	54.2	22.2	137.4	137.3	0.013	0.006	0.11	0.103	0.008
805.0	23.1	65.8	141.6	143.3	127.1	44.0	25.4	144.9	149.5	0.013	0.017	0.12	0.116	0.010
825.4	23.1	70.7	153.8	153.1	136.4	45.7	23.2	155.6	159.6	0.012	0.010	0.12	0.125	0.012
845.8	23.1	75.4	163.5	163.9	144.9	38.0	23.7	164.3	175.7	0.015	0.007	0.15	0.138	0.012
865.1	23.2	79.3	169.7	169.9	152.1	48.4	22.9	172.0	185.6	0.004	0.013	0.16	0.159	0.015
886.5	23.2	84.2	184.4	180.5	160.1	40.2	24.1	184.9	189.8	0.008	0.009	0.17	0.159	0.018
906.9	23.2	89.2	196.9	193.2	167.6	59.7	23.4	196.6	204.7	0.011	0.019	0.16	0.192	0.018

TEST 6-19-80

TIME SEC	A 13 DEG C	A 14 DEG C	A 6 DEG C	A 7 DEG C	A 8 DEG C	A 9 DEG C	A 10 DEG C	A 11 DEG C	A 12 DEG C	B 1 W/CMC MSR	B 2 W/CMC MSR	C 3 1/M	D 4 W/CMC M	D 5 W/CMC M
927.3	23.2	93.9	204.5	203.5	173.2	37.7	22.4	205.5	208.0	0.018	0.018	0.17	0.206	0.022
947.7	23.3	93.3	203.8	202.8	171.3	56.0	25.3	212.7	223.1	0.010	0.015	0.16	0.227	0.023
958.1	23.3	103.0	219.2	200.5	153.4	58.5	25.1	221.2	226.0	0.030	0.016	0.17	0.236	0.025
968.6	23.3	107.7	226.2	205.7	193.2	41.4	25.4	225.3	230.5	0.017	0.018	0.19	0.241	0.027
1008.9	23.3	112.8	238.7	230.5	204.4	60.1	25.2	235.5	231.8	0.018	0.022	0.21	0.271	0.029
1029.3	23.3	117.1	243.8	241.4	214.5	64.2	25.7	244.9	256.1	0.023	0.027	0.22	0.264	0.032
1049.7	23.3	121.2	249.1	247.2	219.9	54.6	25.4	248.6	272.4	0.024	0.028	0.24	0.284	0.035
1070.2	23.4	125.1	263.1	260.4	232.5	65.6	27.5	260.6	234.1	0.024	0.032	0.22	0.306	0.038
1090.7	23.4	131.3	278.5	275.0	242.1	95.8	33.4	279.5	305.7	0.027	0.037	0.25	0.343	0.041
1111.1	23.4	135.4	283.0	270.5	250.0	84.2	30.5	284.1	293.5	0.030	0.035	0.27	0.339	0.045
1131.6	23.5	142.3	285.7	273.9	257.5	75.3	29.0	283.5	311.0	0.027	0.038	0.29	0.404	0.049
1152.1	23.5	147.7	310.7	284.6	282.3	89.9	32.9	312.0	340.2	0.036	0.034	0.30	0.405	0.053
1172.6	23.5	152.7	306.7	306.7	272.8	65.8	29.1	314.8	343.3	0.034	0.036	0.33	0.418	0.056
1192.9	23.6	157.4	310.0	311.3	277.1	94.0	30.9	323.2	344.2	0.035	0.049	0.33	0.408	0.059
1213.3	23.6	161.6	313.9	320.3	256.1	76.9	29.7	330.2	331.6	0.040	0.056	0.34	0.474	0.065
1233.7	23.7	165.6	340.3	342.7	302.4	80.5	34.5	342.6	376.5	0.044	0.058	0.36	0.460	0.070
1254.0	23.8	171.5	343.6	343.8	311.1	84.3	31.7	353.2	385.1	0.046	0.059	0.37	0.481	0.074
1274.5	23.9	176.3	359.4	358.1	321.7	119.8	33.2	366.4	425.0	0.049	0.062	0.39	0.532	0.080
1294.8	23.9	182.0	367.9	363.2	330.9	115.2	34.3	372.4	425.2	0.046	0.068	0.39	0.553	0.086
1315.2	24.0	187.3	375.0	363.7	334.5	145.1	32.2	388.8	433.1	0.059	0.084	0.44	0.533	0.093
1335.6	24.0	193.4	384.1	391.2	351.9	115.3	33.1	401.3	410.2	0.055	0.092	0.44	0.637	0.099
1356.0	24.1	193.9	398.5	393.9	348.7	151.5	33.6	407.9	430.3	0.062	0.074	0.47	0.611	0.106
1376.3	24.2	204.5	402.3	412.8	370.0	185.4	43.1	431.0	432.1	0.071	0.090	0.48	0.709	0.113
1397.7	24.2	212.3	433.4	425.5	384.0	184.2	35.1	435.9	486.9	0.080	0.094	0.49	0.708	0.127
1417.1	24.3	218.6	442.3	443.8	400.5	174.9	37.3	444.7	475.0	0.080	0.102	0.52	0.742	0.136
1437.6	24.4	225.8	443.1	433.3	393.4	139.5	40.0	451.9	455.8	0.085	0.099	0.54	0.766	0.145
1457.9	24.5	231.7	454.9	450.7	399.2	188.3	44.1	472.4	515.2	0.093	0.105	0.56	0.855	0.149
1478.2	24.6	237.4	456.8	454.9	408.6	164.9	40.5	481.9	514.0	0.098	0.116	0.61	0.857	0.160
1498.7	24.8	241.5	461.9	453.4	414.4	208.9	42.5	481.7	572.5	0.101	0.128	0.55	0.847	0.162
1519.0	24.8	246.2	462.1	458.0	423.8	219.4	42.5	476.7	555.3	0.105	0.138	0.58	0.855	0.173
1539.3	24.9	250.3	463.7	454.6	422.4	239.2	52.7	495.2	532.5	0.109	0.146	0.60	0.876	0.179
1559.7	25.0	255.3	473.5	473.6	431.9	222.4	45.3	505.5	576.6	0.113	0.150	0.65	0.972	0.193
1580.1	25.2	260.2	491.1	483.3	432.2	223.1	51.0	515.5	622.5	0.122	0.157	0.71	1.032	0.198
1600.4	25.3	264.1	487.2	481.8	432.6	216.8	49.4	509.6	555.2	0.127	0.159	0.71	0.961	0.202
1620.8	25.4	267.2	485.0	480.0	435.5	233.9	51.7	514.3	613.3	0.130	0.161	0.69	1.026	0.206
1641.2	25.5	270.0	507.1	510.0	445.9	241.6	67.2	530.4	601.3	0.130	0.163	0.67	1.017	0.215
1661.6	25.7	274.7	502.9	493.6	442.1	202.6	45.3	498.0	569.2	0.140	0.165	0.70	1.023	0.223
1681.9	25.9	278.4	509.9	495.0	444.4	262.1	61.4	526.6	636.1	0.149	0.179	0.70	1.116	0.230
1702.3	25.9	282.8	495.9	509.2	456.4	237.8	51.9	533.6	626.1	0.149	0.186	0.72	1.051	0.234
1722.6	26.1	285.6	510.3	512.9	471.7	222.0	54.1	544.9	620.0	0.149	0.185	0.73	1.092	0.248
1742.9	26.3	289.6	507.5	509.6	454.7	261.8	63.2	540.5	656.9	0.150	0.197	0.77	1.090	0.249
1763.3	26.5	293.2	513.3	515.3	453.3	222.1	54.0	550.1	659.4	0.157	0.193	0.77	1.164	0.258
1783.6	26.6	296.7	516.3	525.5	467.7	220.9	51.8	550.9	614.1	0.161	0.200	0.78	1.156	0.270
1804.0	26.7	300.3	525.1	527.7	481.7	247.8	61.1	559.1	667.4	0.174	0.208	0.76	1.201	0.290
1824.3	26.8	305.5	523.6	519.2	468.1	266.0	73.1	545.7	675.0	0.179	0.217	0.77	1.235	0.298

TEST 6-19-80

TIME SEC	A13 DEG C	A14 DEG C	A6 DEG C	A7 DEG C	A8 DEG C	A9 DEG C	A10 DEG C	A11 DEG C	A12 DEG C	B1 W/CMMSR	B2 W/CMMSR	C3 1/M	D4 W/CMCM	D5 W/CMCM
1845.0	27.0	314.0	524.9	544.1	437.4	273.2	51.3	335.3	636.7	0.195	0.245	0.87	1.335	0.330
1845.5	27.2	314.6	539.3	553.5	507.1	281.9	57.6	605.2	609.0	0.209	0.254	0.89	1.375	0.381
1846.0	27.3	320.6	541.5	559.0	433.1	309.1	65.0	585.6	708.2	0.218	0.255	0.87	1.345	0.388
1846.3	27.5	335.0	530.7	535.0	531.2	310.4	54.3	603.3	717.2	0.224	0.266	0.84	1.392	0.378
1846.8	27.7	339.1	527.7	541.0	531.0	275.1	55.4	502.1	711.7	0.228	0.279	0.93	1.354	0.330
1847.2	27.8	343.7	540.3	552.5	532.5	316.5	55.6	583.4	795.9	0.232	0.282	0.93	1.381	0.391
1847.7	28.0	347.6	541.4	544.1	533.6	237.1	61.0	581.6	721.0	0.244	0.280	0.89	1.403	0.408
1848.1	28.3	350.9	557.6	553.4	535.8	233.9	64.0	607.9	737.2	0.266	0.304	0.99	1.530	0.449
1848.5	28.5	352.0	550.1	557.3	534.2	271.1	52.8	695.7	670.6	0.270	0.314	1.00	1.499	0.449
1849.0	28.8	355.5	540.3	551.0	532.7	274.6	53.4	583.4	717.0	0.271	0.314	1.06	1.501	0.453
1849.3	29.0	358.1	550.9	557.2	533.2	233.8	75.2	621.5	737.5	0.283	0.324	1.14	1.519	0.473
1849.7	29.2	371.1	551.1	554.4	535.4	307.1	54.0	612.9	739.3	0.289	0.330	1.08	1.553	0.429
1849.9	29.4	377.8	563.0	574.0	531.0	290.8	64.5	647.5	735.8	0.302	0.340	1.08	1.619	0.524
1850.3	29.6	383.6	551.4	573.9	532.8	345.3	78.4	630.8	751.2	0.312	0.371	1.16	1.648	0.534
1850.7	29.8	384.4	554.3	582.0	532.4	349.5	62.9	629.2	731.8	0.303	0.361	1.11	1.590	0.536
1851.2	30.0	385.8	558.7	584.1	533.8	200.3	59.1	605.9	747.2	0.319	0.363	1.08	1.587	0.530
1851.5	30.2	390.5	566.3	575.3	535.7	275.4	57.1	577.9	733.5	0.326	0.375	1.23	1.617	0.575
1851.9	30.5	392.3	563.3	577.1	533.6	321.1	57.7	577.1	734.1	0.326	0.373	1.12	1.684	0.573
1852.3	30.7	394.8	560.5	575.0	533.0	301.4	65.0	603.0	732.3	0.330	0.388	1.30	1.678	0.503
1852.6	31.0	394.5	558.0	575.6	534.7	295.8	83.1	555.4	741.8	0.335	0.386	1.13	1.684	0.572
1853.0	31.2	392.7	560.3	573.7	535.0	272.8	83.5	635.3	745.0	0.329	0.370	1.22	1.618	0.573
1853.3	31.6	394.6	561.3	583.7	535.9	301.7	65.2	631.2	755.4	0.336	0.376	1.21	1.636	0.592
1853.8	31.8	399.3	584.4	583.1	533.2	314.4	76.4	701.1	739.0	0.346	0.355	1.26	1.719	0.514
1854.2	32.2	401.3	569.6	583.2	535.1	303.0	75.6	634.5	745.2	0.350	0.410	1.43	1.712	0.631
1854.5	32.4	400.8	554.8	583.5	535.1	312.0	74.6	632.5	760.2	0.347	0.394	1.22	1.673	0.622
1854.7	32.6	422.8	562.7	583.5	535.5	312.4	74.6	617.7	750.4	0.337	0.400	1.32	1.681	0.619
1855.4	32.9	433.0	563.9	583.6	535.0	301.9	72.1	700.4	740.9	0.356	0.402	1.25	1.749	0.644
1855.8	33.0	433.7	563.7	583.9	535.5	322.2	85.4	711.1	774.0	0.376	0.432	1.31	1.835	0.658
1856.1	33.4	411.9	574.4	583.9	537.3	332.2	77.1	723.9	779.5	0.367	0.429	1.51	1.836	0.672
1856.6	33.7	412.4	563.9	582.7	533.8	291.8	72.4	703.9	771.3	0.360	0.423	1.46	1.795	0.673
1856.9	34.1	412.4	564.9	584.5	532.9	234.2	74.0	705.3	774.8	0.379	0.447	1.33	1.766	0.674
1857.3	34.4	414.1	560.2	583.9	535.3	334.1	60.8	712.5	769.3	0.377	0.434	1.43	1.879	0.692
1857.7	34.7	415.7	578.3	584.2	534.3	235.8	73.7	703.7	773.3	0.383	0.450	1.34	1.821	0.693
1858.0	34.9	417.7	570.8	583.5	533.6	323.7	101.5	734.1	775.4	0.396	0.457	1.48	1.881	0.706
1858.4	35.3	417.1	565.1	594.2	533.4	320.0	127.9	703.4	775.8	0.393	0.451	1.47	1.868	0.699
1858.8	35.6	415.5	573.6	602.5	533.6	259.4	89.2	735.6	785.2	0.396	0.451	1.38	1.833	0.726
1859.2	35.8	423.2	575.1	593.0	533.9	313.9	88.1	730.9	780.8	0.413	0.457	1.39	1.893	0.754
1859.6	36.1	428.0	574.9	598.2	533.9	297.1	84.3	757.8	786.1	0.424	0.480	1.64	2.033	0.771
1859.9	36.5	429.4	578.3	593.5	541.1	306.1	115.5	725.7	782.9	0.421	0.479	1.53	1.935	0.746
1860.3	36.8	428.6	574.6	593.5	532.0	277.8	83.3	717.8	776.1	0.410	0.477	1.35	1.923	0.763
1860.7	37.2	427.5	567.0	595.7	531.4	272.9	83.3	739.7	782.0	0.418	0.478	1.43	1.976	0.756
1861.1	37.5	429.7	573.0	599.2	534.8	329.2	83.0	742.6	778.3	0.427	0.479	1.35	1.937	0.770
1861.5	37.4	412.0	354.7	356.5	337.3	228.6	134.6	184.3	729.5	0.347	0.422	1.67	1.520	0.567
1861.9	37.0	300.5	216.4	174.5	98.1	77.0	-9.4	202.6	573.0	0.150	0.202	0.71	0.553	0.233
1862.4	36.8	287.3	272.3	222.6	102.2	59.8	44.4	221.9	485.9	0.113	0.145	0.62	0.439	0.176

TEST 6-19-80

TIME SEC	A13 DEG C	A14 DEG C	A6 DEG C	A7 DEG C	A8 DEG C	A9 DEG C	A10 DEG C	A11 DEG C	A12 DEG C	B1 W/CMSR	B2 W/CMSR	C3 I/M	D4 W/CMSR	D5 W/CMSR
2751.8	36.8	271.6	243.7	193.5	77.2	51.2	41.8	182.9	430.7	0.009	0.115	0.45	0.417	0.151
2732.2	36.7	253.4	231.6	175.1	76.5	52.1	39.9	154.4	351.8	0.005	0.105	0.35	0.385	0.133
2702.7	36.9	233.7	214.2	158.0	67.5	50.9	33.9	161.8	352.1	0.078	0.088	0.24	0.357	0.120
2823.0	36.9	228.4	208.3	159.6	60.5	47.9	38.4	151.0	339.7	0.073	0.075	0.18	0.330	0.108
2843.4	37.0	219.3	203.3	152.1	66.4	44.0	35.4	164.9	318.5	0.071	0.076	0.10	0.297	0.101
2853.7	37.0	211.0	190.4	133.2	65.0	48.6	33.4	153.3	302.8	0.064	0.065	0.04	0.280	0.093
2864.0	37.2	204.2	185.8	127.1	55.4	46.0	37.0	154.7	290.8	0.060	0.035	-0.01	0.274	0.095
2904.4	37.3	193.1	187.9	142.2	54.0	39.3	35.0	107.3	275.2	0.053	0.050	-0.04	0.255	0.032
2924.7	37.4	192.5	180.1	124.1	52.8	43.1	33.2	111.9	259.4	0.053	0.055	-0.02	0.253	0.077
2945.0	37.9	187.7	177.5	142.9	53.9	38.3	37.5	128.4	254.7	0.053	0.041	-0.05	0.225	0.072
2955.3	38.0	182.7	177.7	120.5	57.2	38.4	33.6	133.1	243.5	0.045	0.037	-0.07	0.239	0.068
2985.6	38.1	179.3	168.3	115.6	61.3	41.5	34.1	136.6	241.8	0.043	0.048	-0.13	0.238	0.065
3006.0	38.2	174.1	171.1	129.1	53.2	37.6	31.4	128.7	237.7	0.041	0.043	-0.17	0.227	0.061
3026.3	38.4	170.4	166.3	112.8	49.4	39.5	34.1	133.8	230.2	0.033	0.028	-0.18	0.220	0.059

TABLE A-12. TEMPERATURE AND RADIATION MEASUREMENTS

FULL-SCALE TEST 7-9-80, NAFEC #234 CEILING

Time Sec	A6 °C	A7 °C	A8 °C	A9 °C	A10 °C	A11 °C	A12 °C	B1 W/cm ² sr	B2 W/cm ² sr	C3 1/m	D4 W/cm ²	D5 W/cm ²
8.7	22.4	22.7	22.5	20.4	20.0	23.1	22.8	0.006	0.004	0.00	-0.000	-0.001
29.2	22.3	22.4	21.9	20.5	20.1	23.4	22.2	0.004	0.012	0.01	0.000	-0.001
49.8	22.4	22.4	22.0	20.0	20.4	23.3	23.3	0.002	0.004	-0.00	-0.001	0.000
70.3	22.7	22.9	22.3	20.9	20.8	23.7	23.4	0.004	0.016	0.00	0.001	-0.000
90.3	23.1	23.3	22.9	20.7	20.4	23.3	23.6	-0.002	0.000	0.00	-0.000	-0.001
111.4	23.3	23.3	23.1	20.2	20.2	25.4	25.6	0.003	0.004	0.00	-0.000	0.001
132.0	23.5	23.9	23.9	20.3	20.4	25.1	25.5	0.001	0.012	0.00	-0.001	-0.001
152.6	23.1	24.8	24.8	21.2	19.3	26.4	25.5	0.000	-0.001	0.00	0.001	-0.001
173.2	26.1	25.9	24.4	21.2	20.3	27.4	27.3	0.002	0.010	0.00	0.000	-0.000
193.8	27.1	26.7	25.2	21.3	20.4	26.3	27.1	-0.003	0.003	0.00	0.000	-0.001
214.3	27.7	27.1	26.3	22.0	20.3	29.4	29.8	0.002	0.011	0.01	0.000	0.000
234.9	29.4	28.9	27.7	21.6	20.5	30.4	29.5	0.002	0.003	0.01	-0.000	-0.001
255.5	30.2	30.0	26.9	21.9	20.5	31.5	31.6	-0.001	-0.001	0.00	0.001	-0.000
276.0	31.7	31.4	25.1	21.1	22.2	33.0	32.4	0.002	0.005	0.01	0.001	-0.001
296.6	33.2	32.5	23.8	22.0	20.0	33.8	33.6	0.000	0.010	0.02	0.000	-0.000
317.2	33.7	33.4	29.5	21.1	20.2	36.2	35.0	0.003	0.009	0.01	0.001	-0.001
337.8	35.2	35.0	32.5	24.1	23.8	36.7	35.0	0.005	0.007	0.02	0.001	-0.001
358.4	36.3	35.2	32.4	24.8	22.5	37.4	33.8	0.000	0.009	0.02	0.001	-0.002
379.0	38.2	37.4	34.7	24.8	20.9	40.0	39.2	-0.001	0.003	0.02	0.001	-0.002
399.5	40.0	39.3	34.8	22.4	20.4	41.5	42.4	0.002	0.006	0.02	0.002	-0.001
420.1	41.3	40.9	36.5	23.5	20.6	43.0	43.7	0.000	0.005	0.02	0.002	-0.000
440.7	42.9	44.1	39.1	24.1	21.2	45.0	45.4	0.002	0.009	0.02	0.002	-0.001
461.3	45.0	45.2	41.2	25.3	20.4	47.1	45.3	0.003	0.003	0.02	0.003	-0.002
481.8	45.6	45.7	42.9	27.8	21.8	43.1	41.5	0.002	0.012	0.03	0.004	-0.000
502.4	49.8	49.3	43.3	26.0	20.7	50.4	51.3	0.002	0.011	0.05	0.003	-0.000
522.9	52.7	52.1	45.3	25.9	21.6	53.5	52.9	-0.000	0.010	0.05	0.003	-0.000
543.4	53.7	52.9	47.0	24.9	20.5	54.5	53.1	0.002	0.002	0.06	0.003	0.000
564.0	56.7	54.1	47.1	26.1	20.2	57.6	53.7	-0.002	0.005	0.06	0.004	0.001
584.5	58.8	57.8	51.9	27.0	20.3	55.8	61.2	0.006	0.007	0.05	0.004	0.000
605.1	62.3	60.4	53.9	26.4	21.7	62.0	63.6	-0.000	0.004	0.05	0.006	0.002
625.6	64.3	62.7	55.7	26.9	22.3	65.8	67.5	0.003	0.016	0.06	0.004	0.002
645.2	65.8	65.7	59.3	27.1	23.1	68.3	71.7	-0.001	0.001	0.05	0.006	0.001
665.8	71.1	65.4	60.6	25.1	20.3	73.7	73.1	0.002	0.003	0.06	0.005	0.000
687.2	75.5	73.2	63.4	25.8	20.8	73.9	76.8	0.004	0.015	0.06	0.005	0.000
707.8	77.6	75.1	65.7	26.1	23.8	75.6	80.0	0.005	0.002	0.05	0.006	0.002
725.4	82.2	80.9	69.8	30.3	21.1	82.5	81.5	0.004	0.010	0.06	0.007	0.001
745.9	86.6	83.1	73.7	29.2	20.7	87.7	87.5	0.004	0.004	0.06	0.007	0.001
765.5	92.5	88.8	78.9	29.1	21.1	84.4	82.9	0.001	0.013	0.06	0.008	0.001
785.0	95.7	93.2	82.8	27.2	21.0	85.0	83.1	0.001	0.005	0.09	0.010	0.003
805.6	102.6	100.5	85.0	25.5	21.2	102.5	101.3	0.004	0.003	0.08	0.010	0.003
821.1	107.1	105.7	92.7	22.0	20.9	107.8	110.5	0.001	0.011	0.07	0.011	0.002
841.6	113.0	110.7	93.1	30.4	21.1	114.5	113.3	0.004	0.010	0.07	0.013	0.003
861.6	118.7	114.2	97.6	25.9	21.9	118.4	117.4	0.005	0.010	0.10	0.013	0.003
882.2	129.7	123.8	103.9	31.0	22.2	121.1	128.4	0.003	0.015	0.07	0.016	0.005
903.3	135.6	131.0	107.8	30.4	21.3	135.4	135.3	0.007	0.013	0.10	0.018	0.006

TEST 7-9-80

TIME SEC	A 6 DEG C	A 7 DEG C	A 8 DEG C	A 9 DEG C	A 10 DEG C	A 11 DEG C	A 12 DEG C	B1 W/CHCM	B2 W/CHCM	C3 1/M	D4 W/CHCM	D5 W/CHCM
533.9	144.5	139.0	115.2	28.3	21.1	140.3	146.2	0.005	0.017	0.10	0.019	0.008
554.4	149.2	143.5	117.5	28.9	21.3	145.4	147.7	0.009	0.004	0.11	0.020	0.007
575.0	157.0	152.9	121.9	27.2	21.7	151.6	155.2	0.004	0.009	0.13	0.022	0.003
595.6	163.6	154.5	125.5	33.5	21.5	163.7	158.8	0.002	0.006	0.14	0.026	0.003
1016.2	172.8	166.4	133.2	29.6	21.9	168.6	163.5	0.008	0.013	0.14	0.029	0.008
1036.8	177.7	167.8	136.6	32.2	22.1	171.9	170.5	0.007	0.010	0.13	0.031	0.009
1057.4	183.4	175.1	143.2	27.2	22.5	179.5	189.0	0.008	0.020	0.11	0.034	0.009
1078.0	193.7	183.0	149.0	29.5	22.9	189.7	187.7	0.006	0.013	0.09	0.036	0.010
1098.6	194.9	187.1	149.6	28.9	22.2	191.3	183.7	0.011	0.011	0.09	0.038	0.012
1119.2	206.2	197.0	156.7	36.1	24.3	201.3	203.5	0.007	0.021	0.10	0.042	0.013
1139.6	210.4	203.7	156.3	33.3	24.1	202.7	202.9	0.011	0.012	0.10	0.045	0.015
1160.4	220.0	210.3	170.5	22.7	23.2	210.4	213.0	0.011	0.021	0.09	0.043	0.015
1181.1	225.6	219.6	171.0	32.3	23.7	221.4	234.4	0.013	0.023	0.10	0.053	0.017
1201.7	228.6	218.4	177.4	30.0	24.4	223.8	229.8	0.012	0.015	0.12	0.057	0.018
1222.4	245.1	238.3	183.4	45.3	25.6	238.7	243.8	0.015	0.016	0.14	0.059	0.020
1243.0	290.5	255.2	178.9	62.1	28.2	280.5	251.5	0.010	0.021	0.17	0.076	0.025
1263.7	306.2	275.0	174.0	50.0	25.6	304.4	283.7	0.012	0.018	0.17	0.088	0.026
1284.5	323.6	298.4	201.2	62.8	27.3	321.8	307.0	0.021	0.026	0.18	0.098	0.032
1305.2	341.9	309.4	220.9	52.0	26.9	326.0	302.3	0.024	0.024	0.19	0.111	0.038
1325.8	350.5	311.9	216.1	46.9	26.8	343.0	310.2	0.024	0.026	0.20	0.120	0.042
1346.4	374.8	323.1	205.8	44.4	26.8	346.2	321.9	0.025	0.036	0.21	0.139	0.048
1367.1	416.8	354.2	237.9	49.2	27.9	353.0	327.5	0.032	0.047	0.22	0.162	0.057
1387.8	413.7	368.9	260.4	81.1	31.7	410.6	349.0	0.032	0.044	0.23	0.176	0.062
1408.5	417.0	379.8	280.5	62.0	32.8	353.3	340.6	0.035	0.044	0.26	0.184	0.067
1429.2	335.0	377.9	292.0	92.1	30.5	400.5	366.5	0.035	0.052	0.25	0.168	0.069
1439.9	410.0	378.5	296.1	93.0	35.0	423.4	384.1	0.039	0.051	0.25	0.203	0.072
1470.6	449.7	401.4	308.0	78.4	35.4	451.9	400.3	0.044	0.051	0.27	0.227	0.081
1491.3	462.5	427.7	320.5	68.6	32.9	443.7	407.1	0.045	0.051	0.25	0.254	0.092
1511.9	434.6	436.8	290.3	75.2	32.8	456.5	435.3	0.055	0.058	0.27	0.269	0.107
1532.5	508.0	462.3	342.8	76.8	37.3	468.7	403.4	0.061	0.058	0.28	0.311	0.121
1553.1	499.3	452.9	333.2	94.4	35.2	500.6	422.4	0.066	0.071	0.28	0.333	0.129
1573.7	495.4	459.2	342.4	88.7	33.8	482.1	434.8	0.066	0.079	0.30	0.337	0.132
1594.3	501.0	450.7	364.7	98.5	39.3	492.0	441.5	0.065	0.075	0.28	0.339	0.132
1615.0	505.6	453.2	329.5	66.2	35.8	470.9	440.4	0.073	0.075	0.29	0.348	0.136
1635.6	492.7	467.3	341.2	75.5	39.2	448.8	410.3	0.072	0.076	0.31	0.347	0.136
1656.2	479.3	444.9	345.7	70.7	35.5	469.9	439.6	0.063	0.065	0.30	0.344	0.130
1676.9	477.5	458.2	352.8	104.5	39.6	463.4	430.4	0.072	0.079	0.32	0.359	0.135
1697.5	498.3	450.3	341.9	112.5	43.7	483.1	475.8	0.068	0.068	0.33	0.375	0.141
1718.2	479.9	454.8	352.1	90.3	38.9	485.9	435.5	0.057	0.079	0.33	0.380	0.141
1738.8	506.0	457.0	354.6	110.2	38.4	489.3	493.4	0.071	0.089	0.36	0.391	0.146
1759.5	490.6	471.3	369.9	111.7	39.1	494.9	485.3	0.070	0.102	0.37	0.400	0.150
1780.1	502.5	476.1	375.1	97.1	38.4	495.2	473.2	0.077	0.085	0.42	0.411	0.158
1800.8	500.6	475.6	370.9	114.9	41.8	513.0	513.2	0.077	0.080	0.39	0.425	0.158
1821.5	501.1	473.2	388.9	95.1	41.5	505.0	509.9	0.074	0.087	0.38	0.426	0.162
1842.1	509.4	478.1	409.9	113.5	41.6	524.4	521.2	0.074	0.096	0.38	0.446	0.163

TEST 7-9-80

TIME SEC	A 6 DEG C	A 7 DEG C	A 8 DEG C	A 9 DEG C	A 10 DEG C	A 11 DEG C	A 12 DEG C	5' W/CNOMSR	B2 W/CNOMSR	C2 1/M	D4 W/CNOM	D5 W/CNOM
1802.8	495.4	490.9	364.6	109.8	48.9	500.9	500.4	0.079	0.086	0.42	0.450	0.170
1823.5	514.5	491.2	360.0	96.9	43.3	525.4	523.5	0.084	0.091	0.41	0.452	0.170
1904.1	529.3	494.9	333.9	104.3	42.6	524.1	523.9	0.093	0.104	0.42	0.472	0.178
1924.8	504.4	490.1	335.1	115.5	52.6	534.1	521.2	0.090	0.089	0.45	0.477	0.182
1945.5	517.7	504.5	361.8	131.2	0.8	520.1	520.0	0.099	0.102	0.50	0.490	0.187
1956.2	518.0	497.7	367.0	131.1	50.2	521.9	523.2	0.094	0.107	0.50	0.491	0.190
2006.9	515.4	494.5	337.0	118.6	43.4	536.9	521.6	0.091	0.103	0.51	0.515	0.193
2027.6	517.1	502.1	405.3	130.0	50.2	530.9	531.3	0.093	0.110	0.49	0.518	0.194
2038.3	511.3	493.0	402.6	114.0	52.3	540.0	537.8	0.090	0.107	0.50	0.492	0.188
2049.0	497.9	494.0	378.4	115.9	55.7	528.3	530.0	0.093	0.111	0.54	0.530	0.188
2059.7	531.2	497.1	394.3	120.9	50.3	548.6	530.1	0.093	0.105	0.54	0.531	0.198
2090.4	523.5	509.2	426.9	125.2	43.5	545.9	531.5	0.093	0.106	0.55	0.537	0.208
2111.1	509.3	485.0	404.3	121.9	45.4	533.1	530.1	0.099	0.107	0.56	0.537	0.200
2131.8	523.9	500.6	421.4	177.5	49.3	529.0	533.7	0.096	0.106	0.56	0.530	0.208
2152.5	515.5	515.5	414.1	156.3	46.2	541.9	535.7	0.106	0.123	0.59	0.555	0.216
2173.2	520.3	514.0	405.9	129.9	49.1	548.0	573.1	0.103	0.118	0.59	0.573	0.218
2193.9	524.0	496.1	412.9	161.5	53.0	555.1	578.3	0.105	0.122	0.61	0.581	0.222
2214.5	525.7	508.6	431.3	169.6	49.3	552.8	606.2	0.112	0.124	0.58	0.590	0.222
2235.1	533.4	512.9	431.2	162.3	50.5	531.2	594.9	0.111	0.118	0.60	0.518	0.234
2255.6	544.8	522.3	441.5	162.1	40.6	573.2	595.4	0.115	0.134	0.60	0.527	0.246
2276.2	535.5	516.7	415.1	145.6	56.2	502.6	635.4	0.123	0.131	0.60	0.629	0.242
2296.8	329.5	314.8	263.6	100.8	44.1	342.3	437.6	0.117	0.132	0.56	0.447	0.168
2317.4	200.5	156.8	65.2	43.0	35.9	133.8	329.7	0.031	0.069	0.47	0.177	0.093
2338.1	151.1	110.8	41.4	37.4	29.5	121.4	249.6	0.051	0.043	0.30	0.136	0.071
2358.8	125.6	79.7	40.7	36.9	33.6	72.9	205.5	0.040	0.049	0.22	0.109	0.057
2379.3	119.2	82.2	41.6	34.2	30.2	76.8	169.0	0.032	0.035	0.16	0.091	0.047
2399.9	105.7	61.4	34.3	35.7	31.3	86.2	151.7	0.027	0.027	0.12	0.078	0.039
2420.6	92.5	53.0	31.1	33.7	28.8	81.1	121.1	0.022	0.039	0.09	0.065	0.034
2441.2	71.8	40.8	30.2	31.0	27.4	78.6	118.7	0.021	0.022	0.06	0.062	0.028
2461.9	84.3	53.5	31.9	29.3	28.4	84.8	110.2	0.018	0.015	0.03	0.053	0.024
2482.5	87.1	63.9	32.6	31.4	27.1	51.6	106.1	0.018	0.010	0.02	0.039	0.021
2503.1	85.3	62.2	35.4	31.8	27.4	46.3	95.8	0.014	0.010	-0.01	0.043	0.019
2523.8	63.7	53.9	31.9	30.0	27.4	53.4	92.5	0.015	0.007	-0.01	0.042	0.016
2544.4	72.8	49.2	27.2	29.3	25.5	57.4	92.7	0.014	0.013	-0.02	0.035	0.014
2564.9	70.8	43.8	29.6	29.8	27.0	41.6	32.2	0.012	0.013	-0.03	0.033	0.010
2585.5	62.7	46.2	32.9	29.8	27.6	42.1	77.0	0.013	0.005	-0.04	0.031	0.009
2606.1	59.9	46.0	26.7	27.9	27.7	39.0	80.2	0.009	0.004	0.03	0.032	0.009
2626.7	59.2	44.9	31.3	27.9	27.2	34.6	75.3	0.010	0.007	0.03	0.039	0.009
2647.3	32.2	26.7	24.7	26.6	25.9	42.5	71.7	0.006	0.004	0.01	0.026	0.007
2657.9	58.3	39.9	25.9	26.8	25.5	44.9	68.7	0.008	0.007	0.02	0.027	0.005
2668.4	57.1	40.5	25.1	25.5	24.3	53.0	63.6	0.011	0.003	-0.00	0.023	0.005
2709.0	59.8	44.7	25.3	25.7	25.3	34.4	64.6	0.007	-0.005	0.00	0.025	0.004
2729.6	51.2	35.4	26.4	26.5	26.1	37.0	66.1	0.011	0.009	-0.00	0.023	0.003
2750.1	52.8	38.8	27.5	26.2	25.4	32.2	63.9	0.004	0.006	-0.12	0.022	0.002
2770.7	52.0	40.2	27.7	26.3	26.4	27.0	61.4	0.004	0.003	-0.12	0.022	0.001

TEST 7-9-80

TIME SEC	A 6 DEG C	A 7 DEG C	A 8 DEG C	A 9 DEG C	A 10 DEG C	A 11 DEG C	A 12 DEG C	B 1 W/CMMSR	R 2 W/CMMSR	C 3 1/M	D 4 W/CMCM	D 5 W/CMCM
2791.2	37.9	30.7	25.5	25.7	24.8	25.8	58.4	0.003	0.005	-0.11	0.020	-0.000
2811.8	47.3	37.3	27.9	25.9	24.8	35.7	43.6	0.005	-0.004	-0.10	0.017	-0.003
2832.4	48.3	35.8	25.6	25.3	24.7	31.5	54.9	0.008	-0.004	-0.10	0.013	-0.002
2852.9	48.7	35.5	25.2	25.5	24.1	35.4	56.8	0.004	-0.000	-0.11	0.019	0.000
2873.5	42.8	29.8	25.4	25.3	24.7	33.3	52.3	-0.002	0.003	-0.11	0.017	0.001
2934.1	40.9	32.7	25.2	25.5	24.4	29.8	49.8	0.006	0.003	-0.12	0.017	-0.001
2954.6	42.1	34.8	27.2	26.6	24.7	26.4	55.7	0.011	-0.000	-0.13	0.015	-0.002
2955.2	37.5	30.8	24.8	25.1	24.0	28.3	52.7	0.007	0.003	-0.11	0.015	-0.001
2955.7	32.4	28.4	26.3	25.9	24.8	29.3	51.2	0.001	0.010	-0.12	0.015	-0.002
2976.3	30.2	25.4	25.5	24.6	23.5	41.9	46.4	0.005	-0.005	-0.13	0.016	-0.002
2986.8	37.1	31.2	24.5	24.3	23.6	32.6	43.5	0.008	0.005	-0.12	0.014	-0.003
3017.4	28.4	25.7	23.5	24.6	24.2	33.7	44.8	0.002	0.009	-0.11	0.014	-0.003
3036.0	35.7	29.6	25.3	24.0	23.6	32.1	45.9	0.001	-0.004	-0.12	0.014	-0.003
3058.5	30.0	24.2	22.9	23.5	22.9	26.2	41.1	0.001	0.003	-0.09	0.012	-0.004

TABLE A-13. TEMPERATURE AND RADIATION MEASUREMENTS
FULL-SCALE TEST 7-22-80, NAFEC #B8811 CEILING

TIME SEC	A 6 DEG C	A 7 DEG C	A 8 DEG C	A 9 DEG C	A 10 DEG C	A 11 DEG C	A 12 DEG C	B 1 W/CMCMSR	B 2 W/CMCMSR	C 3 1/M	D 4 W/CMCMSR	D 5 W/CMCMSR
7.0	24.6	24.8	23.8	22.9	22.6	26.6	25.7	-0.001	0.000	0.00	0.001	0.000
23.3	24.7	25.1	25.0	23.6	22.7	26.9	26.3	-0.007	-0.008	0.01	0.001	-0.001
39.6	25.3	25.7	25.3	24.4	23.8	26.7	26.3	-0.008	-0.005	0.04	0.001	-0.001
55.9	25.5	25.9	25.8	25.1	24.0	27.4	27.0	-0.009	-0.001	0.03	0.001	-0.000
72.3	25.9	26.3	25.9	24.9	23.7	28.3	27.2	-0.012	-0.004	0.04	0.001	-0.000
88.7	27.0	27.1	25.8	25.0	23.9	28.4	28.8	-0.013	-0.008	0.03	0.001	-0.000
105.0	27.5	27.6	27.1	25.8	23.4	29.2	28.7	-0.008	-0.006	0.04	0.000	-0.000
121.2	28.4	28.4	26.8	27.2	25.5	30.4	30.7	-0.008	-0.002	0.03	0.001	-0.002
137.6	29.0	27.8	26.8	26.0	24.1	30.9	30.4	-0.007	-0.004	0.04	0.002	-0.002
154.0	29.5	29.5	27.6	24.6	23.0	31.5	30.9	-0.008	-0.002	0.02	0.001	-0.002
170.3	30.4	30.3	27.7	25.2	23.5	32.6	32.3	-0.004	-0.007	0.02	0.002	-0.001
186.5	30.7	31.4	28.7	25.2	23.3	33.3	33.2	-0.003	-0.001	0.02	0.002	-0.000
202.8	32.6	32.4	28.1	23.7	22.6	33.7	33.7	-0.008	-0.010	0.03	0.001	-0.001
219.2	32.9	32.7	30.7	27.6	23.7	34.2	34.1	-0.005	-0.015	0.07	0.001	-0.001
235.6	33.2	33.9	31.0	27.6	25.2	35.8	35.3	-0.008	-0.005	0.05	0.001	-0.002
251.8	34.5	34.6	33.3	27.5	24.7	36.5	36.5	-0.009	-0.008	0.06	0.001	-0.001
268.1	35.7	36.4	29.2	27.6	23.8	38.2	37.7	-0.015	-0.002	0.05	0.001	-0.001
284.4	37.6	37.7	33.4	28.1	25.1	39.3	39.6	-0.006	0.002	0.04	0.003	-0.001
300.8	38.7	39.3	32.2	26.9	24.0	41.4	42.6	-0.006	-0.005	0.03	0.004	-0.002
317.2	40.4	40.4	36.9	27.6	26.0	42.5	42.6	-0.005	0.000	0.02	0.003	-0.002
333.6	40.5	41.4	38.9	27.3	23.5	44.0	42.6	-0.012	0.000	0.03	0.004	-0.001
349.9	42.7	43.2	37.6	25.9	24.0	45.3	44.5	-0.008	-0.005	0.04	0.002	-0.000
366.3	44.2	44.8	41.3	29.6	25.0	47.1	46.4	-0.004	0.004	0.03	0.001	-0.000
382.6	45.8	45.5	43.3	28.7	24.0	47.8	48.7	-0.006	-0.008	0.08	0.003	-0.000
398.9	47.3	47.6	45.0	29.5	24.1	48.6	50.5	-0.004	-0.006	0.04	0.003	0.000
415.2	48.0	48.3	45.9	31.7	24.3	49.7	51.0	-0.010	0.001	0.04	0.003	-0.001
431.6	49.7	50.3	45.1	27.7	23.5	51.5	52.6	-0.007	-0.010	0.04	0.003	-0.001
447.9	49.6	49.6	47.4	34.7	25.1	51.9	52.5	-0.008	-0.003	0.01	0.003	0.000
464.3	53.6	53.5	49.2	33.1	24.7	55.6	57.3	-0.004	0.001	0.01	0.003	-0.000
480.5	53.9	54.6	51.2	30.8	25.0	58.0	56.1	-0.007	-0.001	0.01	0.003	0.000
496.8	55.0	55.7	53.0	33.8	24.2	58.1	56.0	-0.011	-0.006	0.01	0.004	0.002
513.1	58.3	59.1	54.7	31.7	23.4	61.1	59.6	-0.005	-0.003	0.00	0.005	0.001
529.4	59.3	60.0	56.4	31.6	24.9	63.6	64.2	-0.008	-0.008	0.01	0.005	0.001
545.8	61.1	62.1	57.7	33.3	25.9	66.7	66.2	-0.010	-0.006	0.02	0.005	0.000
562.1	65.5	66.9	61.5	32.5	24.2	67.4	70.0	-0.009	-0.013	0.04	0.005	0.002
578.5	67.1	66.9	62.6	33.4	24.6	69.2	69.5	-0.003	0.001	0.03	0.007	0.003
594.8	71.7	71.3	66.2	33.1	23.4	73.7	75.7	-0.002	0.001	0.03	0.008	0.002
611.2	72.2	71.6	65.7	29.1	24.0	75.9	78.8	-0.010	0.011	0.02	0.006	0.001
627.5	73.1	72.1	68.2	30.9	27.3	76.2	73.9	-0.005	-0.006	0.01	0.006	0.002
643.8	78.2	78.2	73.3	31.9	26.6	83.9	82.1	-0.010	-0.005	0.00	0.008	0.002
660.1	80.6	81.2	76.9	33.1	24.1	82.6	86.4	-0.008	0.002	0.01	0.007	0.004
676.5	82.3	82.8	76.8	29.9	24.9	86.7	88.1	-0.012	0.005	0.01	0.008	0.005
692.9	86.3	89.7	82.4	33.3	24.3	90.2	95.3	-0.004	0.009	0.01	0.009	0.004
709.2	89.4	90.8	84.3	31.5	24.7	99.3	100.9	-0.008	-0.010	-0.00	0.011	0.003
725.6	96.6	96.7	90.3	32.9	24.8	98.8	96.7	-0.008	-0.005	-0.00	0.011	0.003

TEST 7-22-80

TIME SEC	A 6 DEG C	A 7 DEG C	A 8 DEG C	A 9 DEG C	A 10 DEG C	A 11 DEG C	A 12 DEG C	B 1 W/CMCWSR	B 2 W/CMCWSR	C 3 1/M	D 4 W/CMCM	D 5 W/CMCM
741.9	102.1	101.5	92.0	40.3	25.9	104.5	106.0	-0.005	-0.011	0.00	0.012	0.003
758.2	105.6	105.5	98.0	31.6	25.5	115.4	109.8	-0.007	-0.011	0.01	0.014	0.004
774.6	112.2	112.0	99.0	34.2	25.4	116.4	115.5	-0.005	-0.004	0.01	0.014	0.004
791.0	114.6	114.9	104.5	30.3	26.6	118.5	123.5	-0.006	0.010	0.01	0.015	0.005
807.3	119.3	120.6	109.0	34.0	25.3	126.1	126.1	-0.005	0.002	0.01	0.016	0.006
823.5	131.1	130.8	115.3	50.4	27.3	131.0	131.1	-0.009	0.003	0.04	0.017	0.007
839.9	133.3	134.7	120.0	48.5	25.9	138.0	134.6	-0.003	0.003	0.02	0.021	0.008
856.2	138.9	137.2	125.0	39.4	26.6	143.2	142.2	0.002	-0.008	0.07	0.022	0.008
872.5	141.9	140.5	126.7	61.1	31.9	150.5	161.6	-0.000	-0.006	0.07	0.023	0.007
888.8	152.8	151.4	129.1	56.3	31.9	158.5	165.1	-0.001	0.005	0.06	0.027	0.007
905.1	155.6	160.3	145.7	35.3	25.0	162.6	158.7	-0.003	0.007	0.06	0.028	0.011
921.4	168.7	169.8	147.8	46.3	28.2	168.7	178.4	0.001	0.008	0.06	0.030	0.012
937.6	171.2	175.5	156.8	40.1	27.0	179.6	170.1	-0.005	0.003	0.07	0.035	0.013
953.9	182.4	182.4	160.6	36.8	27.6	191.1	188.6	-0.001	-0.001	0.07	0.037	0.014
970.2	191.0	191.5	169.4	41.0	25.9	198.2	199.5	0.003	0.010	0.07	0.041	0.016
986.6	204.7	202.9	181.4	47.4	25.3	206.4	212.4	-0.004	0.017	0.06	0.046	0.017
1002.9	214.2	214.6	182.8	54.0	25.0	215.2	225.4	0.004	0.014	0.08	0.051	0.020
1019.2	215.1	218.3	196.1	45.0	26.6	224.2	223.7	0.000	0.002	0.11	0.053	0.022
1035.5	227.9	232.2	200.6	57.1	26.9	241.6	235.5	0.003	0.008	0.09	0.058	0.023
1051.8	229.9	227.2	201.7	59.0	29.0	232.3	234.7	0.001	0.019	0.10	0.065	0.026
1068.2	249.4	246.9	217.0	63.3	28.6	259.5	251.3	0.002	0.015	0.11	0.072	0.029
1084.6	253.7	252.2	217.6	75.0	27.1	258.6	247.7	0.003	0.017	0.09	0.076	0.031
1100.9	262.4	254.8	220.2	55.8	27.2	255.4	280.3	0.003	0.015	0.10	0.081	0.032
1117.3	258.7	259.6	220.2	73.7	28.9	265.9	277.1	0.006	0.017	0.11	0.085	0.034
1133.6	263.9	269.5	230.5	116.3	33.7	283.0	299.9	0.004	0.021	0.11	0.091	0.037
1150.0	277.3	278.4	236.0	97.0	29.4	285.1	311.1	0.007	0.021	0.13	0.100	0.038
1166.4	282.9	282.0	245.4	88.9	29.4	286.0	328.7	0.008	0.030	0.18	0.105	0.040
1182.8	294.9	295.5	251.7	126.8	39.3	314.4	327.7	0.010	0.022	0.13	0.113	0.044
1199.2	310.8	311.6	259.8	86.0	29.4	321.0	332.3	0.011	0.022	0.15	0.123	0.048
1215.7	306.8	310.8	266.7	112.1	34.2	312.3	366.6	0.011	0.028	0.16	0.129	0.051
1233.1	323.1	325.8	280.6	90.6	31.1	330.6	355.7	0.014	0.027	0.17	0.142	0.055
1258.8	328.7	328.9	289.1	103.5	31.0	342.5	368.5	0.013	0.030	0.19	0.153	0.061
1277.8	353.0	344.7	290.4	117.6	36.3	364.2	373.6	0.020	0.040	0.20	0.163	0.063
1294.2	367.8	368.3	310.6	144.1	32.9	390.7	407.6	0.020	0.042	0.19	0.181	0.071
1310.7	409.3	403.0	337.1	174.0	38.6	420.1	390.3	0.025	0.049	0.23	0.212	0.083
1327.1	422.2	407.8	313.6	156.6	35.1	422.4	411.9	0.028	0.049	0.25	0.233	0.094
1343.6	431.1	418.3	338.0	136.5	32.6	448.4	447.9	0.033	0.057	0.27	0.246	0.099
1360.1	427.0	417.2	329.2	152.1	34.8	444.1	449.4	0.035	0.055	0.26	0.256	0.105
1376.6	444.0	436.8	333.8	168.9	38.0	445.1	424.9	0.034	0.065	0.29	0.273	0.111
1393.0	434.0	425.0	339.7	123.0	33.6	461.4	469.2	0.038	0.065	0.29	0.287	0.116
1409.4	461.2	442.2	356.9	169.2	35.7	492.1	455.9	0.042	0.071	0.29	0.310	0.125
1425.7	468.5	455.7	364.7	192.3	39.4	499.3	461.9	0.047	0.070	0.30	0.326	0.133
1442.1	471.0	460.4	364.9	176.3	37.0	516.4	470.0	0.050	0.072	0.30	0.339	0.139
1458.5	455.0	449.9	371.6	220.3	46.8	499.6	536.6	0.047	0.085	0.32	0.350	0.143
1474.8	467.2	466.0	379.1	205.7	45.3	498.8	459.2	0.058	0.095	0.34	0.356	0.149

TEST 7-22-80

TIME SEC	A 6 DEG C	A 7 DEG C	A 8 DEG C	A 9 DEG C	A 10 DEG C	A 11 DEG C	A 12 DEG C	B1 W/CMCHSR	B2 W/CMCHSR	C3 1/M	D4 W/CMCM	D5 W/CMCM
1491.2	459.0	465.8	393.7	173.0	50.1	516.7	510.4	0.059	0.084	0.34	0.365	0.152
1507.6	454.9	477.6	418.0	194.0	41.7	509.8	512.8	0.063	0.090	0.38	0.389	0.166
1524.0	474.7	483.0	413.8	190.6	43.0	522.3	536.5	0.062	0.090	0.37	0.394	0.166
1540.4	469.0	467.9	421.6	241.7	51.5	491.9	546.0	0.060	0.086	0.35	0.375	0.161
1556.8	459.1	468.1	402.4	197.9	42.6	496.7	563.2	0.062	0.095	0.37	0.392	0.167
1573.2	475.7	478.2	431.3	244.5	40.4	522.4	572.4	0.066	0.102	0.38	0.397	0.172
1589.6	459.1	463.0	438.7	214.2	43.7	516.3	573.8	0.063	0.101	0.34	0.406	0.176
1606.0	494.8	495.2	408.8	258.0	49.4	495.0	538.6	0.065	0.095	0.36	0.428	0.184
1622.5	494.9	499.2	419.5	244.6	49.2	542.4	511.7	0.068	0.109	0.41	0.459	0.200
1638.9	492.6	499.8	440.8	248.0	48.6	538.3	564.5	0.075	0.111	0.40	0.460	0.199
1655.3	487.1	495.8	422.0	262.8	64.2	554.4	569.0	0.084	0.110	0.41	0.483	0.206
1671.8	491.5	497.1	454.5	276.2	47.5	542.6	600.7	0.081	0.113	0.41	0.490	0.212
1688.2	503.7	517.0	431.6	217.0	44.4	538.3	585.3	0.086	0.115	0.44	0.499	0.218
1704.6	500.5	508.4	442.0	230.2	59.2	578.0	570.0	0.087	0.108	0.44	0.509	0.220
1721.1	509.6	501.4	436.0	250.5	56.9	574.6	593.5	0.097	0.126	0.47	0.551	0.238
1737.6	503.0	518.5	458.1	277.1	57.3	578.6	596.9	0.104	0.132	0.50	0.563	0.247
1754.0	522.7	524.5	448.2	261.7	57.0	595.2	590.9	0.099	0.132	0.50	0.580	0.255
1770.5	522.1	521.0	458.5	267.5	69.9	573.8	630.8	0.103	0.134	0.53	0.585	0.260
1787.0	504.0	500.3	442.3	269.7	52.0	559.3	629.3	0.102	0.138	0.49	0.547	0.245
1803.4	511.7	518.0	465.4	283.9	73.7	586.4	624.7	0.108	0.134	0.54	0.567	0.260
1819.9	523.1	529.9	455.7	260.0	59.2	585.2	630.1	0.107	0.129	0.55	0.586	0.260
1836.4	507.5	518.8	448.3	280.3	78.7	575.3	661.6	0.111	0.143	0.57	0.588	0.260
1852.9	520.6	521.3	463.9	249.8	60.6	592.7	605.8	0.119	0.141	0.56	0.627	0.279
1869.4	531.8	526.8	474.6	306.0	70.8	613.4	620.1	0.118	0.151	0.64	0.641	0.289
1885.8	521.1	533.8	472.6	249.4	58.4	599.7	661.0	0.126	0.152	0.58	0.653	0.290
1902.3	516.7	530.1	484.1	273.1	60.2	588.0	652.8	0.125	0.146	0.57	0.636	0.287
1918.8	525.6	525.9	466.2	287.3	58.3	600.3	664.7	0.117	0.148	0.51	0.626	0.282
1935.3	535.6	533.7	470.9	292.6	59.3	600.3	606.1	0.124	0.146	0.57	0.651	0.291
1951.8	528.5	540.6	472.2	283.6	63.6	606.6	682.1	0.121	0.145	0.54	0.666	0.299
1968.3	519.5	529.9	491.1	260.4	57.1	590.7	655.5	0.124	0.152	0.54	0.650	0.294
1984.8	531.9	541.8	502.4	297.5	63.1	604.7	693.5	0.123	0.156	0.52	0.677	0.297
2001.3	536.9	546.9	491.7	263.3	62.9	631.9	705.9	0.133	0.152	0.53	0.698	0.310
2017.9	533.6	542.7	485.8	274.8	63.3	619.0	699.4	0.144	0.159	0.57	0.721	0.322
2034.4	535.9	539.7	489.6	302.7	56.8	644.7	692.5	0.139	0.159	0.55	0.711	0.323
2050.9	541.3	543.3	479.6	288.4	60.2	604.7	675.7	0.134	0.165	0.54	0.730	0.331
2067.4	543.2	551.6	461.0	241.9	69.7	649.5	652.0	0.145	0.165	0.64	0.777	0.349
2084.0	541.8	557.9	488.9	235.9	49.7	630.0	713.1	0.144	0.165	0.57	0.765	0.336
2100.5	358.8	351.9	264.2	141.8	54.7	425.6	578.6	0.133	0.157	0.38	0.543	0.261
2116.9	241.9	210.4	106.2	53.9	40.4	207.2	321.1	0.049	0.069	0.36	0.195	0.117
2134.4	130.5	154.7	75.0	44.4	35.7	177.8	264.6	0.033	0.037	0.20	0.144	0.083
2150.8	179.1	142.5	81.7	38.8	35.1	152.6	215.2	0.019	0.028	0.08	0.114	0.066
2167.2	160.4	127.2	51.1	39.6	35.2	146.8	196.2	0.012	0.029	0.02	0.096	0.052
2183.6	150.0	128.0	64.0	37.0	35.3	126.5	176.5	0.003	0.023	-0.04	0.083	0.044
2200.0	142.5	117.4	65.3	37.0	34.5	117.0	156.9	0.009	0.013	-0.07	0.074	0.037
2216.4	131.3	113.4	60.1	34.3	33.1	106.5	150.1	0.001	0.014	-0.13	0.068	0.030

TEST 7-22-80

TIME SEC	A 6 DEG C	A 7 DEG C	A 8 DEG C	A 9 DEG C	A 10 DEG C	A 11 DEG C	A 12 DEG C	B 1 W/C/CMR W/C/CMR	B 2 W/C/CMR	C 3 1/M	D 4 W/C/CMR	D 5 W/C/CMR
2232.7	127.0	110.1	45.6	32.9	32.0	109.9	142.0	-0.000	0.035	-0.15	0.059	0.027
2233.1	120.3	99.4	52.2	30.6	32.5	100.5	133.9	-0.003	0.009	-0.19	0.054	0.025
2233.5	117.1	92.5	40.2	25.8	29.9	114.5	139.8	0.001	0.011	-0.22	0.051	0.022
2234.8	111.3	82.3	38.3	34.4	30.0	106.5	132.4	0.002	-0.003	-0.25	0.048	0.020
2235.2	111.1	85.3	35.3	31.7	29.4	105.3	128.3	-0.001	0.005	-0.27	0.042	0.019
2235.6	108.9	92.2	41.2	33.8	30.3	105.8	112.3	-0.001	0.001	-0.32	0.032	0.016
2236.0	104.6	91.2	30.3	34.9	31.3	91.8	123.5	-0.003	-0.009	-0.34	0.043	0.015
2237.3	93.4	84.3	40.3	31.0	29.9	93.8	114.8	-0.008	0.000	-0.36	0.039	0.014
2238.6	93.3	84.3	37.8	32.5	30.3	93.5	106.3	-0.005	0.002	-0.36	0.036	0.013
2239.0	93.6	87.7	31.6	29.0	27.8	93.6	118.1	-0.006	-0.007	-0.39	0.035	0.013
2239.3	93.2	82.9	38.8	31.0	28.9	87.7	104.6	-0.007	0.002	-0.40	0.033	0.010
2239.6	93.4	78.4	34.6	29.2	27.6	90.4	109.2	-0.003	0.004	-0.41	0.032	0.010
2239.8	93.9	77.8	33.9	29.2	27.7	93.1	103.6	-0.005	0.007	-0.42	0.030	0.010
2240.0	97.0	75.0	33.3	30.6	27.6	90.5	95.5	-0.009	0.002	-0.42	0.030	0.009

AD-A107 590

FACTORY MUTUAL RESEARCH CORP NORWOOD MASS

F/G 21/2

MODELING OF CEILING FIRE SPREAD AND THERMAL RADIATION.(U)

OCT 81 R L ALPERT, M K MATHEWS, A T MODAK

DOT-FA79NA-6019

UNCLASSIFIED

RC81-BR-3

DOT/FAA-CT-81-70

NL

2-2

AD-A107 590



END

DATE

FILED

1-82

DTIC

TABLE A-14. TEMPERATURE AND RADIATION MEASUREMENTS
FULL-SCALE TEST 7-30-80, NAFEC #223 CEILING

TIME SEC	A 6 DEG C	A 7 DEG C	A 8 DEG C	A 9 DEG C	A 10 DEG C	A 11 DEG C	A 12 DEG C	B2 W/CMCMR	C3 1/M	D4 W/CMCM	D5 W/CMCM
7.0	22.8	22.7	21.1	20.1	20.1	24.4	23.9	-0.000	-0.05	-0.002	-0.002
23.5	22.7	22.8	21.7	20.8	20.3	24.7	23.2	-0.006	-0.06	-0.002	-0.002
39.9	23.4	22.9	22.7	20.8	20.3	25.3	25.3	0.003	-0.04	-0.002	-0.001
56.4	23.7	23.8	23.3	20.5	20.1	25.6	25.2	-0.001	-0.05	-0.001	-0.001
72.8	24.3	24.0	23.4	22.0	21.1	25.7	25.3	0.014	-0.05	-0.001	-0.001
89.1	24.7	24.8	24.3	22.1	20.4	26.4	27.0	0.001	-0.04	-0.002	-0.002
105.6	25.5	24.7	24.1	20.6	20.6	27.2	27.0	0.007	-0.04	-0.001	-0.002
122.0	26.3	26.1	24.1	21.8	20.6	27.5	28.4	0.003	-0.05	-0.001	-0.001
138.4	26.8	26.1	24.6	22.9	21.7	28.6	28.9	-0.003	-0.04	-0.001	-0.001
154.8	27.6	27.3	25.7	23.6	21.4	29.3	29.5	0.003	-0.04	-0.000	-0.002
171.2	28.8	29.1	26.5	23.4	21.7	30.0	30.5	-0.014	-0.03	0.000	-0.002
187.7	29.3	28.7	25.3	21.2	20.4	30.9	31.2	0.001	-0.04	-0.001	-0.002
204.1	29.7	29.8	27.8	22.5	20.9	32.4	32.1	0.003	-0.04	-0.002	-0.002
220.4	30.6	30.7	26.5	23.2	20.9	32.8	34.2	-0.004	-0.04	-0.002	-0.003
236.8	32.4	32.3	27.4	23.4	20.6	34.1	35.3	0.003	-0.03	-0.001	-0.001
253.3	32.7	32.9	30.0	24.4	21.6	34.8	35.9	-0.005	-0.03	-0.002	-0.001
269.6	34.5	34.2	27.9	22.9	20.8	36.9	37.5	0.012	-0.05	-0.001	-0.002
286.1	35.1	35.0	33.6	26.3	21.4	36.9	38.4	-0.001	-0.03	-0.001	-0.002
302.5	36.3	36.8	33.4	23.6	22.6	38.6	40.1	0.010	0.10	0.001	0.000
318.9	37.5	38.0	35.3	27.4	23.3	39.7	41.9	-0.008	0.11	0.000	-0.002
335.2	38.5	38.6	36.0	22.6	20.7	41.5	42.5	-0.002	0.12	-0.001	-0.003
351.6	39.7	39.9	38.4	25.9	21.4	42.5	45.5	0.009	0.11	-0.001	-0.002
368.0	41.5	41.6	39.3	23.3	21.2	43.8	44.4	0.003	0.12	-0.001	-0.000
384.4	43.0	42.8	40.5	26.6	21.7	45.8	48.2	0.002	0.10	-0.000	-0.000
400.8	44.1	44.3	41.4	23.5	21.0	47.5	48.4	-0.000	0.11	-0.000	-0.001
417.2	45.9	46.1	43.7	26.1	21.6	49.1	52.6	-0.002	0.11	0.000	-0.001
433.7	48.1	48.4	44.4	25.2	22.4	50.5	53.7	0.000	0.11	0.000	-0.002
450.1	49.8	49.7	48.3	27.4	23.9	53.5	55.1	0.008	0.12	0.003	-0.002
466.5	52.0	52.7	49.8	29.5	24.5	53.3	57.1	0.002	0.13	0.001	-0.000
482.9	53.7	54.1	51.5	26.3	21.9	55.8	58.3	0.000	0.12	0.002	0.000
499.3	55.7	55.8	53.0	29.0	23.1	57.8	61.5	0.013	0.11	0.002	-0.000
515.7	57.4	57.6	54.5	28.2	22.5	61.0	62.4	0.020	0.11	0.003	0.000
532.1	58.2	59.3	56.6	27.1	22.6	63.5	63.5	0.001	0.12	0.003	0.001
548.5	62.6	62.8	58.9	29.2	22.3	65.6	70.3	0.013	0.09	0.003	0.002
564.9	64.1	65.3	61.6	26.8	22.4	69.6	63.8	0.000	0.02	0.003	0.001
581.4	66.0	65.9	61.7	29.2	22.0	70.1	73.7	0.008	-0.01	0.003	0.002
597.8	68.5	68.8	64.9	30.9	21.6	71.5	77.8	0.004	-0.01	0.004	0.000
614.2	71.1	71.7	66.3	26.8	22.9	75.2	78.4	0.007	-0.01	0.004	0.000
630.6	73.4	72.8	68.1	28.2	21.9	77.0	80.4	0.007	-0.01	0.004	0.002
647.0	75.8	75.8	72.0	32.2	21.6	81.5	86.8	0.004	-0.01	0.005	0.003
663.4	79.7	79.3	74.1	29.2	21.5	83.9	90.0	-0.002	0.00	0.006	0.002
679.8	83.7	83.3	75.9	27.0	21.3	89.9	91.8	0.015	0.01	0.006	0.002
696.2	87.3	86.3	80.5	30.4	21.1	91.5	90.2	0.011	-0.00	0.006	0.003
712.6	90.5	89.6	81.1	31.2	21.6	94.6	102.8	-0.003	0.03	0.007	0.003
729.1	94.4	95.2	86.9	31.6	23.3	101.7	106.3	-0.003	0.15	0.009	0.004

TEST 7-30-80

TIME SEC	A.6 DEG C	A.7 DEG C	A.8 DEG C	A.9 DEG C	A.10 DEG C	A.11 DEG C	A.12 DEG C	B2 W/CMCNR	C3 1/M	D4 W/CMCM	D5 W/CMCM
745.5	100.9	101.2	91.6	30.8	23.2	104.5	106.2	0.010	0.13	0.009	0.005
761.9	103.2	103.4	96.5	27.8	23.4	106.4	114.0	0.013	0.12	0.010	0.005
778.3	108.1	108.0	97.6	36.1	22.6	112.7	118.8	0.019	0.11	0.012	0.005
794.7	112.9	113.7	102.9	37.6	22.4	118.7	120.7	0.005	0.10	0.013	0.006
811.1	116.5	117.6	107.3	40.6	24.6	125.1	136.9	0.010	0.10	0.014	0.006
827.5	121.6	121.0	112.1	34.1	22.7	128.9	139.3	0.004	0.17	0.015	0.006
843.9	127.9	127.9	117.0	36.5	22.7	133.9	134.1	0.008	0.16	0.017	0.007
860.4	133.8	131.9	118.7	38.4	24.2	135.0	151.7	0.006	0.10	0.020	0.009
876.8	140.1	140.9	125.2	27.9	22.7	144.4	164.9	0.013	0.09	0.022	0.009
893.2	149.9	145.7	125.4	39.6	23.5	150.9	187.1	0.019	0.09	0.024	0.009
909.5	161.5	156.3	135.0	32.6	23.4	164.0	192.0	0.010	0.08	0.027	0.011
925.9	166.6	164.3	137.1	31.5	23.1	173.8	209.9	0.006	0.06	0.028	0.012
942.2	169.8	164.7	141.5	32.7	23.5	174.7	214.7	0.014	0.07	0.030	0.013
958.6	175.6	172.6	145.7	31.0	23.0	184.7	216.0	0.012	0.10	0.033	0.014
974.9	185.4	178.8	155.8	36.6	24.2	193.8	224.8	0.013	0.07	0.037	0.015
991.3	190.9	193.2	163.8	32.8	23.8	204.6	241.1	0.011	0.04	0.039	0.018
1007.8	197.2	195.4	158.7	30.7	24.8	214.0	237.7	0.020	0.08	0.044	0.019
1024.2	204.9	202.8	165.5	33.9	24.9	224.5	279.1	0.011	0.05	0.046	0.020
1040.5	208.7	203.5	174.9	32.9	23.7	215.7	258.3	0.017	0.06	0.049	0.022
1056.8	209.6	211.7	185.6	52.3	25.7	231.8	259.0	0.016	0.06	0.055	0.023
1073.1	233.5	229.4	201.3	63.3	28.3	255.6	274.3	0.016	0.07	0.063	0.027
1089.5	236.6	237.0	204.4	67.1	29.3	264.3	279.2	0.019	0.08	0.071	0.029
1105.8	249.8	242.7	210.3	79.4	27.6	280.9	291.2	0.029	0.07	0.079	0.031
1122.0	272.8	266.8	228.4	68.8	28.6	291.3	283.1	0.022	0.19	0.089	0.036
1138.3	268.9	257.8	229.3	82.6	28.6	286.9	306.3	0.026	0.18	0.093	0.040
1154.6	272.0	272.6	238.8	56.1	26.0	287.0	291.9	0.024	0.19	0.097	0.041
1171.0	268.6	268.9	236.5	65.6	27.6	301.1	308.1	0.034	0.19	0.101	0.043
1187.3	286.1	279.0	246.9	109.0	28.0	294.8	315.4	0.034	0.20	0.107	0.046
1203.6	294.8	285.4	251.8	117.8	29.0	316.1	323.6	0.036	0.21	0.116	0.051
1220.1	319.6	316.4	266.0	89.1	30.3	342.5	334.2	0.037	0.23	0.131	0.056
1237.1	309.9	313.4	283.9	85.0	29.1	340.8	367.6	0.035	0.19	0.142	0.060
1254.9	303.1	304.9	282.1	85.0	29.8	372.1	405.0	0.035	0.15	0.158	0.069
1271.2	298.1	286.5	236.9	60.4	27.9	378.0	377.0	-0.042	0.16	0.172	0.076
1287.6	300.9	291.0	321.0	259.8	141.2	376.0	412.4	-0.158	0.23	0.181	0.081
1303.9	370.5	364.9	319.6	152.0	37.5	373.8	384.7	0.055	0.19	0.189	0.084
1320.3	369.1	354.5	313.8	146.1	34.3	371.7	382.8	0.052	0.17	0.200	0.088
1336.7	377.4	382.8	325.1	109.5	33.0	394.3	433.5	0.063	0.17	0.212	0.093
1353.1	394.4	387.9	339.6	122.5	34.3	406.3	423.5	0.058	0.17	0.229	0.100
1369.5	393.7	393.3	351.6	155.5	34.6	405.2	430.5	0.064	0.17	0.243	0.107
1385.9	412.7	405.4	369.4	266.2	45.1	446.1	459.1	0.065	0.18	0.263	0.119
1402.2	427.3	422.7	378.0	204.3	42.5	440.0	459.3	0.069	0.22	0.289	0.132
1418.6	409.3	413.8	367.1	191.1	44.2	449.4	462.6	0.073	0.21	0.290	0.131
1434.9	447.1	437.0	384.7	227.2	44.2	477.1	523.0	0.083	0.21	0.320	0.148
1451.2	460.2	455.3	391.7	221.5	40.6	483.0	497.7	0.096	0.25	0.353	0.163
1467.5	474.1	468.4	412.1	211.4	43.6	487.0	497.5	0.108	0.26	0.382	0.177

TEST 7-30-80

TIME SEC	A 6 DEG C	A 7 DEG C	A 8 DEG C	A 9 DEG C	A 10 DEG C	A 11 DEG C	A 12 DEG C	B2 W/CMCM	C3 1/M	D4 W/CMCM	D5 W/CMCM
1483.8	456.3	465.2	411.6	206.1	46.3	492.9	522.5	0.113	0.30	0.395	0.185
1500.2	479.6	485.5	418.1	251.1	45.6	511.5	535.4	0.110	0.26	0.417	0.196
1516.5	497.7	493.4	422.5	215.0	46.7	515.8	575.4	0.119	0.28	0.430	0.206
1532.9	506.2	485.8	432.4	212.1	46.5	542.5	591.5	0.124	0.29	0.469	0.224
1549.2	507.6	494.3	439.6	205.0	47.3	571.0	606.5	0.128	0.46	0.500	0.241
1565.6	512.2	512.4	446.9	242.9	46.7	570.6	615.5	0.137	0.63	0.517	0.247
1581.9	509.8	510.5	448.6	238.8	51.4	553.1	569.0	0.140	0.62	0.535	0.256
1598.2	488.8	493.9	445.1	185.9	47.0	558.3	579.9	0.139	0.58	0.522	0.254
1614.6	510.3	508.7	463.3	219.7	47.9	569.9	633.2	0.139	0.60	0.552	0.270
1631.0	513.8	508.7	449.2	225.2	54.0	580.1	672.1	0.138	0.59	0.556	0.271
1647.3	521.6	525.7	469.0	237.3	63.1	593.4	628.8	0.151	0.62	0.597	0.289
1663.7	522.2	509.1	457.3	262.5	50.7	566.1	610.7	0.152	0.65	0.601	0.292
1680.0	504.2	507.7	444.6	215.3	50.9	572.5	679.8	0.153	0.56	0.591	0.287
1696.4	517.0	517.9	471.0	261.6	57.4	592.9	607.3	0.154	0.50	0.608	0.296
1712.8	516.6	515.2	459.8	250.2	53.7	609.6	690.6	0.154	0.51	0.637	0.309
1729.2	518.6	513.3	458.9	261.9	54.5	602.3	648.7	0.174	0.54	0.647	0.318
1745.6	532.7	529.7	467.1	214.9	46.3	592.3	647.5	0.166	0.54	0.660	0.329
1762.0	533.3	525.5	464.2	263.8	59.3	593.8	683.5	0.172	0.51	0.696	0.344
1778.4	525.7	532.5	479.6	247.6	54.2	600.4	703.3	0.181	0.48	0.697	0.347
1794.8	516.5	524.3	468.2	276.0	60.8	599.1	709.0	0.175	0.47	0.687	0.343
1811.2	529.7	523.0	479.7	248.9	56.3	601.4	676.3	0.172	0.49	0.676	0.340
1827.6	519.5	516.3	474.3	283.5	60.0	582.1	677.2	0.169	0.49	0.681	0.340
1844.0	514.7	510.9	467.8	313.5	54.1	591.2	710.0	0.172	0.50	0.678	0.336
1860.4	521.6	529.9	471.9	281.1	77.2	611.3	660.0	0.173	0.51	0.702	0.349
1876.8	534.4	535.0	480.1	266.9	56.4	616.1	705.7	0.182	0.57	0.739	0.363
1893.2	523.8	529.3	480.1	209.5	49.4	621.9	671.4	0.184	0.53	0.748	0.367
1909.6	514.6	508.1	461.0	289.7	78.6	600.8	630.7	0.158	0.47	0.718	0.351
1926.0	545.6	545.7	489.5	254.6	61.4	614.8	695.8	0.187	0.54	0.766	0.375
1942.5	525.3	532.4	481.0	261.5	66.9	641.7	690.9	0.200	0.57	0.761	0.371
1958.9	519.4	525.4	485.7	296.7	73.3	580.4	699.5	0.195	0.57	0.773	0.384
1975.4	520.0	531.6	484.4	276.3	57.3	641.5	710.9	0.192	0.55	0.770	0.380
1991.8	546.7	546.6	491.6	280.4	60.7	662.5	705.3	0.196	0.56	0.831	0.414
2008.2	533.1	531.9	474.8	291.7	72.2	651.1	731.4	0.204	0.61	0.863	0.431
2024.7	541.0	542.3	496.2	223.7	53.9	649.5	731.4	0.214	0.65	0.859	0.433
2041.2	537.5	543.2	500.8	274.2	69.0	632.9	723.8	0.201	0.68	0.855	0.420
2057.6	539.3	558.4	514.1	283.3	74.7	673.5	703.7	0.206	0.63	0.883	0.440
2074.1	546.1	551.7	481.8	273.3	70.1	694.0	738.8	0.211	0.62	0.897	0.457
2090.6	536.0	545.1	495.9	282.5	80.9	661.9	742.8	0.210	0.55	0.890	0.447
2107.0	547.2	555.5	511.8	262.6	68.7	631.1	738.8	0.161	0.65	0.913	0.460
2123.5	515.7	176.6	111.2	73.8	55.0	223.6	429.9	0.147	0.50	0.316	0.201
2139.7	226.6	190.0	99.1	44.4	33.0	208.5	301.6	0.075	0.33	0.202	0.130
2156.3	200.4	165.0	78.6	40.2	31.7	184.7	334.4	0.056	0.05	0.149	0.092
2173.3	171.9	142.3	59.8	40.4	31.8	177.3	400.7	0.031	0.05	0.123	0.073
2189.5	164.9	136.7	58.7	35.6	30.0	152.7	355.6	0.028	0.02	0.103	0.061
2205.8	156.9	126.2	49.9	38.5	33.3	145.2	336.5	0.021	-0.03	0.087	0.051

TEST 7-30-80

TIME SEC	A 6 DEG C	A 7 DEG C	A 8 DEG C	A 9 DEG C	A 10 DEG C	A 11 DEG C	A 12 DEG C	B2 W/CMCM	C3 1/M	D4 W/CMCM	D5 W/CMCM
2222.1	145.6	115.1	42.9	34.6	29.0	138.0	312.8	0.014	-0.06	0.079	0.044
2238.4	139.9	112.7	51.2	35.5	29.6	131.6	292.4	0.023	-0.06	0.068	0.039
2254.7	125.5	99.1	44.5	34.2	30.9	129.0	274.1	0.013	-0.10	0.064	0.034
2271.0	129.1	99.0	49.3	34.9	29.3	122.5	259.1	0.014	-0.14	0.057	0.030
2287.4	122.7	105.2	48.8	31.6	28.2	120.7	246.0	0.015	-0.18	0.052	0.027
2303.7	119.1	98.0	43.3	33.0	29.2	125.0	233.4	0.010	-0.21	0.050	0.026
2320.1	114.1	93.7	46.9	30.5	27.6	117.8	223.1	0.015	-0.24	0.045	0.023
2336.5	106.8	87.4	42.6	31.4	28.6	102.6	213.5	0.019	-0.26	0.044	0.021
2352.8	107.7	85.0	35.2	30.4	28.5	110.2	205.3	0.014	-0.29	0.038	0.019
2369.1	101.5	76.4	31.9	29.1	26.6	98.5	197.7	0.001	-0.29	0.039	0.017
2385.4	99.2	81.5	36.3	30.5	27.0	91.9	190.6	0.018	-0.31	0.035	0.016
2401.7	95.6	75.5	35.0	29.2	26.2	91.4	183.4	0.023	-0.32	0.034	0.014
2418.0	92.8	75.8	33.8	29.2	28.2	97.9	177.1	0.012	-0.34	0.033	0.014
2434.3	94.8	71.4	35.7	32.1	27.3	90.8	171.2	0.013	-0.35	0.030	0.012

TABLE A-15. TEMPERATURE AND RADIATION MEASUREMENTS

FULL-SCALE TEST 8-5-80, PMMA CEILING

TIME SEC	A 6 DEG C	A 7 DEG C	A 8 DEG C	A 9 DEG C	A 10 DEG C	A 11 DEG C	A 12 DEG C	B 1 W/CMMSR	B 2 W/CMMSR	C 3 1/M	D 4 W/CMCM	D 5 W/CMCM
2.9	22.2	22.1	21.9	21.2	20.9	24.1	23.4	-0.004	-0.004	0.01	-0.001	0.002
10.3	22.4	22.2	21.9	21.1	20.9	24.4	23.8	-0.003	-0.004	0.00	-0.000	0.002
17.8	22.5	22.7	22.3	21.7	21.5	24.3	23.2	0.003	0.009	-0.00	0.001	0.002
25.3	22.8	22.9	22.7	21.2	21.1	24.2	23.9	-0.001	-0.010	0.00	0.000	0.002
32.8	23.0	23.3	22.2	21.2	20.6	24.5	24.7	-0.001	-0.008	0.01	0.001	0.001
40.3	23.5	23.8	23.0	22.3	22.6	24.5	24.5	0.002	0.001	-0.01	0.002	0.001
47.8	23.5	23.1	23.0	21.7	20.6	25.2	24.4	0.002	0.004	0.00	0.003	0.001
55.3	22.9	23.4	23.5	21.1	20.8	25.4	24.7	0.001	0.001	-0.01	0.003	0.002
62.9	24.1	24.2	22.6	22.5	21.5	25.6	24.8	0.001	0.001	0.00	0.002	0.003
70.4	24.2	24.5	23.0	21.8	21.2	25.9	24.8	-0.004	-0.004	0.02	-0.000	0.002
77.9	24.5	24.6	23.0	21.5	21.3	25.6	24.7	0.004	0.005	-0.03	0.002	0.002
85.4	24.7	25.0	21.8	21.7	21.4	26.3	25.5	0.001	0.002	-0.03	0.001	0.002
92.9	25.0	25.1	23.0	21.3	20.8	26.5	26.0	0.001	-0.013	-0.01	0.002	0.001
100.4	25.2	25.2	23.5	22.1	20.8	26.7	26.5	-0.001	0.003	-0.03	0.002	0.001
107.9	25.7	26.0	24.7	22.1	21.0	26.9	26.8	0.002	0.008	-0.03	0.001	0.002
115.4	26.2	26.3	23.6	21.7	20.6	27.4	27.8	-0.004	-0.003	-0.03	0.000	0.003
122.9	26.4	26.4	24.3	22.4	21.5	27.7	27.1	0.006	0.003	-0.03	0.002	0.002
130.5	26.3	25.3	24.0	22.6	21.3	27.6	27.3	-0.001	0.007	-0.02	-0.000	0.002
138.0	26.4	26.4	23.7	23.2	21.5	28.5	29.1	0.009	-0.002	-0.03	-0.000	0.002
145.5	27.2	26.7	24.2	22.1	21.1	29.0	29.4	0.002	0.002	-0.03	0.000	0.003
153.0	27.1	27.3	24.9	24.4	21.8	29.1	29.2	-0.004	0.007	-0.02	0.001	0.002
160.5	27.7	28.2	25.8	23.3	22.3	29.7	29.1	-0.001	-0.011	-0.03	0.002	0.002
168.0	28.4	28.4	26.9	23.9	20.6	29.7	30.0	0.008	-0.005	-0.03	0.000	0.001
175.5	29.2	29.3	22.6	22.1	20.8	30.5	30.9	-0.000	-0.010	-0.02	0.001	0.002
183.0	29.1	29.4	26.8	23.2	20.4	29.9	30.6	-0.000	-0.005	-0.02	0.001	0.002
190.5	29.1	29.4	28.2	22.1	20.6	30.6	30.8	0.002	-0.006	-0.02	0.002	0.001
198.0	29.7	30.1	27.3	23.9	21.4	31.8	31.7	-0.004	-0.005	-0.02	0.001	-0.000
205.5	30.4	30.5	29.2	24.9	21.3	32.3	32.2	0.002	-0.015	-0.02	0.002	0.002
213.0	30.6	30.4	27.6	22.9	21.4	32.2	32.1	0.005	-0.002	-0.03	0.001	0.002
220.5	31.2	31.3	27.4	22.6	21.6	32.5	33.1	0.002	-0.007	-0.02	0.003	0.005
228.0	31.3	31.3	30.1	24.2	21.0	33.6	34.0	0.009	-0.008	-0.01	0.000	0.004
235.5	32.2	32.3	28.0	23.2	20.7	33.6	33.1	-0.005	0.003	-0.02	0.000	0.002
243.0	32.0	32.2	28.3	21.8	20.7	33.9	33.4	0.001	0.010	-0.02	0.001	0.003
250.5	31.6	32.5	29.3	24.6	21.3	35.0	36.1	0.010	-0.012	-0.01	0.001	-0.000
258.0	33.5	33.9	29.4	23.0	21.2	35.2	36.2	0.003	0.000	-0.02	0.000	0.000
265.5	33.5	33.8	30.2	23.2	20.9	35.8	37.1	0.003	0.002	-0.01	0.001	0.002
273.0	34.6	35.0	31.4	24.1	21.1	38.2	38.5	0.007	-0.008	-0.02	0.000	0.003
280.4	35.4	35.5	28.2	21.6	20.8	36.7	39.1	0.005	0.001	-0.01	0.001	0.002
287.9	34.4	35.0	29.9	23.8	20.9	37.8	38.6	-0.005	0.005	-0.02	0.001	0.001
295.4	36.2	36.3	34.4	21.7	21.1	37.5	38.7	0.002	-0.002	-0.01	0.000	0.000
302.9	35.4	36.0	34.7	25.2	21.1	38.6	38.2	0.002	-0.017	-0.01	-0.000	0.000
310.4	35.6	36.5	35.3	24.6	21.6	38.6	39.1	0.004	-0.003	-0.02	-0.000	0.001
317.9	37.4	37.1	36.2	24.9	21.9	40.1	40.4	0.004	-0.007	-0.01	-0.000	0.002
325.4	37.4	38.1	36.3	23.8	21.1	40.1	41.3	0.001	-0.012	-0.01	-0.000	0.001
332.9	38.6	38.4	36.3	24.0	21.0	40.9	40.8	-0.004	0.001	-0.00	0.001	0.001

TEST 8-5-80

TIME SEC	A 6 DEG C	A 7 DEG C	A 8 DEG C	A 9 DEG C	A 10 DEG C	A 11 DEG C	A 12 DEG C	B 1 W/CMC MSR	B 2 W/CMC MSR	C 3 1/M	D 4 W/CMC MSR	D 5 W/CMC MSR
340.4	39.2	39.4	37.7	24.1	21.8	42.9	44.9	-0.002	0.001	0.00	0.001	0.001
347.9	40.3	40.4	38.4	22.7	20.7	40.6	43.0	0.004	0.003	-0.00	0.001	0.001
355.4	40.1	40.4	37.4	21.9	21.8	41.9	43.4	-0.002	-0.010	0.00	0.001	0.002
362.9	41.1	41.0	38.7	24.0	22.0	42.9	45.1	-0.005	-0.016	0.00	0.001	0.002
370.4	41.6	41.6	39.5	24.2	21.6	44.7	43.8	0.003	0.007	0.00	0.000	0.000
377.9	41.5	42.0	40.2	24.2	21.6	44.5	44.9	0.002	0.001	-0.00	0.002	0.001
385.4	41.9	42.2	40.2	29.0	21.2	44.1	43.8	0.000	0.010	-0.00	0.000	0.001
392.8	43.5	44.3	42.1	25.2	21.8	45.4	47.4	0.001	-0.011	0.00	-0.000	0.002
400.4	45.0	44.8	42.5	24.0	21.0	45.8	51.5	0.001	0.005	0.00	0.001	0.003
407.9	45.6	45.2	41.7	27.7	20.9	46.5	45.3	0.005	0.004	0.00	0.003	0.002
415.4	45.4	45.6	43.1	24.1	21.7	48.2	49.8	-0.001	-0.001	0.00	0.003	0.003
422.9	45.1	46.0	44.0	22.5	21.9	48.6	50.2	-0.010	0.005	0.01	0.002	0.003
430.4	45.5	45.9	41.9	24.4	21.5	48.5	50.5	-0.001	-0.000	0.01	0.002	0.003
437.9	46.9	47.5	44.9	24.6	21.4	49.7	48.5	0.004	-0.012	0.02	0.002	0.003
445.4	48.7	48.6	44.4	24.0	21.7	49.9	54.8	0.005	-0.002	0.02	0.003	0.003
452.9	47.2	49.3	46.4	22.9	26.4	51.4	51.3	0.004	-0.001	0.01	0.003	0.004
460.4	49.1	49.5	46.4	25.1	21.2	50.8	50.8	0.001	-0.007	0.02	0.002	0.003
467.9	49.5	51.4	48.4	23.7	22.0	53.6	53.9	0.006	-0.009	0.02	0.002	0.002
475.3	51.0	52.0	48.4	28.1	22.1	53.6	53.5	0.004	-0.010	0.02	0.002	0.005
482.8	50.7	51.4	49.6	22.5	23.0	54.6	52.8	-0.001	-0.010	0.02	0.002	0.004
490.3	52.5	53.0	51.7	23.9	21.1	55.6	53.7	0.006	0.000	0.02	0.003	0.004
497.8	53.1	53.4	52.2	23.4	23.1	56.9	57.4	-0.003	-0.007	0.02	0.003	0.004
505.3	55.7	55.9	50.6	24.5	21.4	57.3	58.6	0.017	-0.004	0.02	0.003	0.004
512.8	54.8	55.5	53.2	24.0	23.2	56.5	61.3	0.005	-0.007	-0.00	0.003	0.004
520.3	53.8	55.1	54.0	27.7	21.8	60.5	63.1	-0.004	0.002	0.01	0.002	0.002
527.8	57.1	57.7	55.1	25.4	23.2	60.2	63.9	-0.002	-0.007	0.04	0.003	0.003
535.3	58.9	59.0	54.4	23.9	22.4	61.7	61.7	-0.003	-0.005	0.04	0.003	-0.000
542.8	59.3	60.3	56.4	27.4	22.4	62.4	63.8	-0.005	-0.015	0.04	0.003	-0.000
550.3	57.9	60.0	58.1	24.2	22.5	65.5	65.8	-0.012	-0.013	0.05	0.003	-0.001
557.8	60.7	61.7	59.7	23.4	22.0	65.6	66.5	0.000	-0.004	0.05	0.002	-0.001
565.3	64.7	64.9	59.5	25.0	21.4	65.7	69.6	0.001	0.003	0.08	0.004	-0.000
572.8	62.4	62.5	59.1	30.0	22.9	65.0	66.1	0.003	-0.001	0.09	0.002	0.003
580.2	62.1	63.9	58.7	24.9	22.6	64.8	67.5	0.004	-0.007	0.11	0.003	0.003
587.7	66.6	66.4	60.9	24.4	22.5	70.8	72.7	0.003	-0.003	0.14	0.002	0.002
595.2	67.0	68.0	62.4	23.9	22.2	69.3	68.3	0.004	0.003	0.15	0.002	0.003
602.7	67.8	70.0	63.4	23.6	22.7	71.9	72.2	-0.005	-0.003	0.13	0.004	0.003
610.2	68.4	68.4	63.2	22.6	22.1	70.5	76.0	0.007	0.005	0.12	0.002	0.004
617.7	70.3	71.4	66.8	22.8	22.4	72.1	77.8	0.000	-0.006	0.12	0.003	0.004
625.2	69.9	71.9	65.8	26.4	23.8	74.5	77.6	-0.000	-0.006	0.11	0.004	0.004
632.7	72.7	73.3	68.7	40.6	24.8	77.2	81.9	0.002	-0.004	0.10	0.005	0.004
640.2	74.3	74.4	68.9	29.4	23.0	80.0	78.8	-0.000	-0.012	0.11	0.003	0.004
647.7	77.0	78.2	71.3	26.9	22.5	81.7	83.5	0.001	-0.013	0.12	0.003	0.004
655.1	76.8	76.8	70.9	26.6	22.0	79.2	80.2	-0.007	0.004	0.12	0.005	0.005
662.6	77.4	77.4	72.1	24.5	22.2	83.8	82.8	-0.000	-0.005	0.12	0.005	0.005
670.1	77.7	79.4	76.6	25.8	21.1	81.1	88.9	0.004	0.002	0.14	0.007	0.006

TEST 8-5-80

TIME SEC	A 6 DEG C	A 7 DEG C	A 8 DEG C	A 9 DEG C	A 10 DEG C	A 11 DEG C	A 12 DEG C	B 1 W/CMCMR	B 2 W/CMCMR	C 3 1/M	D 4 W/CMCM	D 5 W/CMCM
677.6	80.2	80.8	78.5	30.5	21.2	83.8	87.9	0.002	-0.008	0.13	0.006	0.006
685.1	81.6	83.0	77.4	23.0	22.2	86.3	83.0	0.008	-0.006	0.14	0.007	0.006
692.6	82.5	82.7	79.3	24.9	29.7	89.9	88.3	0.001	-0.011	0.15	0.008	0.007
700.1	85.9	87.0	77.5	24.9	22.8	90.8	94.6	-0.003	-0.009	0.16	0.008	0.006
707.6	87.9	88.6	81.8	25.5	23.2	90.2	90.6	0.002	0.006	0.14	0.006	0.005
715.1	88.5	90.2	83.6	26.3	23.2	93.3	96.3	0.007	0.005	0.16	0.007	0.004
722.6	90.3	89.7	85.0	29.3	23.5	94.2	103.5	0.004	-0.009	0.15	0.008	0.004
730.1	92.0	93.8	88.7	23.4	22.0	97.7	97.2	0.001	0.007	0.16	0.009	0.005
737.6	91.8	92.8	89.5	53.2	21.9	97.0	90.7	0.006	0.004	0.16	0.009	0.006
745.1	91.9	93.9	86.2	24.9	22.5	103.8	95.9	-0.003	-0.005	0.16	0.007	0.004
752.6	94.3	95.3	88.4	23.4	24.2	101.9	105.7	-0.002	-0.008	0.17	0.008	0.004
760.1	99.2	99.2	94.8	30.6	21.9	104.5	108.8	0.002	0.003	0.18	0.007	0.004
767.6	97.4	99.4	94.1	26.2	21.6	111.1	107.8	0.001	0.006	0.19	0.009	0.008
775.1	104.9	103.5	95.5	31.7	22.4	106.4	101.5	0.006	-0.002	0.19	0.010	0.008
782.6	107.7	108.5	97.3	26.0	22.8	112.4	117.0	-0.003	0.014	0.19	0.011	0.007
790.1	106.9	106.9	94.6	40.8	27.5	111.1	123.9	0.000	0.004	0.20	0.009	0.006
797.6	109.4	109.6	100.7	33.5	25.6	119.6	113.3	0.006	-0.008	0.21	0.011	0.006
805.1	111.2	111.0	105.2	56.3	26.2	119.1	128.8	0.012	0.009	0.21	0.012	0.007
812.6	111.9	112.5	107.9	35.1	22.9	120.7	127.6	0.008	-0.006	0.22	0.012	0.007
820.1	116.4	119.9	106.8	29.9	22.3	124.3	129.9	-0.005	0.005	0.22	0.011	0.010
827.5	119.0	123.1	109.6	34.0	22.2	122.4	126.7	-0.002	-0.001	0.23	0.013	0.009
835.1	125.5	124.6	112.0	37.6	21.8	128.0	133.5	0.005	-0.009	0.22	0.014	0.009
842.6	132.1	131.1	113.6	43.7	26.2	135.0	139.6	0.004	-0.007	0.23	0.013	0.008
850.1	125.3	126.3	117.8	33.8	22.4	136.0	145.6	0.004	0.006	0.24	0.014	0.008
857.6	135.1	136.0	124.0	37.2	22.3	139.2	144.6	0.005	0.002	0.25	0.014	0.007
865.1	133.5	133.8	123.5	31.6	22.9	140.8	140.2	0.003	-0.013	0.25	0.015	0.008
872.6	134.9	136.6	127.3	42.7	21.9	144.5	139.6	0.004	-0.005	0.26	0.017	0.009
880.1	142.1	141.7	128.0	31.3	22.4	146.6	154.8	0.001	0.005	0.28	0.016	0.009
887.6	137.1	139.1	131.6	38.2	22.3	145.0	157.4	0.003	0.006	0.29	0.017	0.009
895.2	147.3	144.5	133.4	37.2	22.8	156.3	172.3	0.006	0.010	0.28	0.016	0.010
902.6	148.2	147.5	137.8	37.6	22.6	158.1	169.8	0.005	-0.009	0.30	0.018	0.011
910.1	148.5	152.0	139.5	56.4	23.0	153.3	160.3	0.004	-0.001	0.31	0.019	0.010
917.6	154.1	154.7	143.6	57.3	23.6	158.3	161.4	0.008	-0.006	0.32	0.020	0.010
925.1	155.8	157.7	142.9	44.5	23.8	157.4	153.9	0.007	0.006	0.33	0.021	0.010
932.6	152.8	158.8	144.1	50.2	22.6	160.9	160.4	0.012	-0.001	0.33	0.021	0.010
940.1	161.7	162.9	149.5	57.1	23.5	165.8	170.5	-0.004	0.007	0.35	0.023	0.012
947.6	159.4	166.5	151.8	46.2	24.1	167.5	180.0	-0.005	-0.000	0.35	0.023	0.011
955.1	163.8	165.1	145.8	32.3	23.2	172.7	177.9	0.006	-0.004	0.36	0.024	0.012
962.7	165.0	167.5	154.3	51.5	24.8	179.4	166.9	0.007	-0.002	0.37	0.024	0.011
970.2	166.1	173.1	162.2	71.0	29.0	180.5	170.0	0.005	0.009	0.37	0.026	0.011
977.7	179.8	179.0	164.9	46.4	23.1	181.4	182.5	0.008	-0.011	0.39	0.026	0.011
985.2	176.0	177.3	160.7	89.1	23.1	185.4	179.9	0.000	0.002	0.40	0.028	0.012
992.7	169.9	183.4	167.5	70.1	22.7	190.2	180.1	0.000	-0.014	0.42	0.028	0.013
1000.2	179.7	182.0	173.1	73.8	22.6	185.8	190.2	0.009	-0.008	0.42	0.029	0.013
1007.7	182.3	189.1	168.8	57.9	23.3	188.4	203.1	0.011	-0.003	0.43	0.029	0.013

TEST 8-5-80

TIME SEC	A 6 DEG C	A 7 DEG C	A 8 DEG C	A 9 DEG C	A 10 DEG C	A 11 DEG C	A 12 DEG C	B 1 W/CMMSR	B 2 W/CMMSR	C 3 1/M	D 4 W/CMCM	D 5 W/CMCM
1015.2	181.6	186.0	173.5	36.8	24.1	192.2	178.6	0.009	-0.009	0.45	0.030	0.014
1022.7	189.5	190.1	169.2	63.0	25.0	201.1	201.5	0.002	0.011	0.47	0.030	0.013
1030.1	190.6	192.5	169.7	69.0	23.9	198.0	200.8	0.005	0.002	0.49	0.032	0.015
1037.7	193.3	199.0	178.3	61.4	24.8	198.9	201.0	0.008	-0.001	0.49	0.033	0.015
1045.2	192.1	195.9	179.3	68.0	25.3	200.6	190.0	0.009	-0.008	0.50	0.034	0.015
1052.7	194.8	190.6	183.0	98.6	24.9	209.9	222.2	0.010	-0.000	0.51	0.035	0.016
1060.2	193.4	201.5	183.2	55.7	24.6	210.6	219.0	0.012	0.013	0.53	0.036	0.016
1067.7	207.5	211.5	189.6	35.6	23.4	217.8	218.0	0.006	0.015	0.53	0.038	0.017
1075.2	213.0	215.7	191.1	79.5	27.8	223.2	213.4	0.007	0.000	0.56	0.039	0.018
1082.8	246.3	250.7	228.7	56.7	26.3	278.9	321.7	0.005	0.014	0.58	0.047	0.021
1090.3	313.6	312.9	258.7	46.0	25.9	317.9	355.8	0.008	0.007	0.61	0.059	0.027
1097.9	335.8	348.7	273.5	47.8	25.0	366.0	386.2	0.003	0.013	0.66	0.077	0.034
1105.4	395.8	399.0	270.7	82.7	27.6	442.3	531.5	0.012	0.029	0.73	0.098	0.042
1113.0	453.9	442.1	306.2	50.2	28.7	454.1	583.2	0.012	0.005	0.80	0.125	0.054
1121.0	477.5	495.7	379.2	121.7	31.0	566.2	673.9	0.039	0.013	0.87	0.164	0.071
1129.3	557.1	542.5	362.4	43.2	30.5	599.8	669.2	0.039	0.035	0.90	0.228	0.107
1137.7	597.2	605.1	361.8	50.6	34.7	663.8	670.8	0.038	0.042	0.99	0.295	0.140
1146.0	682.5	689.4	452.9	168.6	38.5	760.1	725.4	0.060	0.067	1.15	0.399	0.214
1154.3	739.0	745.9	481.5	179.4	45.7	794.5	724.6	0.085	0.106	1.31	0.494	0.294
1162.6	733.3	779.5	555.4	221.1	52.7	833.0	907.7	0.140	0.158	1.48	0.588	0.374
1171.0	746.4	790.5	650.9	230.1	55.9	853.2	848.9	0.188	0.198	1.64	0.713	0.502
1179.4	685.7	710.5	787.5	290.3	70.5	821.9	978.6	0.226	0.257	1.66	0.825	0.626
1187.8	677.9	715.6	772.4	387.0	68.9	838.2	896.3	0.293	0.320	1.97	0.955	0.770
1196.3	707.9	717.8	796.1	542.7	72.5	813.6	895.3	0.338	0.373	2.17	1.144	0.929
1204.9	679.9	729.5	802.4	631.0	115.3	790.2	985.0	0.384	0.434	2.33	1.156	0.961
1213.4	676.0	704.2	774.0	713.6	146.7	765.3	980.6	0.391	0.437	2.66	1.250	1.093
1221.8	676.4	754.8	774.4	762.1	277.7	809.5	915.2	0.411	0.468	2.58	1.297	1.127
1235.2	700.2	711.4	759.3	609.0	127.7	763.9	910.9	0.485	0.480	3.02	1.371	1.220
1248.7	659.3	668.0	750.7	795.3	171.7	766.9	941.9	0.478	0.501	3.26	1.475	1.295
1257.6	669.7	704.8	750.6	780.8	271.0	772.7	464.2	0.459	0.541	3.53	1.489	1.302
1266.4	125.7	122.8	76.8	54.9	37.0	193.1	301.0	0.156	0.156	3.12	0.187	0.184
1274.7	247.2	236.6	97.9	60.4	36.9	230.5	280.4	0.070	0.077	2.57	0.188	0.154
1287.1	191.1	173.7	79.8	40.8	43.1	163.0	245.4	0.054	0.062	2.33	0.142	0.112
1299.2	177.9	159.7	85.6	44.8	35.1	165.0	209.1	0.046	0.049	1.86	0.126	0.102
1306.8	170.3	153.7	59.5	44.1	33.4	157.1	206.1	0.036	0.040	1.70	0.114	0.093
1314.3	170.3	143.5	57.0	41.8	31.0	139.6	191.7	0.040	0.033	1.61	0.107	0.084
1321.9	154.9	130.1	49.5	43.3	32.6	140.3	186.3	0.035	0.038	1.62	0.103	0.080
1329.4	152.1	123.6	42.8	40.7	31.0	125.3	175.6	0.037	0.030	1.39	0.096	0.073
1337.0	124.5	86.5	38.3	36.3	29.2	113.4	174.7	0.028	0.030	1.32	0.091	0.068
1344.5	140.4	117.6	40.6	38.1	31.2	122.2	154.3	0.031	0.031	1.29	0.086	0.064
1352.1	122.9	104.0	40.3	37.6	27.5	110.4	149.9	0.022	0.053	1.23	0.079	0.062
1359.6	133.9	124.3	44.3	41.8	26.7	89.2	147.0	0.030	0.033	1.21	0.075	0.059
1367.1	124.2	92.7	42.3	33.9	27.1	105.3	152.4	0.033	0.032	1.18	0.075	0.055
1374.6	119.0	100.6	39.0	33.4	28.6	97.6	140.7	0.033	0.008	1.15	0.068	0.053
1382.2	111.0	100.0	33.6	32.7	27.8	101.8	126.3	0.026	0.061	1.11	0.066	0.050

TEST 8-5-80

TIME SEC	A 6 DEG C	A 7 DEG C	A 8 DEG C	A 9 DEG C	A 10 DEG C	A 11 DEG C	A 12 DEG C	B 1 W/CMCM	B 2 W/CMCM	C 3 1/M	D 4 W/CMCM	D 5 W/CMCM
1389.7	112.3	92.8	38.1	32.7	26.7	100.5	112.2	0.024	0.030	1.11	0.063	0.048
1397.2	85.6	80.2	40.2	34.5	29.1	103.3	128.2	0.021	0.024	1.10	0.062	0.047
1404.7	108.5	81.7	34.5	34.6	28.5	94.0	127.9	0.017	0.036	1.06	0.060	0.046
1412.2	112.3	89.3	43.8	36.1	30.5	91.6	122.1	0.019	0.007	1.08	0.057	0.043
1419.7	94.5	81.2	34.2	33.9	29.5	91.2	120.9	0.022	0.014	1.06	0.057	0.041
1427.3	90.3	65.8	34.7	31.8	28.5	89.1	109.3	0.019	0.017	1.04	0.056	0.040
1434.8	84.1	63.3	36.2	30.2	27.6	89.8	116.6	0.016	0.017	1.04	0.051	0.038
1442.3	99.1	88.9	35.5	30.4	24.8	81.2	109.1	0.021	0.020	1.04	0.051	0.038
1449.8	94.0	73.8	39.4	35.0	26.8	70.5	114.1	0.014	0.015	1.05	0.049	0.037
1457.3	101.4	82.3	32.2	27.3	26.1	80.5	110.5	0.010	0.019	1.03	0.051	0.034
1464.8	95.8	73.5	33.9	31.3	29.0	83.9	102.9	0.009	0.005	1.01	0.048	0.034
1472.3	90.2	68.9	35.8	29.5	25.0	82.3	112.2	0.011	0.015	0.99	0.046	0.033
1479.8	92.1	71.7	38.7	30.1	27.0	77.1	102.0	0.012	0.015	1.00	0.049	0.033
1487.3	84.5	80.8	34.0	26.9	25.7	75.1	96.0	0.018	0.022	1.00	0.042	0.031
1494.8	89.9	75.3	31.4	30.6	25.0	73.9	101.7	0.011	0.021	0.99	0.044	0.030
1502.3	82.6	68.4	30.1	28.2	24.0	76.9	99.4	0.014	0.011	0.99	0.042	0.029
1509.8	78.6	62.3	32.1	31.7	29.5	82.0	94.3	0.011	0.022	0.99	0.041	0.029
1517.3	88.1	78.1	36.3	26.6	23.9	76.6	107.2	0.022	0.017	1.00	0.039	0.029
1524.8	81.3	71.4	33.0	24.2	23.6	76.3	86.3	0.009	0.012	0.97	0.039	0.028
1532.3	67.4	49.3	33.4	31.2	25.7	75.3	92.9	0.011	0.022	0.98	0.038	0.028
1539.8	60.2	51.7	28.3	27.5	26.0	73.4	92.4	0.013	0.017	0.96	0.037	0.027
1547.3	73.4	52.4	31.0	27.8	24.4	72.7	93.6	0.009	0.012	0.95	0.038	0.026
1554.8	72.6	50.3	30.0	30.3	27.1	71.6	82.0	0.007	0.006	0.95	0.036	0.026
1562.3	72.3	63.4	28.6	28.9	25.4	69.3	88.6	0.013	0.020	0.94	0.039	0.026
1569.8	77.8	64.7	29.3	29.2	25.2	68.9	90.1	0.017	0.025	0.94	0.034	0.026
1577.3	78.6	62.0	31.2	26.0	25.6	72.0	90.3	0.006	0.009	0.94	0.035	0.024
1584.8	77.2	65.0	29.7	25.5	24.6	73.9	83.5	0.007	0.019	0.94	0.034	0.024
1592.3	75.4	59.3	29.8	23.6	23.2	67.3	89.7	0.006	0.006	0.94	0.035	0.024
1599.8	73.2	64.5	31.6	25.0	24.0	71.4	81.4	0.016	0.019	0.92	0.033	0.022
1607.3	72.7	62.7	28.6	24.7	23.6	71.4	90.7	0.007	0.016	0.91	0.032	0.023

TABLE A-16
 TEMPERATURE AND RADIATION MEASUREMENTS
 FULL-SCALE TEST 8-20-80
 FULLY DEVELOPED PMMA CEILING FIRE

Instrument I.D.	Measurement	
	Average	Standard Deviation
A6	633°C	23°C
A7	708°C	32°C
A8	782°C	14°C
A9	847°C	29°C
A10	764°C	19°C
A11	757°C	26°C
A12	793°C	5.7°C
B2	0.643 W/cm ² sr	0.027 W/cm ² sr
C3	3.51 m ⁻¹	0.02 m ⁻¹
D4	2.122 W/cm ²	0.063 W/cm ²
D5	1.882 W/cm ²	0.040 W/cm ²